











# NAVAL POSTGRADUATE SCHOOL

## Monterey, California



# THESIS

VERIFICATION OF A MICRO-THRUSTING MODEL TO  
MAINTAIN SATELLITES IN LOW ORBIT

by

Christopher David Noble

June 1987

Thesis Advisors:

Maurice D. Weir

Richard D. Wood

Approved for public release; distribution is unlimited

T234312



UNCLASSIFIED

SECURITY CLASSIFICATION OF THIS PAGE

## REPORT DOCUMENTATION PAGE

a REPORT SECURITY CLASSIFICATION UNCLASSIFIED			1b RESTRICTIVE MARKINGS			
2a SECURITY CLASSIFICATION AUTHORITY			3 DISTRIBUTION/AVAILABILITY OF REPORT Approved for public release; distribution is unlimited			
4b DECLASSIFICATION/DOWNGRADING SCHEDULE						
1 PERFORMING ORGANIZATION REPORT NUMBER(S)			5 MONITORING ORGANIZATION REPORT NUMBER(S)			
a NAME OF PERFORMING ORGANIZATION Naval Postgraduate School		6b OFFICE SYMBOL (If applicable) Code 67		7a NAME OF MONITORING ORGANIZATION Naval Postgraduate School		
c ADDRESS (City, State, and ZIP Code) Monterey, California 93943-5000			7b ADDRESS (City, State, and ZIP Code) Monterey, California 93943-5000			
a NAME OF FUNDING/SPONSORING ORGANIZATION		8b OFFICE SYMBOL (If applicable)		9 PROCUREMENT INSTRUMENT IDENTIFICATION NUMBER		
c ADDRESS (City, State, and ZIP Code)			10 SOURCE OF FUNDING NUMBERS			
			PROGRAM ELEMENT NO	PROJECT NO	TASK NO	WORK UNIT ACCESSION NO
11 TITLE (Include Security Classification) VERIFICATION OF A MICRO-THRUSTING MODEL TO MAINTAIN SATELLITES IN LOW ORBIT						
12 PERSONAL AUTHOR(S) Noble, Christopher D.						
13a TYPE OF REPORT Master's Thesis		13b TIME COVERED FROM _____ TO _____		14 DATE OF REPORT (Year, Month Day) 1987, June		15 PAGE COUNT 168
16 SUPPLEMENTARY NOTATION						
COSATI CODES			18 SUBJECT TERMS (Continue on reverse if necessary and identify by block number)			
FIELD	GROUP	SUB-GROUP	Drag Compensation; Micro-thrusting; Satellite			
			Orbital Lifetime Model; Propellant Longevity;			
			Atmospheric Drag; Orbital Element Design			
19 ABSTRACT (Continue on reverse if necessary and identify by block number) New concepts in aerospace travel have renewed interest in modeling and compensating for the effects of upper atmospheric drag. In particular, the SDI constellation requires strict orbital element maintenance. This thesis is a qualitative verification of a propellant longevity model for low-altitude earth orbit satellites doing intrack micro-thrusting to overcome atmospheric drag. The original model was developed at the Naval Surface Weapons Center. Pertinent orbital mechanics and atmospheric concepts are reviewed. The model and its computer program are described. The results of trend and sensitivity analysis reasonableness tests are presented. Finally suggestions for use are made. Many plots of mission life predictions are presented. The model computer program and sample input and output are also included.						
20 DISTRIBUTION/AVAILABILITY OF ABSTRACT <input checked="" type="checkbox"/> UNCLASSIFIED/UNLIMITED <input type="checkbox"/> SAME AS RPT <input type="checkbox"/> DTIC USERS				21 ABSTRACT SECURITY CLASSIFICATION Unclassified		
22a NAME OF RESPONSIBLE INDIVIDUAL Prof. Maurice D. Weir			22b TELEPHONE (Include Area Code) (408) 646-2608		22c OFFICE SYMBOL Code 63Wc	

Approved for public release; distribution is unlimited.

Verification of a Micro-Thrusting Model  
to Maintain Satellites  
in Low Orbit

by

Christopher David Noble  
Lieutenant, United States Navy  
B.S., University of the State of New York, 1979

Submitted in partial fulfillment of the  
requirements for the degree of

MASTER OF SCIENCE IN ENGINEERING SCIENCE

from the

NAVAL POSTGRADUATE SCHOOL  
June 1987



## ABSTRACT

New concepts in aerospace travel have renewed interest in modeling and compensating for the effects of upper atmospheric drag. In particular, the SDI constellation requires strict orbital element maintenance. This thesis is a qualitative verification of a propellant longevity model for low-altitude earth orbit satellites doing intrack micro-thrusting to overcome atmospheric drag. The original model was developed at the Naval Surface Weapons Center. Pertinent orbital mechanics and atmospheric concepts are reviewed. The model and its computer program are described. The results of trend and sensitivity analysis reasonableness tests are presented. Finally suggestions for use are made. Many plots of mission life predictions are presented. The model computer program and sample input and output are also included.

## TABLE OF CONTENTS

I.	INTRODUCTION -----	5
II.	BACKGROUND -----	13
	A. ORBITAL MECHANICS -----	13
	B. THE ATMOSPHERE MODEL -----	30
III.	PROPELLANT LONGEVITY MODEL DESCRIPTION -----	52
	A. PROPELLANT LONGEVITY MODEL THEORY -----	52
	B. COMPUTER CODE DESCRIPTION -----	53
	C. MODEL CODE OPERATION -----	65
IV.	MODEL VERIFICATION -----	68
V.	SUMMARY -----	126
	APPENDIX A: COMPUTER PROGRAM LISTING -----	129
	APPENDIX B: SAMPLE INPUT AND OUTPUT -----	155
	LIST OF REFERENCES -----	166
	INITIAL DISTRIBUTION LIST -----	167

## I. INTRODUCTION

All current low-earth-orbit satellites are simply placed in orbit and then tracked as their orbits decay deeper into the atmosphere. This orbital decay is due to forces on the satellite produced by atmospheric drag and the non-spherical earth.

Modified exponential-type models for the atmosphere produce sufficiently accurate drag predictions to track the satellites.

New concepts in scientific and military uses of space require greater accuracy in predicting atmospheric drag effects than produced by the modified exponential models. These new uses include the Aero-assisted Orbital Transfer Vehicle (AOTV), orbiting space stations, the Trans Atmospheric Vehicle (TAV), and the strategic defense initiative satellite constellation.

The environment of all of these vehicles is called the thermosphere, an atmospheric layer studied in depth only recently. An accurate empirical model of the thermosphere has also been produced.

One idea under investigation at the Naval Surface Weapons Center is the placement of many low-earth-orbital defensive satellites in precisely controlled and maintained orbits. This set of defensive satellites is termed a

constellation. All low earth-orbital-satellites drift from their initial orbits due to perturbing accelerations caused primarily by the aspherical earth and atmospheric drag. In order to be functional, the orbits of the satellites in an SDI constellation must be exactly maintained. The drift of a satellite must be cancelled out by using an onboard propulsion system to produce forces to offset the perturbing accelerations.

One model, proposed by Dr. Dan Parks of the Naval Surface Weapons Center, calculates the mission lifetime expected of a satellite doing intrack micro-thrusting to overcome atmospheric drag effects. The end of mission life corresponds to depletion of all the maneuvering fuel. This model is here-after referred to as the propellant longevity model. The propellant longevity model incorporates a Bessel function expansion for the fuel-mass decrement on each revolution. However, the model does not calculate the fuel necessary to cancel out orbital drift due to the aspherical earth.

This thesis gives a verification of the low-altitude earth satellite propellant longevity prediction model developed by Dr. Parks. The theory for the model development itself is presented in Naval Surface Weapons Center Technical Report (NSWC TR) 83-243 (Parks [Ref. 1]). Computer code for the model was developed at NSWC under the direction of Dr. Parks. In addition to the computer code of



the model, several other NSWC publications with applications to the model were forwarded to the Naval Postgraduate School.

The Thesis is organized as follows. Chapter I presents a general introduction to the propellant longevity model and discusses the changes made to the computer code for use at the Naval Postgraduate School. A basic description of the orbital mechanics necessary to operate the model is provided in Chapter II. Chapter II also presents an overview of the atmospheric physics necessary to understand the density and compositional variations in the thermospheric layer of the thermosphere. A description of the propellant longevity model is given in Chapter III. Instructions for operation of the computer code are also included there. Chapter IV contains the results of the verification process sensitivity analysis and reasonableness tests. A summary is given in Chapter V. Appendix A contains the propellant longevity Fortran computer code for the IBM 3033. Appendix B shows input sets and their corresponding outputs. Graphical presentation of the tabular results is included.

The coding of the model by NSWC was completed in Fortran for the Control Data Corporation (CDC) 6700 computer. Because of software and hardware differences, extensive modifications to the model coding were required to install the program as an operational model on the IBM 3033 computer at the Naval Postgraduate School. To optimize the utility

of the model, some adjustments were also made to the original computer coding of the propellant longevity model. Great care was taken when modifying the code to preserve the model theory as contained in NSWC TR 83-243.

The alterations to the computer program fall into two categories: changes to transport and implement the model on our IBM 3033, and changes made to mainstream the model verification process. Changes to transport the model from the CDC environment to the IBM environment involved some logical revision and syntax, hardware word-size considerations.

The hardware word-size problems were extensive. The CDC 6700 uses a 60-bit word size for single precision calculations, whereas IBM's standard is a 30-bit word. The propellant longevity model requires 60 bit precision. Thus all real numbers, library functions, and input constants were promoted to double precision accuracy. Another precision-related problem involved the use of fractional exponentiation. All one-half exponents were changed to call the SQRT function to increase precision and speed.

Syntactical changes were mostly related to the software environment transportation from CDC Fortran to IBM Fortran 77. Library functions calls, and input and output format statement changes, were the bulk of the syntactical changes made. (Examples of library function changes are the ARQTAN function changed to the ATAN2 function, the BESI Bessel

function call changed to the MMBSIR Bessel function call and so forth).

Examples of changes in the logic to in order to transport and implement the model code include using the Fortran 77 block IF-THEN-ELSE statement for the CDC Fortran IF statement and the use of DIMENSION statements in each subroutine that is processing a particular array.

The second category of changes to the program addressed mainstreaming the model verification process. The model code as down-loaded from the NSWC tape contained little code-internal documentation. Looking towards future implementation and maintenance of the model code, extensive documentation was added as code internal comments. Most of this documentation was based on the research literature of NSWC. Extensive reference to the current publications is made in the code documentation itself.

Two changes were made in the way the code solves the model in order to implement the theory with greater precision. The first change turned on the subroutine THRST which was designed to allow for preplanned changes to the semi-major axis of the orbit at the expense of onboard maneuvering fuel. (The subroutine code down-loaded from tape did not return the fuel consumed for the orbit adjust, record the resultant change in the semi-major axis, or receive the correct intended adjust parameter. All these functions are performed in the IBM 3033 version.)

A second change in the code alters the way in which the satellite velocity relative to the atmosphere is computed. In the original code this parameter had to be entered as part of the input file and was assumed to be constant. Since this relative velocity is actually a function of other transient orbital parameters, recomputation is now automatically accomplished for each satellite revolution based on current values of the changing orbital parameters. In place of the satellite-to-atmospheric-relative-velocity input, the user now inputs the atmospheric-to-earth relative rotation rates. The physics associated with this change is discussed later on, in the section describing the atmospheric model.

A few other changes to the propellant longevity code customize the output, or state the input element initial conditions. Several control inputs now allow for a range of model predictions. These are explained in Chapter III.

The actual model verification is accomplished in three steps. First does the model address the original problem? Second, does the model meet the criteria of common sense? Finally, how well does the model solution compare when tested against real-world data?

No real-world data sets exist for testing the propellant longevity model. The only low-earth-orbit satellite having a propulsion system to maintain orbital parameters is highly classified under the auspices of the United States Air



Force. The data from this program is not available in an unclassified state. In lieu of actual data, several additions to the program code were made to assist in the model verification process. The major adjustment is the addition of a feature to allow for a sensitivity analysis. The subroutine SNALYS, allows the user to linearly scan any combination of the 20 input elements, from a user specified minimum to any maximum, with user specified granularity. The output of the sensitivity analysis can be descriptive and tabular, or graphical in nature. The SNALYS subroutine allows for a plot of model prediction against the entire range of the input elements. Results of input element sensitivity analysis are presented in the Chapter IV. The sensitivity analysis feature allows for optimum orbital-element and satellite-ballistic-coefficient design.

Thought was given to possible model installation on other computers. The model is large and requires about 20 minutes of dedicated central processor time to complete an average run. As such the model is rather limited to mainframe computers. Initial calculations based on processor time indicate an IBM AT microcomputer with the requisite 80287 co-processor and additional RAM memory might require about ten hours to complete an average run.

This chapter presented an overview and motivation for the propellant longevity model. Changes made to the computer program at the Naval Postgraduate School were also

discussed. The next chapter presents the necessary background in orbital mechanics and atmospheric concepts to operate and understand the model.

## II. BACKGROUND

This chapter presents the orbital mechanics and atmospheric concepts required for the understanding and operation of the propellant longevity model. The orbital mechanics presented in the first section discusses only the orbital element sets, concepts, and coordinate systems specific to the model. In the second section of this chapter, Thermosphere specific atmospheric concepts and cycles are presented.

### A. ORBITAL MECHANICS

This section covers the orbital mechanics for operating the mass decrement model. If the coordinate and orbital element systems discussed are familiar, this basic orbital mechanics section can be skipped. Orbital mechanics references are cited in the text.

Early celestial mechanics models were based on increasingly accurate observations. As observations and record keeping improved so did the empirical model fit to the observations. The model that fathered modern orbital mechanics was the empirical model derived by Johannes Kepler, 1571-1630. In 1619 Kepler formulated three laws (models) of planetary motion. These models were based on life long observations recorded by Tycho Brahe, 1564-1601. Kepler's models were formulated as follows:

1. The orbit of each planet is an ellipse with the sun at one focus.
2. The line joining a planet to the sun sweeps out equal areas in equal times.
3. The square of the period of a planet is proportional to the cube of its mean distance from the sun.

Later, Sir Isaac Newton, 1643-1727 validated Kepler's laws by establishing their equivalence with his law of universal gravitational attraction.

Newton's model for gravitational attraction states that two bodies attract with a force that is proportional to the product of their masses and inversely proportional to the square of the distance between them. Symbolically, the force on the mass  $m$  due to the mass  $M$  is given by:

$$\vec{F_g} = - \frac{GMm}{r^2} \frac{\vec{r}}{r} \quad (1)$$

where  $G$  is the universal gravitational constant and  $r$  is the vector from the center of mass of  $M$  to the center of mass  $m$ .  $r$  is the magnitude of the distance vector  $r$ .

A body experiences an acceleration due to the resultant of all the forces acting on the body. If only a gravitational force acts on the body, then the acceleration of the body is given by:

$$\vec{r}'' = \vec{a} = - \frac{G(M+m)}{r^3} \vec{r} \quad (2)$$



In this model,  $r''$  is the acceleration vector on  $m$  caused by gravitational attraction of  $M$  on  $m$ . The remaining variables are defined as in the previous model. If  $M$  is much greater than  $m$  (as in an earth satellite system),  $G(M+m)$  is very nearly  $GM$ . Another constant can then be defined called the gravitational potential parameter  $u$ :

$$u = Gm \quad (3)$$

The gravitational acceleration of a satellite in earth orbit can then be expressed as:

$$r'' + u/r^3 * r = 0 \quad (4)$$

The gravitational field is conservative. This means that an energy constant of motion can be defined for a body moving in a gravitational field. For a two body, atmospheric, elliptic orbit system the specific mechanical energy is:

$$\xi = v_t^2/2 - u/r \quad (5)$$

In this model  $\xi$  is the specific mechanical energy,  $v_t$  is the satellite tangential speed, and  $u$  and  $r$  are as previously defined. Note that  $E$  is the sum of the kinetic

energy per unit mass of the satellite and its potential energy per unit mass.

The model, (5), requires satellites at specific radii to have specific tangential speeds. As  $r$  increases,  $v$  must decrease to maintain  $\xi$  constant. This orbital energy model is important when modelling the effects of atmospheric drag which is the major topic of the next section.

Newton's inverse square law of gravitational force requires gravitational field orbits to be elliptical in the shape. The mathematics of the ellipse is important in the description of orbits and Figure 1 presents some of the important parameters.

The parameters shown in Figure 1 are defined as follows:

- a: the semi-major axis.
- b: the semi-minor axis.
- e: the eccentricity where

$$e = \text{SQRT} [1 - (b/a)^2].$$

- C: the ellipse center.
- O: the ellipse focus (earth center).
- p: the semi-latus rectum.
- r: the distance from a position on the ellipse the focus O.
- v: the true anomaly.
- rp: the radius at perigee (in an earth system).
- ra: the radius at apogee (in an earth system).

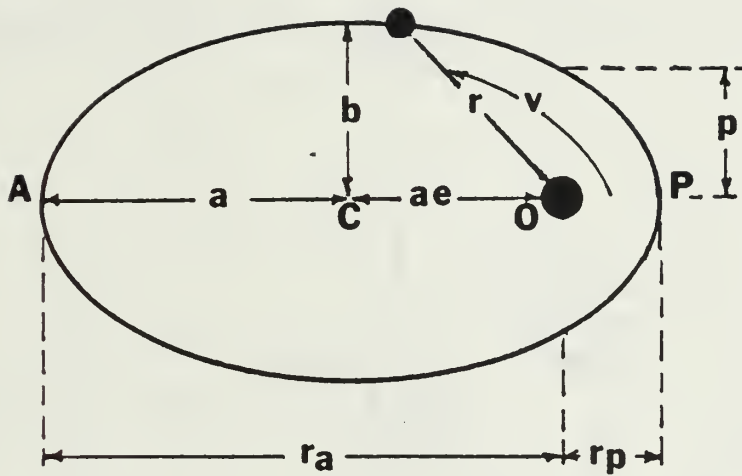


Figure 1. The Elliptical Orbit

A: the apogee (point farthest from the focus).

P: the perigee (point closest to the focus).

No real orbits occur in just two dimensions. To describe real orbits a third dimension must be added. A suitable reference must also be chosen. One of the most convenient reference frames is the geocentric reference depicted in Figure 2. In this system a fixed nonrotating earth forms

the center of the celestial sphere. The earth's projected north pole, south pole, and equator become the north celestial pole (NCP), the south celestial pole (SCP), and celestial equator respectively.

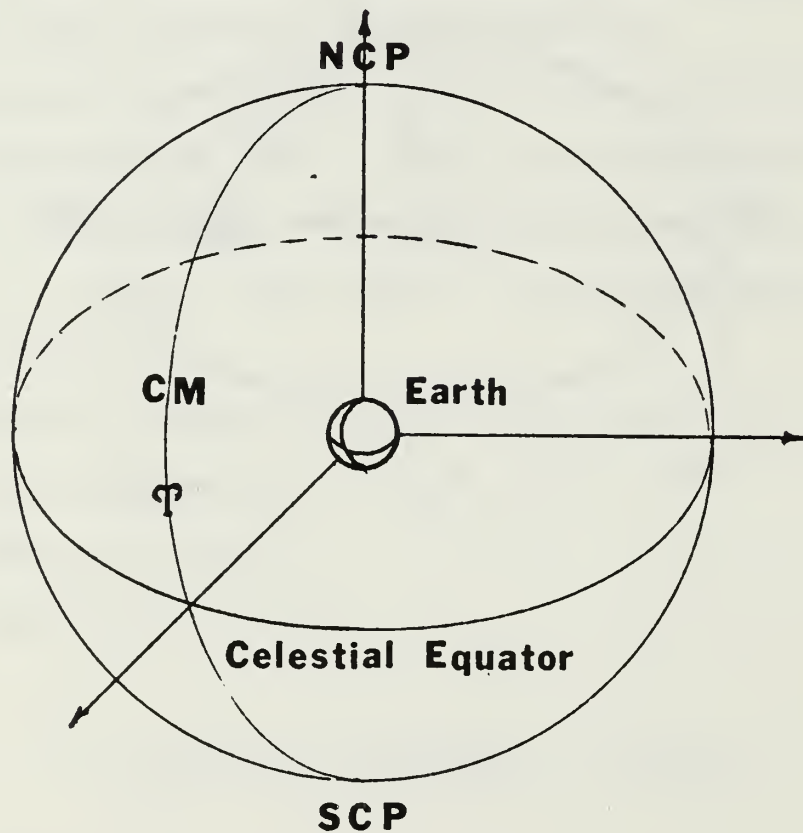


Figure 2. The Geocentric Celestial Sphere

To account for the apparent motion of the celestial sphere as viewed from the earth, a reference point on the celestial sphere must be chosen. Traditionally this has been the First Point of Aries, describing the constellation



where the vernal equinox occurred when the celestial reference was defined. The vernal equinox does not now occur in the constellation Aries. Tradition still uses the first point of Aries as the Celestial Meridian (CM) of reference. Figure 3 illustrates the vernal equinox reference. The vernal equinox is defined as the time when the sun is directly over the equator at noon in the spring.

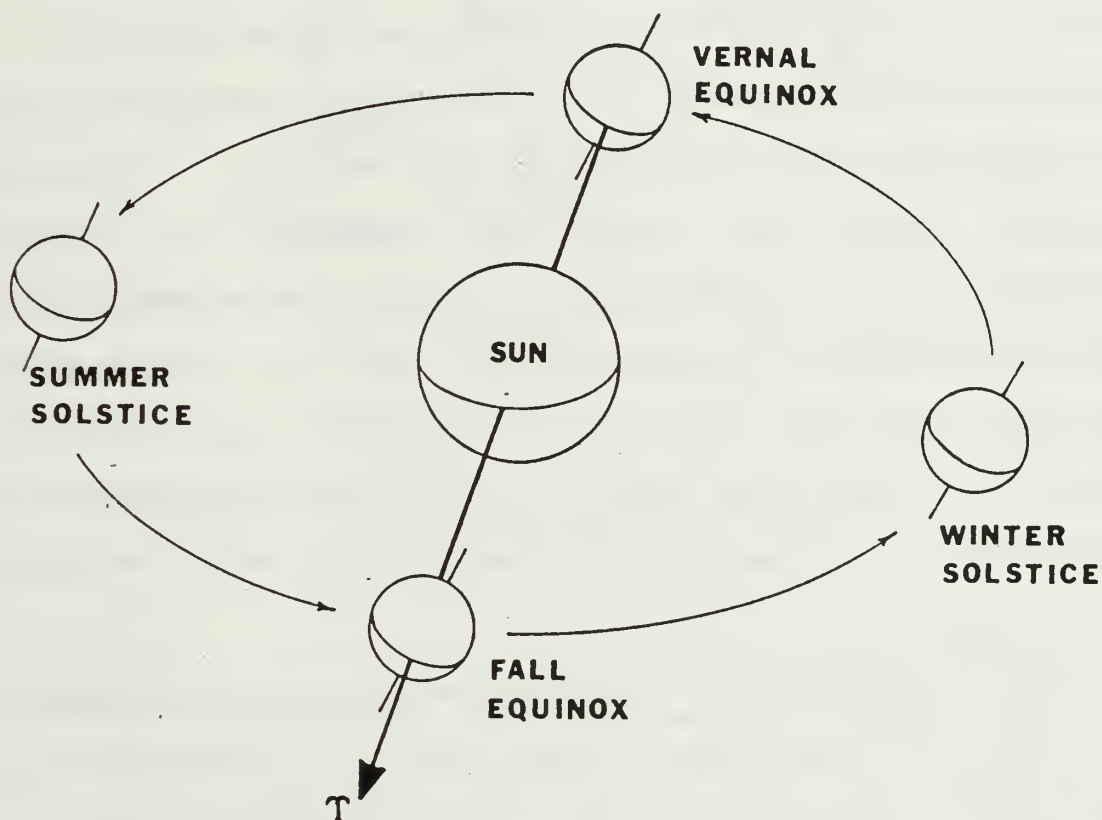


Figure 3. The Vernal Equinox

Figure 4 is a representation of an orbit in real space using the geocentric system. The points where the projection of the satellites orbit on the celestial sphere crosses the celestial equator are called the nodes of the orbit. The ascending node (N) is where the projected orbit crosses the celestial equator heading for the north celestial pole. The descending node is where the projected orbit crosses the celestial equator heading for the south celestial pole. The angular measurement from the reference celestial meridian to the ascending node along the celestial equator is called the longitude of the ascending node, and usually given the symbol  $\Omega$ . The angular measurement from the ascending node to the point of perigee (P) along the projected orbit is called the argument of perigee, symbolized by  $\omega$ . Both the longitude of the ascending node and the argument of perigee range from 0 to 360 degrees. The angle from the plane of the celestial equator to the plane of the projected orbit is called the inclination and denoted by  $i$ . Values for the inclination range between 0 and 180 degrees.

Inclinations of 0 and 180 degrees are termed equatorial. In equatorial orbits the longitude of the ascending node is not defined. Orbits with an inclination of 90 degrees are called polar. Prograde orbits are those with an inclination of between 0 and 90 degrees and retrograde orbits have an inclination range of 90 to 180 degrees.

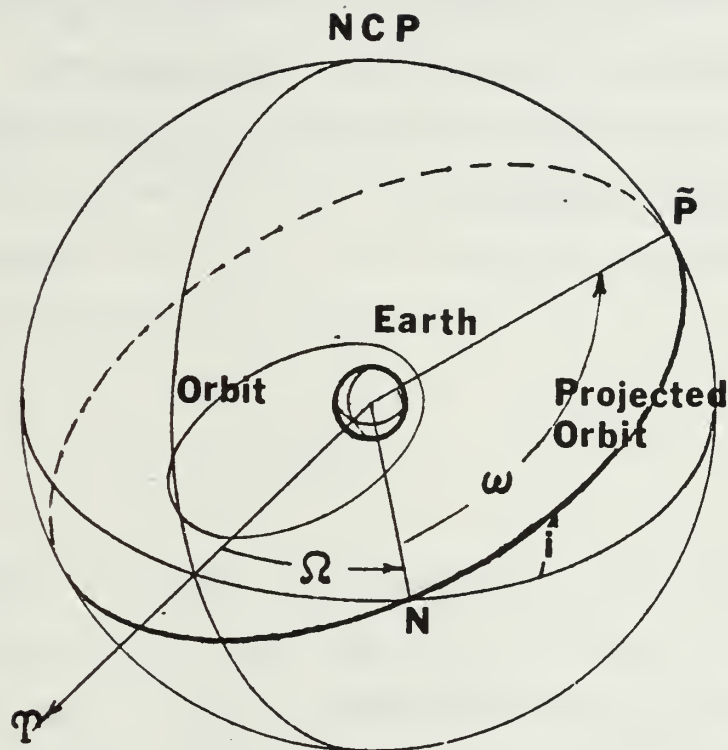


Figure 4. A Geocentric Orbital System

Historically, it was difficult to tell much about the orbit specific parameters from the earth vantage point. However, a value that could be measured was the time for one complete orbit. If the radius vector moved uniformly along the projected orbit with the average rate of mean motion  $n$  ( $n$  is also referred to as the mean angular velocity) at an epoch  $T$ , it would be at a position  $M$  called the mean

anomaly. The mean anomaly has a range of 0 to 360 degrees. It is measured from the perigee along the projected orbit. The mean anomaly corresponds to positions on the orbital ellipse. An eccentric anomaly ( $E$ ), is defined as the angle between the projected position and the point of perigee subtending at the center of the ellipse. Figure 5 illustrates eccentric anomaly.

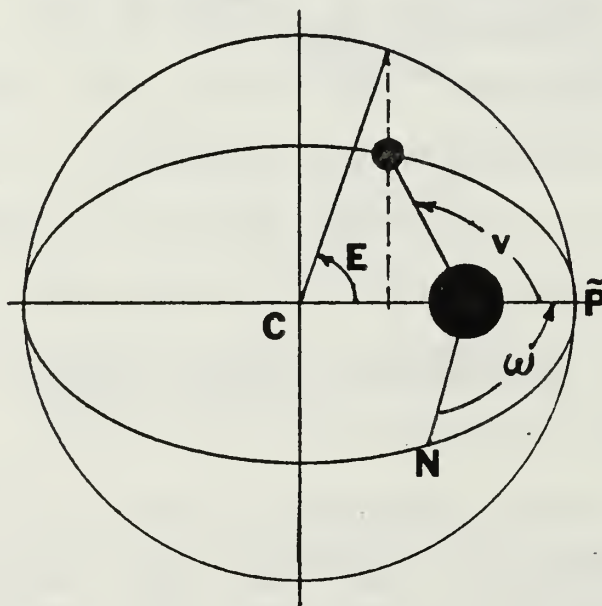


Figure 5. Orbital Anomalies



The difference between the eccentric anomaly and the mean anomaly is important. The mean anomaly is a mathematical concept corresponding to an imaginary position of a satellite past the perigee if it moved at an average angular velocity. The eccentric anomaly is the actual projected angular position of a real satellite on the celestial sphere. The eccentric and mean anomalies are equal in circular orbits ( $e = 0$ ). The eccentric and mean anomalies are related by Kepler's equation:

$$M = E - e \sin E \quad (6)$$

The solution to model (6) has been the source of much investigation. By a solution it is meant for a given  $M$ , determine  $e$  and  $E$ . In 1817 Friedrich Wilhelm Bessel, 1784-1846 invented Bessel functions to provide an infinite series approximation for the solution of the model (6). Newton developed a converging algorithm for its solution. The mass decrement submodel of the propellant longevity model uses Newton's method for the solution of Kepler's equation.

All anomalies are concerned with the measurement of the position of a body in orbit. All anomalies are measured angularly from the point of perigee in the orbital plane, and vanish at perigee.

When  $e$  and  $E$  have been found from Kepler's equation (6), then using the equations for an ellipse in Taff [Ref. 2:p.

67], the remaining elliptical parameters can be solved for when any one of  $a$ ,  $b$ ,  $r_p$ , or  $r_a$  is known.

The minimum number of parameters needed to describe an orbit is called an orbital element set. Five parameters are needed to describe an orbit. One more is needed to position an object in the orbit. Many orbital element sets have been used and are in use. The classical orbital elements are:

semi-major axis ( $a$ )

eccentricity ( $e$ )

inclination ( $i$ )

longitude of the ascending node ( $\Omega$ )

argument of perigee ( $\omega$ )

time of perigee passage or epoch ( $T$ ).

The Keplerian set replaces the time of perigee passage with the mean anomaly ( $M$ ). The orbital element set used in the mass decrement submodel is the Kozai mean element set, very similar to the Keplerian set. The name "Kozai mean element set" refers to the Kozai perturbation approximations used to solve for the Keplerian orbital element set. The perturbation theory approximation of Y. Kozai is discussed later.

Up to now all orbital considerations have been limited to the classical two-body problem. The two body problem limits the forces on the orbiting body to the gravitational force. The two-body problem also requires all masses be concentrated at a single point. A real earth satellite

experiences many forces resulting in many discrete accelerations. The theory of perturbations was developed to account for the motion of real satellites.

In perturbation theory the original orbit, with only the point-mass gravitational acceleration, is called the osculating orbit. Orbital elements describing the osculating orbit are the osculating element set. The osculating orbit is then adjusted periodically to account for the action of all the nonpoint-mass gravitational accelerations.

Accelerations result from forces. Examples of perturbing forces on an earth satellite are: oblate earth gravitational, atmospheric drag, sun gravitational, moon gravitational, solar radiation pressure, and satellite motor thrust.

To remain in a closed orbit, the point-mass gravitational force must be the dominant force on the satellite. For low earth orbit satellites, the oblate earth gravitational force is the next greatest force and is termed the dominant perturbation. Satellites below 600 kilometers in altitude experience an atmospheric drag force of the same order of magnitude as the oblate earth force. The atmospheric drag and oblate earth effects are so large for low earth orbit satellites that the effects of the other perturbations (except motor thrust) are lost in the background error.

Central to the problem of perturbation theory is the that the three body problem has never been solved mathematically in general closed form. Most modern approximations involve power series or Legendre polynomial expansions. The state of the art in orbit perturbation prediction only uses only the first-order terms of these expansions, termed first-order effects. An exception is a theory advanced in 1959 by Y. Kozai. His approximations are computationally efficient and allow for the use of more of the oblate earth effects (called J2, J3, and J4 terms and discussed later). Kozai's theory is flawed in the higher-order terms due to the introduction of mathematical singularities. Nevertheless, proponents for its use argue that it does work and predicts the oblate earth effects to a reasonable degree of accuracy. The mass decrement submodel of the propellant longevity model presented in this thesis uses Kozai's theory.

The gravitational potential parameter  $u$  was presented as singularly determining the gravitational potential in the earlier development of the gravitational acceleration model. In earth systems, the gravitational potential is a complex function of the earth's mass distribution.

The earth is not a point mass. Neither is it a homogenous sphere. It's true mass distribution is complex. The real distribution of matter on the earth forms a body



termed the geoid. This geoid determines exactly the gravitational potential function.

The determination of the geoid is based on ground and satellite measurements. Many military programs depend on the precise position of a point on the surface of the earth. The military has led the way in geoid determination in the past two decades.

Geoidal studies reveal important facts about the aspherical shape of the earth. A fluid spinning sphere should exhibit a bulge at the equator and flattening at the poles. This is termed **oblateness**. The oblate deviation is the dominant deviation for the earth as a sphere. Measurements of the earth's oblateness indicate that it is more oblate than the current spin rate could produce by itself. This excess oblateness indicates two factors: the earth's core is more solid than previously thought, and the earth's spin has slowed.

The earth deviates in other ways from being a sphere. Since all deviations can be expressed in terms of sines and cosines they are referred to as **spherical harmonics**. Harmonics are divided into categories. **Zonal harmonics** are symmetric about the earth's spin axis and are not longitude dependent. **Sectorial harmonics** are only longitude dependent. Harmonics dependent on both longitude and latitude are termed **tesseral**. Odd numbered harmonics are antisymmetric about the equatorial plane; even numbered



harmonics are symmetric about the equatorial plane. Harmonics are also classified by number. The number refers to the subscript of the J coefficient (defined later).

Bate et al., [Ref. 3], offers a simplified development of the gravitational potential function. If the gravitational potential function  $\Phi$  of a geoid is known, the acceleration due to this gravitational function is modeled by:

$$\vec{r}'' = \nabla \Phi \quad (7)$$

One common expression for the gravitational potential or geoid function  $\Phi$  is:

$$\Phi = \frac{u}{r} \left[ 1 - \sum_{n=2}^{\infty} J_n \left( \frac{r_e}{r} \right)^n P_n \sin L \right] \quad (8)$$

In this model  $u$  is the gravitational potential parameter,  $J_n$  is an experimentally determined J coefficient,  $r_e$  is the radius of the earth,  $P_n$  is a Legendre polynomial of order  $n$ ,  $L$  is the geocentric latitude, and  $r$  is the radius of the satellites position. Taking the gradient of the potential function yields an expression for the acceleration due to the gravitational potential. Bate et al., [Ref. 3:pp. 419-423] details the resultant potential induced acceleration to the first seven terms.

Recent studies have determined the geoid function out through the J44 term. Values used by the mass decrement model by the subroutine GEOP are  $1082.76 \times 10^{-6}$ ,  $-2.55 \times 10^{-6}$ , and  $1.56 \times 10^{-6}$ , for the J2, J3, and J4 terms respectively. The J2 and J4 terms are even numbered, and refer to even harmonics symmetric about the equator. The J3 term is odd numbered, and refers to odd harmonics which are antisymmetric about the equator. The J2, J3, and J4 terms are all zonal.

Current perturbation theory expresses  $\Phi$  to the J2 term. The theory advanced by Kozai in 1959 appears to use the J2, J3, and J4 coefficients in a first-order perturbation theory approximation (because singularities occur in terms higher-order than J2). Taff [Ref. 2:pp. 332-342] takes strong exception to the theory.

The subroutine GEOP in the propellant longevity model uses Kozai's theory to calculate the geoidal effects on orbital parameters through the first three zonal coefficients (J2, J3, and J4 terms). Their effect is calculated once each orbital revolution, and the Kozai mean element set is adjusted accordingly. While using the model, it is important to understand that as the altitude of the satellite decreases, The aspherical earth perturbations become much greater. The orbital element drift due to the aspherical earth is thus much faster in lower altitude orbits.

In summary, the computer program of the propellant longevity model uses three orbital element sets in a geocentric reference. The input orbital element set is the Brouwer mean element set of the Naval Space Surveillance System (NAVSPASUR)<sup>1</sup> system. Chapter III and Appendix A explain the input elements in detail in the input description. The Brouwer mean elements are first converted into a Brouwer osculating set. These osculating orbital elements are then transformed into a Keplerian-like Kozai mean set. Half of the computer program of the propellant longevity model transforms the Brouwer mean element set into the Kozai mean set. These element set transformations are used to prepare real-world orbital element sets for use in the propellant longevity predictions. Once the computer program has solved for the Kozai mean element set all perturbation effects result in adjustments to the Kozai mean set. Adjustments are made once per revolution.

#### B. THE ATMOSPHERE MODEL

Central to the validation of any model is an understanding of the system to be modeled. The model under investigation determines the propellant longevity for low earth orbital satellites doing in track micro-thrusting to

---

<sup>1</sup>The NAVSPASUR system publishes a semiannual report on the 1000+ orbiting objects they track in The Satellite Situation Summary. The orbits are described in a five card, 80 column, Fortran style input format. The report is available on request from the Commanding Officer, Naval Space Surveillance System, Dahlgren, Virginia.

overcome the effects of atmospheric drag. The fuel required by a particular rocket motor on a satellite to perform a known amount of work can be computed from the rocket equation. The problem occurs in computing the amount of work required.

To compute the required work by the satellite propulsion system to overcome atmospheric drag requires knowledge of the atmospheric environment of the satellite. For low earth satellites the atmospheric environment is the thermosphere. The physics of the thermosphere is discussed in this section. Before discussing the thermosphere, some preliminary thermospheric properties are presented.

For low earth orbital satellites, the drag-induced change in the orbital elements is significant. The oblate earth (referred to as the "J2 term") orbital perturbation is normally the dominant perturbation term. The perturbations due to drag are of the same order of magnitude as those due to the oblate earth for orbits below 600 kilometers.

The drag force caused by the satellite moving through the atmosphere always acts against the motion of the satellite. Neglecting the lift effects due to the satellite's shape and attitude, the drag force causes work to be done on the atmosphere by the satellite.

From Bate et al., [Ref. 3:pp. 15-16] a satellite in orbit has a constant specific mechanical energy  $\xi$  given by



$$\xi = \frac{v_t^2}{2} - \frac{u}{r} \quad (9)$$

where  $\xi$  is the mechanical energy per unit mass,  $v_t$  the satellite speed,  $u$  the gravitational potential constant, and  $r$  the radius of the orbit.

The above model says that the mechanical energy per unit mass of a body in an an-atmospheric, two body, circular orbit is the sum of its kinetic energy per unit mass and gravitational potential energy per unit mass.

Conservation of energy requires that the work done on the atmosphere by the satellite must reduce the orbital energy of the satellite. The differential element of work done on the atmosphere by the satellite results in a differential reduction in the specific kinetic energy of the satellite. Assuming the specific mechanical energy is a constant, the radius,  $r$ , of the orbit must therefore decrease. As the radius decreases, the velocity tends to increase in order to maintain the an-atmospheric conservation of specific mechanical energy.

In non-circular (real elliptical) orbits, the atmospheric effects are greatest at perigee (Figure 1). Orbital mechanics requires a differential reduction in orbital velocity at perigee to result in a reduction in the semi-major axis and orbital eccentricity. The major effect of transatmospheric satellite motion is to reduce the semi-major axis and the eccentricity of the elliptical orbit.



Taff [Ref. 2:pp. 352-353] develops the mathematical equations for the drag-induced changes in the semi-major axis, eccentricity, argument of perigee (Figure 4), and mean anomaly (Figure 5). The changes in the argument of perigee and the mean anomaly are shown to be periodic. The net effect on the orbit due to atmospheric drag is to circularize the orbit closer to the earth, with little change to the other orbital elements.

An accepted model for the magnitude of the drag force as presented in Taff [Ref. 2:p. 352] is:

$$F_D = \frac{A \rho C_D}{2m} v_{rel}^2 \quad (10)$$

In this equation,  $F_D$  is the drag force magnitude,  $A$  the effective satellite cross-sectional area,  $C_D$  the drag coefficient,  $m$  the satellite mass,  $\rho$  the atmospheric density, and  $v_{rel}$  the velocity of the satellite relative to the atmosphere.

The upper atmosphere is dynamic. The changes that must be modeled to achieve a valid prediction for the drag force are those that effect the drag force factors. The factors in the drag force model that are dependent on the atmosphere are density, a drag coefficient (dependent on satellite physical and fluid-flow characteristics), and the relative velocity of the satellite in the atmosphere.

To model the atmospheric effects on density, drag coefficient, and relative velocity, some background in upper atmosphere physics is needed. The descriptive presentation here is carefully developed to be relative to the above three drag force dependent factors. A more comprehensive treatment of atmospheric physics can be found in a work of Fleagle [Ref. 4]. An excellent technical treatment of thermospheric dynamics can be found in the works of Jacchia [Refs. 5,6,7].

Jacchia formulated the most widely used thermospheric model currently employed by professional orbital analysts (known as the Jacchia J60 model or simply J60). His latest comprehensive empirical thermospheric model (Jacchia J77 or J77) is many orbital analysts' preferred refinement for modeling the atmosphere.

The Jacchia J77 model is highly tabular, uses considerable computer time, and requires an extensive input file. However, these negative aspects are balanced by the orders-of-magnitude increase in accuracy of density predictions. Jacchia [Ref. 7:p. 2] presents a table of residuals for predicted versus observed densities for various satellites, as well as time intervals for the Jacchia J77 atmosphere model. All density residuals are much smaller than those produced by exponential models in the same time intervals. When extremely accurate density predictions are required in some submodel, the use of the

Jacchia J77 atmosphere model may well be worth the additional computer time and expense.

A simple model of the atmosphere considers it as a homogeneous mass of constant density. A refinement is made by modeling the density as decreasing exponentially with altitude. The exponential model predicts pressure and density will fall one tenth for every ten kilometer increase in altitude. Prior to 1960 this exponential model was used extensively for upper air calculations involving meteor trails. With the advent of low earth orbital satellites, a greater degree of accuracy in predicting atmospheric effects is required. The predicted satellite decays from the exponential model are very different from the observations. The Jacchia J60 atmosphere model was formulated to improve decay predictions. It was based on measurements from high altitude balloons, sounding rockets, and ground stations.

The atmosphere is divided roughly into concentric shells, each with specific properties. The properties used in this subdivision are after Fleagle. [Ref. 4]

From the early days of atmospheric studies, temperature and moisture have been recorded. The division system described by Fleagle [Ref. 4] is based primarily on a height versus temperature profile.

The height versus temperature profile is graphed in Figure 6. The temperatures and altitudes are those of the 1975 U.S. standard atmosphere. This temperature behavior

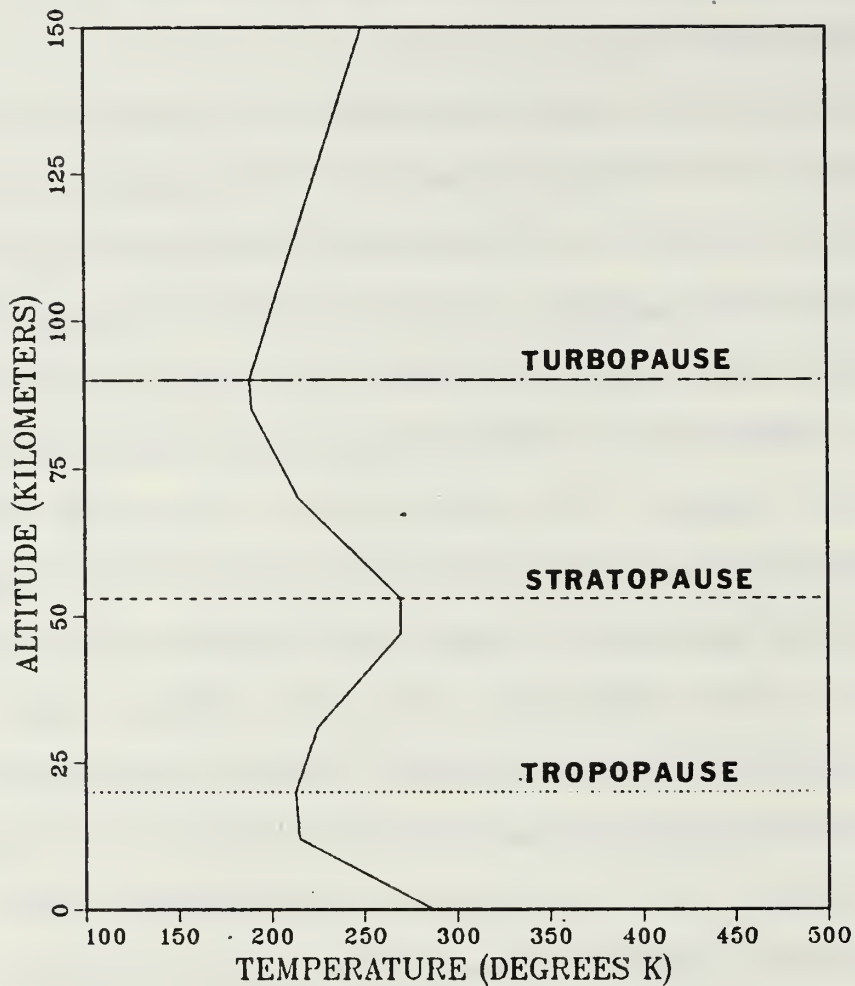


Figure 6. Atmospheric Temperature Profile

approximates general conditions (large transient variations have been observed). Figure 6 also shows the boundaries between concentric shells, called pauses. The following description of the atmospheric layers is presented in Fleagle [Ref. 4:pp: 79-84].

The region of the atmosphere closest to the earth is the troposphere and contains eighty percent of the atmospheric



mass. This region is characterized by near linearly decreasing temperature with altitude. The dynamics are due to earth surface energy transitions. All of the earth's weather occurs in this region. The height of the troposphere is variable and depends on both latitude and season. Along the equator the maximum altitude is 16 to 18 kilometers. At the poles the troposphere is highly seasonal, being nearly absent during the winter months and extending to eight to ten kilometers in the summer. Capping the troposphere is a region of constant temperature with altitude, called the tropopause.

Next in the series of atmospheric layers is the stratosphere. The stratosphere is characterized by linearly increasing temperature with height. The physical dynamics are due mainly to the absorption of solar ultra-violet radiation by the ozone. The maximum altitude of the stratosphere is about 50 kilometers where it is capped by an area of local maximum temperature termed the stratopause.

Above the stratopause is the mesosphere. This atmospheric layer exhibits linearly decreasing temperature with height. The energy physics of the mesosphere are not well understood. Bulk mixing of the gasses still dominates diffusion as thermodynamic processes. Any molecular dissociation of atmospheric molecules produced by radiation absorption is rapidly consumed by chemical recombination of



these dissociated species. The mesosphere is topped by the turbopause at an altitude of about 90 kilometers.

Above the turbopause the gross physics of the atmosphere changes drastically. This region is the environment of all current low earth orbit satellites. Termed the thermosphere, it extends from the turbopause to an altitude of 1000 to 2500 kilometers. Here bulk molecular mixing is dominated by diffusion. Lighter gasses diffuse upwards and heavier ones remain at the lower altitudes. Disassociation of molecular species becomes increasingly important, this results in an increase of individual atomic species. Standard flow equations (Navier-Stokes) are extremely difficult to apply, and physical descriptions are more discrete (quantum mechanical). Flight by flow-supplied lift is not possible. The standard methods of computing drag coefficients do not apply. The ideal gas approximation is also not valid ( $P*V = n*R*T$  does not apply). Above the turbopause, density is an increasing function of temperature. Only about one millionth of the atmosphere remains above the tropopause.

The stratification of gaseous components in the thermosphere is significant. The drag coefficient has been shown to be composition dependent. Thus, as the gaseous composition changes the drag coefficient must be adjusted to reflect the observed drag-induced orbital decays (Jacchia [Ref. 7]). Figure 7 shows the dominant atmospheric species

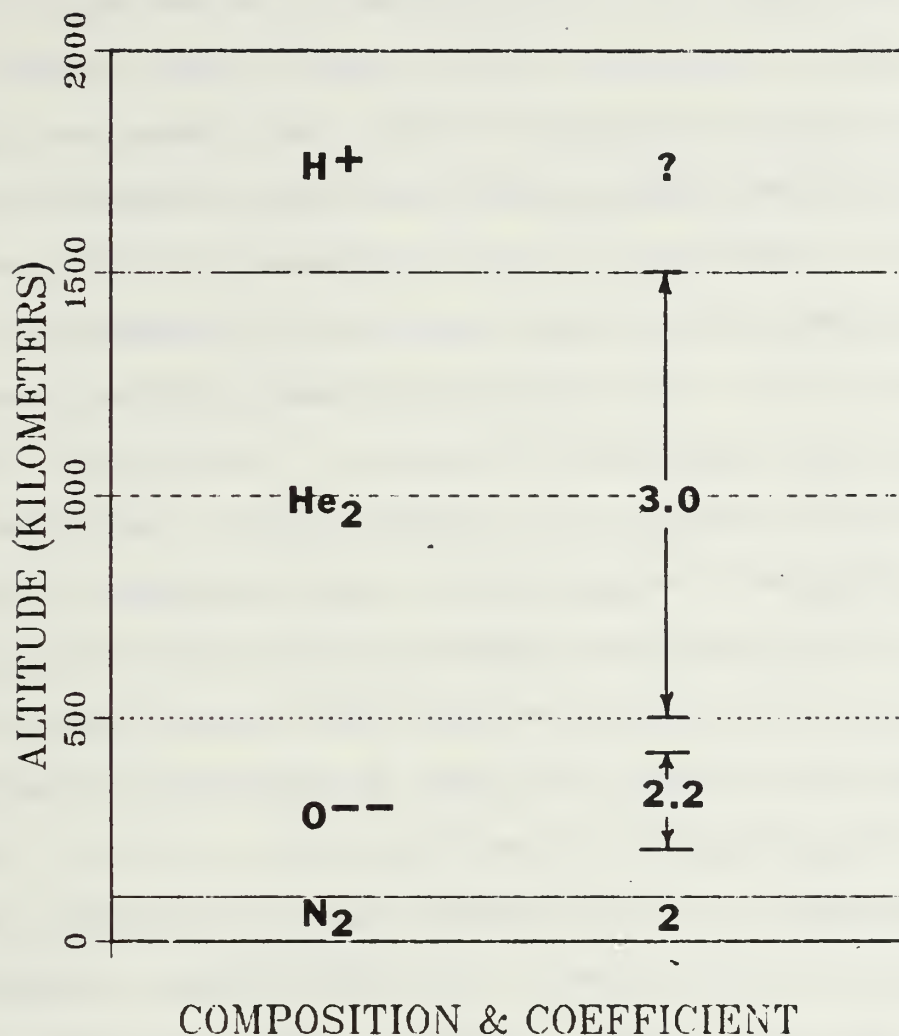


Figure 7. Atmospheric Composition

by altitude with the accepted drag coefficients. The drag coefficients are predictions obtained analyzing the drag coefficient needed to produce the observed drag effects on orbital decay for a satellite at a particular altitude. Thus the drag coefficient is a proportionality constant in the drag force model.

For altitudes below 110 kilometers, molecular nitrogen is the main atmospheric gas. Above this region the dissociation of the molecular oxygen by ultra-violet light absorption causes atomic oxygen to become increasingly the main gaseous constituent. At an altitude of 500 kilometers, helium replaces atomic oxygen as the main atmospheric gas. At altitudes above 1500 kilometers atomic hydrogen becomes the dominant gas (see Figure 7).

Traditional research has assigned a drag coefficient of 2.20 to altitudes between 200 and 400 kilometers. As the altitude of the satellite increases above 500 kilometers, corresponding to satellite movement through helium, a drag coefficient of at least 3.00 must be assigned to maintain agreement with observation (see Figure 7).

Jacchia [Ref. 7] lists the observed variational changes in density and composition in the thermosphere. They are the two component solar activity related, semiannual, diurnal, seasonal latitudinal, and geomagnetic.

The two component solar thermospheric variations are consequences of changes in solar ultra-violet (EUV) flux. The EUV flux changes periodically due to two solar cycles. These are the 27 day rotational or disk cycle and the 11 year sunspot or active area cycle.

EUV flux is not measurable from the ground due to almost complete absorption in the atmosphere. Empirical evidence has suggested a strong parallel of the EUV flux and the

ground measurable 10.7 centimeter flux (F10.7) which has been used in some successful thermospheric models. The Jacchia 1960 model used the 10.7 centimeter flux as an input to model thermospheric density resulting in an improvement of decay predictions over the exponential model. (Indeed, it is only recently that there has been a requirement for greater accuracy in drag predictions.)

The thermosphere responds to increased EUV flux by absorbing more energy, causing increased heating. This increased heating causes an increase in temperature and density. The thermospheric response to changes in the EUV flux is nonlinear. Increases in EUV flux due to disk (rotational) effects produce more thermospheric heating than a like increase in flux due to active area effects. However, Jacchia noticed in 1973 that the disk component of the EUV flux can be linearly related to an average 10.7 centimeter flux. He recommends using a 71 day average corresponding to three solar rotations [Ref. 7]. Tables for the 10.7 centimeter flux have been developed.<sup>2</sup> The Jacchia 1977 atmosphere incorporates the average 10.7 centimeter flux as an input, used as an indicator of the thermospheric heating capacity of the sun's radiation.

---

<sup>2</sup>Orr [Ref. 8:Appendix B] lists values compiled and predicted by the NASA Marshall Space Flight Center. Values range from a minimum of 73.3 to a maximum of 242.9. The units for the 10.7 centimeter flux are  $10^{-22}$  watts/meter<sup>2</sup>/Hz.



The semiannual temperature and density variation has been modeled in many ways. Jacchia [Ref. 7:pp. 47-50] fits a modified harmonic empirical model to the biannual, sinusoidal cycle of observed density. Maxima occur in April and October. The Jacchia 1971 and 1977 models for the semiannual density variation are based on observations of 12 years of satellite data. The observed density variations are thought to be a consequence of the earth-sun orientation. The mechanism for the observed effect is unknown, but may be related to the maximum equatorial heating at the equinoxes. Equinoxes (sun at maximum altitude over the earth's equator) occur in late March and September. Figure 8 illustrates the semiannual bulge in temperature and density observed just after the equinoxes. Due to the earth's oblation, the bulk mass of the atmosphere is concentrated at the equator. The most direct exposure of the equatorial atmosphere occurs at the equinoxes. The temperature and density thus peak shortly after periods of maximum heating.

Seasonal-latitudinal thermospheric variations are again earth-sun orientation related. Variations in density and composition are dependent on the season and latitude. The Jacchia 1977 model fits modified harmonic empirical models to observed data. The seasonal latitudinal variations interact strongly with the semiannual variation, complicating the modeling. The winter helium bulge is the best known



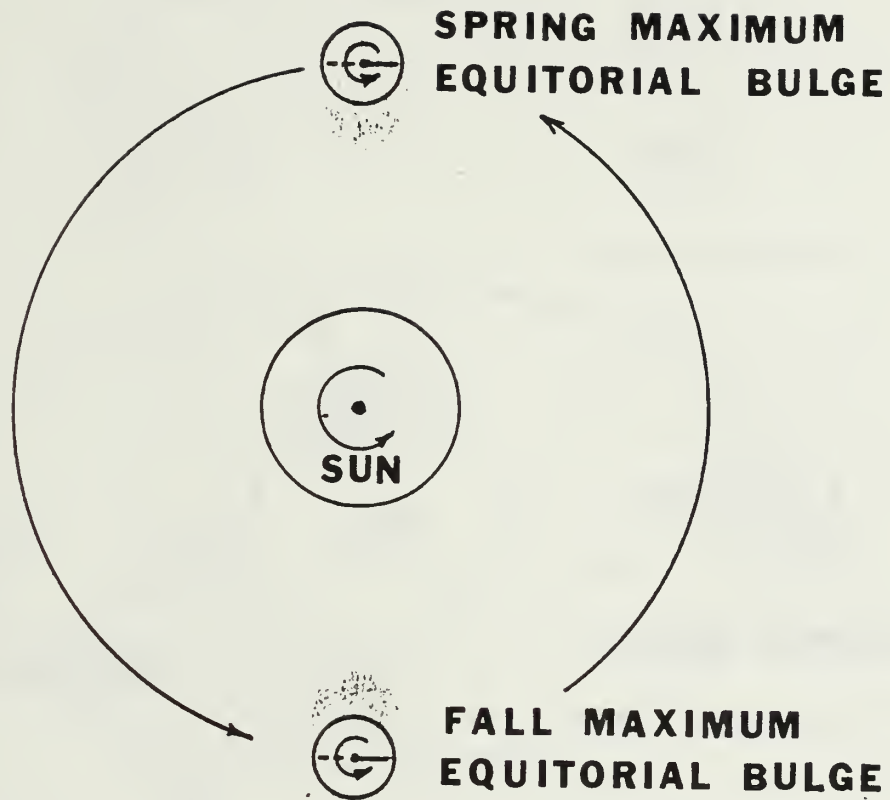


Figure 8. The Semiannual Atmospheric Density Bulge

effect of this variational factor. Figure 9 shows the general shape change of the temperature and density bulge with season. Note that during the June solstice the bulge is centered at about 45 degrees north latitude whereas during the December solstice the bulge is centered at about 45 degrees south latitude.

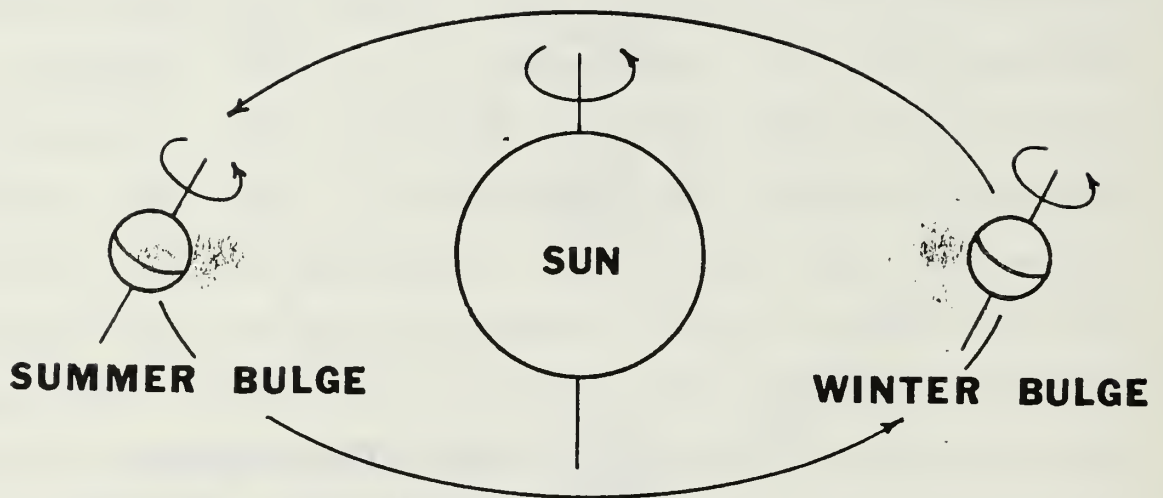
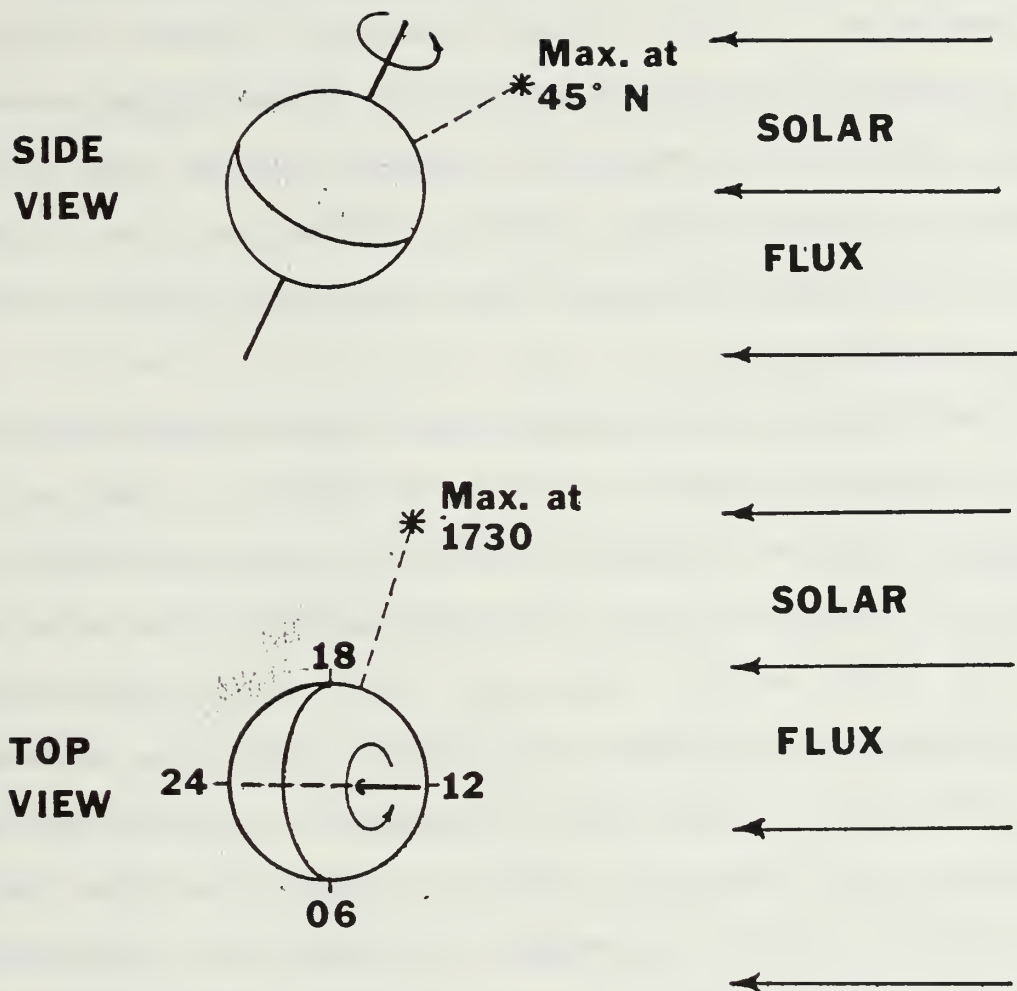


Figure 9. The Seasonal-Latitudinal Atmospheric Density Bulge

The diurnal bulge is shown in Figure 10. It is caused by the daytime heating of the side of the atmosphere facing the sun. Lagging the actual (most direct) solar exposure by about four hours, the heated side shows a marked increase in temperature and density. Many current models track and predict the position of the diurnal bulge.



## EARTH AT SUMMER SOLSTICE

Figure 10. The Diurnal Atmospheric Density Bulge

Geomagnetic heating of the thermosphere is not well understood. At times of high geomagnetic activity (corresponding to an index of 7) large heating effects are produced. The combined effects of geomagnetic and EUV heating can produce changes in density of three orders of magnitude at 600 kilometers (Jacchia [Ref. 5:p. 82]).

In summary, the thermosphere is a very dynamic region of the atmosphere. Many of the observed changes require further research to complete analytical models. The current modified exponential empirical models can be orders of magnitude in error in their density predictions. At higher earth orbits orders of magnitude error in density is of little consequence.<sup>3</sup>

The model chosen for density and compositional effects in the atmosphere depends on the importance of the short-term cyclic effects. Computations for orbits of months in duration and less than 600 kilometers in altitude will be subject to large errors using the simple empirical models (Jacchia 1966). For these short missions the more accurate Jacchia 1977 model seems more appropriate. (Performance of the Jacchia 1977 empirical model has been remarkable with density errors rarely exceeding two percent.) Missions lasting for decades may be able to use the computationally more efficient Jacchia J60 model to predict very long term drag effects.

The one drag force dependent factor not yet discussed is the satellite-to-atmosphere relative velocity. This relative motion is influenced by three gross factors: local

---

<sup>3</sup>Above 800 kilometers the drag term in the orbital decay model used by the Satellite Control Facility in Sunnyvale, California is very small. Its main function is a catch-all for errors in other perturbing terms.

winds, satellite tangential velocity, and atmospheric rotation.

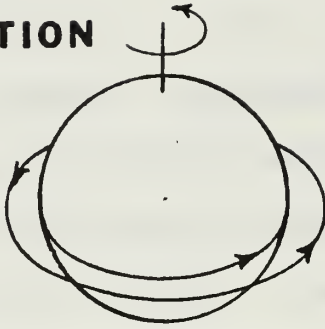
Thermospheric wind has not been measured. Mesospheric wind has been measured based on the observation on meteor trails. Fleagle [Ref. 4:p. 82] reports mesospheric winds exceeding 0.150 kilometers per second. This may sound large, but must be compared with the satellite's velocity (which is on the order of 10 kilometers per second).

Satellite tangential velocity is a major factor in the satellite-to-atmosphere relative velocity. When combined with the rotating atmosphere it accounts for the bulk of relative motion.

Most earth orbit calculations simplify computation of perturbation-induced changes in the orbital elements by assuming a fixed earth. When considering drag a non-rotating earth assumption can lead to a severe error. The earth is not fixed. The atmosphere is pulled along with its rotation, and lags the earth rotation by a small fraction. Figure 11 shows the rotating atmosphere effect. For low inclination (prograde) orbits the atmosphere is actually following the satellite. In high inclination (retrograde) orbits the atmosphere is moving against the satellite. When comparing a typical 16 revolution per day satellite tangential velocity in a prograde atmosphere to the same satellite in a retrograde atmosphere, a 15 percent variation in relative velocity can occur. This is compared to the

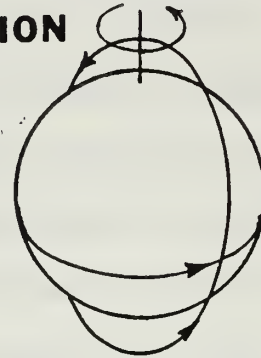


**SAME  
ROTATION**



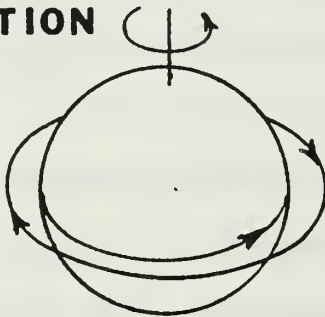
**PROGRADE ORBIT**

**PERPENDICULAR  
ROTATION**



**POLAR ORBIT**

**OPPOSITE  
ROTATION**



**RETROGRADE ORBIT**

**Satellite to Atmosphere**

**Relative Rotation**

Figure 11. Orbital Inclinations in a Rotating Atmosphere

unknown (but probably less than two percent effect) of atmospheric winds.

A model used by Parks [Ref. 1:p. 4] to account for the rotating atmosphere separates the relative velocity of the satellite in relation to atmosphere into two parts. The model is given by:

$$v_{rel} = v_t \sqrt{\delta} \quad (11)$$

Here  $v_{rel}$  is the satellite to atmosphere relative velocity,  $v_t$  is the satellite tangential velocity, and  $\delta$  is a factor accounting for orbital orientation (inclination) with respect to a rotating atmosphere (see Figure 11).

Equation 11 in Parks [Ref. 1:p. 4] models the inclination factor in the following way:

$$\delta = \left[ 1 - \left( \frac{r_p}{v_p} \right) \Lambda \omega_e \cos i \right]^2 \quad (12)$$

In this model,  $\delta$  is the rotation factor,  $r_p$  the radius at perigee,  $v_p$  the satellite velocity at perigee,  $\omega_e$  the earth's angular rotation rate (assumed constant),  $i$  the orbital inclination, and  $\Lambda$  the ratio of rates of rotation of the atmosphere to the earth's rotation.

The model for  $\delta$  used in the propellant longevity model neglects the effect of the atmospheric wind, but this should introduce only a small error. Recent atmospheric work, Jacchia [Ref. 7], suggests a significant gravity wave induced motion in the upper atmosphere. As more experimental information on this bulk motion becomes available, the incorporation of the gravity wave wind may become increasingly important.

The parameter  $\Lambda$  used by the propellant longevity model in the satellite velocity multiplier submodel is probably

not constant. Atmospheric theory suggests it may be dependent on both altitude and latitude. The range of values for the  $\Lambda$  parameter is assumed to be from a maximum of about 1.0 (at low altitudes) to a minimum of around 0.9 (at high altitudes).

The coding of the theory in NSWC TR 83-243 for satellite fuel mass decrement did not compute  $\delta$  internally. It was user supplied input in the original version. As part of the mass decrement model validation at the Naval Postgraduate School, code internal computation of  $\delta$  was added. This allows  $\delta$  to automatically adjust the satellite-to-atmosphere relative velocity  $v_{rel}$  for the results predicted by the theory as perturbation-induced changes to the inclination occur. For a long mission life that exhibits significant inclination drift, the internal computation of  $\delta$  should add accuracy to the mass decrement submodel. In place of the original user input for  $\delta$ , the  $\Lambda$  is now specified by an input file. The input file default value for  $\Lambda$  is 0.9.

A model atmosphere used for drag computations must be able to correctly predict the effects on density, drag coefficient, and satellite-to-atmospheric velocity. There are many variations in the atmosphere that affect density. The sum of all these effects creates a density bulge in the atmosphere, the location and shape of which follow maximum heating.

The drag coefficient is atmosphere composition dependent. Thus the model atmosphere must be able to predict the dominant species in the satellite environment.

Satellite-to-atmosphere relative velocity is a function of satellite tangential speed, atmospheric rotation, and orbital inclination.

The Jacchia J60 model atmosphere used in the propellant longevity model only includes the effects of diurnal heating on the density bulge. There are no computations of atmospheric composition. The newer Jacchia J77 model incorporates all the known density variations currently observed. The Jacchia J77 atmosphere also predicts thermospheric composition.

The background concepts for the propellant longevity model understanding and operation have been presented. The next chapter describes the model and its computer program.

### III. PROPELLANT LONGEVITY MODEL DESCRIPTION

This chapter describes the propellant longevity model. First, a brief summary of the model theory is presented. The second part of this chapter describes the coding of the model as installed at the Naval Postgraduate School. Finally, the third section gives the model code compiling and handling instructions specific to the system at the Naval Postgraduate School.

#### A. PROPELLANT LONGEVITY MODEL THEORY

A detailed development of the propellant longevity model is presented by Dr. Parks [Ref. 1]. The propellant longevity model hinges on the prediction of the fuel mass used by a satellite to compensate for atmospheric drag. The mass decrement submodel predicts the amount of fuel consumed after each revolution of the satellite.

The mass decrement submodel for a low-earth-orbit satellite in an oblate diurnal atmosphere is presented in Reference 1 as Equation 56. The diurnal density bulge is the only density and compositional atmospheric variation considered in the model.

The integrals of the mass decrement model (Equation 56) are next expressed in terms of Bessel functions of the first kind and order  $n$  as defined by:



$$I_n(\beta ae) = \frac{1}{2\pi} \int_0^{2\pi} \cos(nE) \exp(\beta ae \cos E) dE \quad (13)$$

Here  $I_n$  is the Bessel function of the first kind and order  $n$ ,  $\beta$  the inverse density scale height (assumed constant),  $a$  the semi-major orbital axis,  $e$  the orbital eccentricity,  $n = 0, 1, 2, \dots, 6$ , and  $E$  the orbital eccentric anomaly. All of these orbital mechanics terms were presented in Chapter II.A. The integral is to be evaluated over one revolution.

The Bessel function expansion of the mass decrement model is given in equation 58 of Reference 1. This particular expansion is central to the model. Provided accurate values for other multipliers are produced by the model atmosphere, (accurate values for atmospheric density, satellite drag coefficient, and satellite-to-atmosphere relative velocity are essential) greatly increased accuracies should result in predicting the fuel consumed to compensate for atmospheric drag. The main draw back to the use of the this type of Bessel function is the known slowness of its convergence.

## B. COMPUTER CODE DESCRIPTION

A detailed description of the model code and its input elements is contained in the code and included in Appendix A. An operational description is presented here.

The computer code calculates the propellant mass remaining together with the cumulative mission life after

each revolution of the satellite. When propellant fuel is exhausted, the computation terminates.

Computer output is available in several forms and is specified by the user through the use of some control parameters. The user can select one of two modes; standard mode or a sensitivity analysis mode. The input elements used as control parameters for output and mode control are: maximum number of revolutions ITER1, sensitivity analysis granularity PSIZE, output print frequency ITER2, mode control PSENS, anomalistic period print control IET, number of scheduled orbit adjusts NOA, scheduled orbit adjust array IRV(K), and the amount of each adjust array DA(K). These terms are discussed below.

The most basic form of output available is a tabulation of propellant remaining and accumulated mission life for 20 specified satellite-orbital initial conditions. The 20 initial conditions are specified in an input file. Accumulated mission life is expressed in modified Julian days (MJD)<sup>4</sup> and revolution number. Frequency of output printing is selectable from a maximum of once per revolution to a minimum of once per 10000 revolutions by user specification of ITER2.

A cap on runaway computer time is available by selection of ITER1. Satellites with small cross-sectional areas, high

---

<sup>4</sup>A description of the modified Julian day time measurement is in Taff [Ref. 2:p. 103]. The modified Julian day is reckoned from 0<sup>h</sup> Nov. 17 1858.

altitudes, and large amounts of maneuvering fuel can have very long orbital life-times. By defining a maximum number of revolutions to be considered in the calculations through the reasonable selection of ITER1, unnecessary expenditure of computer time can be avoided.

As part of the model verification a sensitivity analysis option was added to the program. It can be selected by setting PSENS = 1. The standard operating mode is selected if PSENS = 0. In the sensitivity analysis mode, the subroutine SNALYS creates an array of elements selected by the user to be linearly scanned from a specified minimum to maximum with a given granularity.

Granularity is specified by the selection of the control parameter PSIZE. A granularity of 1/100 (code specified as PSIZE = 100) will cause 100 executions of the propellant longevity code to complete fuel exhaustion. This specification can lead to excessive computer execution times for high altitude satellites. A granularity of 1/5 will cause five executions of the code to fuel exhaustion. However, only five iterations from a given minimum to a given maximum may be too coarse to reveal the true trend of the satellite mission life.

Each time the code is sequentially executed in the sensitivity analysis mode, the elements selected by the user for analysis are incremented linearly. The output in the sensitivity analysis mode is a table of mission lifetimes,

resulting from the initial values of input elements not selected for analysis, and the current value of the elements selected for analysis.

The output always echoes the initial input element conditions as read from a user supplied input file. Further choice of output and mode control parameters allow the user to tailor the output.

Three more input control elements allow for the specification by revolution number of up to ten adjusts to the semi-major axis. The element IRV(K) is an array whose elements specify the orbital revolution number for axis adjust. The element DA(K) specifies the amount of change in the semi-major axis in kilometers for each scheduled adjustment. Finally, NOA specifies the total number of orbital adjusts to be performed. If the user does not desire any changes to the semi-major axis, NOA must be set to 0 and no values for IRV(K) and DA(K) input to the file stream.

An additional twenty input elements must be specified by the user in the input file. Five of these are satellite physical parameters, five are atmosphere specific parameters, and ten are the Brouwer mean orbital element set of the NAVSPASUR system.

The five satellite physical parameters are: propulsion motor specific impulse (SPI in seconds), initial mass of the satellite including fuel (WT in kilograms), initial mass of



the maneuvering fuel ( $W$  in kilograms), satellite atmospheric drag coefficient ( $CD$ ), and satellite cross-sectional area ( $A$  in square kilometers).

Motor specific impulse  $SPI$  can range from 220 seconds for monopropellants to 3000 seconds for ion drives. The default value is 230.

The initial satellite mass  $WT$  depends on the satellite mission and design. A typical communications satellite has a mass of about 3500 kilograms. An SDI satellite may be considerably more massive. The default value for the satellite mass is 9100 kilograms.

Initial maneuvering fuel mass  $W$  of the satellite depends on the design life of the satellite as well as its ballistic coefficient. Low altitude satellites need at least one percent of their initial mass as maneuvering fuel if mission lives of years are to be achieved. The default value for initial maneuvering fuel is 100 kilograms.

The drag coefficient  $CD$  is a measure of the slowing power of the atmosphere on a given satellite. In the thermosphere it is very atmosphere composition dependent. A value of 2.2 has been settled on by orbital analysts for altitudes of 200 to 400 kilometers. A value of at least 3.0 must be assigned at altitudes above 500 kilometers (corresponding to the helium atmosphere). The default value for the drag coefficient is 2.2.



Satellite cross-sectional area is again very design dependent. The echo series satellites had cross-sections measuring in hundred's of square meters. Some SDI satellites may also have very large cross-sections. The default for cross-sectional area is  $50.0 \times 10^{-6}$  square kilometers, corresponding to 50 square meters.

The five atmosphere specific parameters are: atmosphere-to-earth relative rotation rate D, 10.7 cm solar flux F107 described in Chapter II, ninety-day average solar flux FBAR, geomagnetic activity index AKP, and the time of vernal equinox passage TVE.

The atmosphere-to-earth relative rotation rate D is the factor explained at the end of Chapter II. The default value is 0.9.

The decimetric solar flux and the average decimetric solar flux F107 and FBAR are again explained in Chapter II. Default values of 100 are assigned to each.

The geomagnetic index AKP is discussed in Chapter II. It ranges from 0 to 7 and is set at a default value of 2.00.

With the current atmospheric model Jacchia J60, both FBAR and AKP are read as input but not used for the density computation. As seen from a sensitivity analysis, these parameters currently have no effect on mission life. The Jacchia J77 model atmosphere uses these now stranded input parameters. The future incorporation of the Jacchia J77 atmosphere model will be able to use these input elements.

The ten NAVSPASUR orbital elements are the final input elements in the standard input file. They are all explained in the orbital mechanics section, and in the code included in Appendix A. Briefly, they are:

UJD: time of epoch in modified julian days

ETU: initial mean anomaly

GO: argument of perigee

H0: right ascension of the ascending node

ES: eccentricity

XI: inclination

AO: semi-major axis

RND: rate of change of mean motion

ESD: eccentricity decay rate

ADOT: semi-major axis decay rate.

The first seven of these are orbital elements and the final three are the results of perturbations. The NAVSPASUR orbital element set is the result of orbital measurements of actual satellites.

The final block of input in the input file is the sensitivity analysis specification array. It must be included only when the sensitivity analysis mode is specified. The array consists of 20 lines used to make up the array of elements to be scanned by the program when the sensitivity analysis mode is selected.

The sensitivity analysis specification array is divided into four columns. The first column contains the input

element variable name. These are the same names as specified in the satellite physical, atmosphere specific, and orbital elements input discussions.

The second column is a control parameter. When set to 1.0, the corresponding input element is included in the sensitivity analysis. Columns three and four are in a Fortran F16.9 format and they specify the minimum and maximum range of the element to be scanned. Defaults for the minimum and maximum have been provided in specific cases corresponding to logical and physical ranges of the input elements. In some cases zeros appear in the minimum and maximum columns. These zeros correspond to input elements not physically constrained. An example of an input element not physically constrained is the time of epoch (UJD).

If a 1.0 is entered in column two of a particular row of the sensitivity analysis specification array, that input element is included in the analysis. Any number of the input elements may be selected for simultaneous analysis. When selecting a multivariable sensitivity analysis, the user must understand the interactions of the incrementing variables and ensure that a solution exists in the mission life range being considered.

When a variable is included in the sensitivity analysis, the incrementing values override the initial conditions. All input elements not user selected for analysis (those with zeros in the second column) are reset to their initial

values after each iteration during the analysis. Appendix B contains sample input element files and their corresponding outputs.

Input elements and output forms have been explained. The program flow is discussed next. The 16 subroutines and eight functions comprising the propellant longevity model are explained in Appendix A in the Fortran code. The routine PLEP initializes the system, including inputting program control parameters and initial values for all elements. If the sensitivity analysis mode is selected, subroutine SNALYS generates the array to be scanned linearly, complete with the necessary increments for each iteration. Analysis mode causes completion of all computations to propellant exhaustion PSIZE times. The routines SNALYS and PLEP are completed only once even in analysis mode.

Program control is transferred from the initialization routine PLEP to the subroutine KOZAI, the main driver and bookkeeper of the system. The routine KOZAI first causes the NAVSPASUR Brouwer mean element set to be converted into a Keplerian (Kozai-like) mean orbital set, by calling the subroutines BRAUER, PERIOD, and MEAN.

Subroutine MEAN calls functions XSPA-XSPM to convert the Brouwer osculating elements generated in BRAUER to Keplerian orbital elements. The Keplerian elements are then returned



to the subroutine KOZAI. In standard mode the mean element set is given as output.

All of the above computations have simply conditioned the input elements to conform to the requirements of the propellant longevity model. The routine KOZAI now causes calculation of the fuel used to compensate for atmospheric drag after each revolution. The computation is continued until the fuel is exhausted or the maximum number of revolutions (ITER1) is reached. When the computation terminates, program control is transferred back to PLEP.

To calculate the drag-compensating fuel required for each revolution, KOZAI calls the subroutines PERIOD, GEOP, THRST, and DRAG.

The subroutine GEOP calculates the change in orbital elements due to the aspherical earth. It uses the J2, J3, and J4 terms in a Legendre polynomial expansion, as explained in Chapter II. Aspherical earth calculations are performed once each revolution.

The subroutine THRST checks each revolution for a scheduled orbital adjust. If a change to the semi-major axis is scheduled, it calculates the change to the axis, the argument of perigee, the eccentricity, and the mean anomaly. It also computes the amount of maneuvering fuel required to perform the adjustment. All changes are returned to the subroutine KOZAI.



The subroutine DRAG calculates the fuel mass needed to overcome the atmospheric drag. This calculation is accomplished by calling four subroutines: SOLOC, SATLOC, SALT, and JAC60.

The routine SOLOC computes the right ascension and declination of the sun for the model atmosphere diurnal density bulge. The routine SATLOC computes the right ascension, declination and geomagnetic latitude of the satellite. This is accomplished by first calling the subroutine POSVEL to calculate satellite position and velocity. The routine POSVEL in turn calls the subroutine NWTRPH to solve Kepler's equation (see Chapter II). The routine SALT computes the satellite altitude.

Atmospheric density is computed by the subroutine JAC60 based on the Jacchia J60 model atmosphere discussed in Chapter II. A maximum, minimum, and mean density that the satellite will encounter in the oblate diurnal atmosphere are calculated.

The mass decrement equation (Equation 58 of Reference 1) is contained in the subroutine DRAG. The function MMBSIR is used to perform the Bessel function expansion. The routine DRAG returns the fuel mass decrement due to atmospheric drag computation to KOZAI. The routine KOZAI then decrements the remaining fuel by this amount and checks for fuel exhaustion and maximum orbital number. If fuel is less than zero, or the current revolution number equals ITER1, calculations are

terminated and control is returned to PLEP. In standard mode, program execution now halts.

In sensitivity analysis mode, all input elements not selected for analysis are returned to their initial values, elements selected for analysis are linearly incremented, and KOZAI is again called by PLEP. The subroutine KOZAI then is executed, as previously described, with the new values for the selected elements. Upon fuel exhaustion or reaching the maximum revolution number, KOZAI terminates calculation and passes program control back to PLEP. This process continues until the elements user selected for analysis have been incremented from their minimum to maximum. When the maximum value of the elements user selected for analysis is reached, program execution terminates in the sensitivity analysis mode.

The tabular output in the analysis mode is printed line-by-line in KOZAI upon reaching fuel exhaustion or maximum revolution number. The result is a table of data, PSIZE long, that represents the linear scan of the specified elements. The first line is the mission life corresponding to the minimum value of the scanned elements. Each subsequent line represents the total mission life resulting from an increment of the elements selected for analysis and the initial conditions of the elements not selected. The final line is the mission life resulting from selected

elements at their maximum value and non-selected elements at their initial conditions.

Mission life is expressed in revolution number and modified Julian days. The last column of the tabular output in analysis mode represents the current value of the incremented input element. When more than one element is analyzed, the last column is the current fraction of scan, a real number between 0 and 1.

The tabular output can easily be converted into an input file for a graphics routine by deleting the first 98 lines of output.

### C. MODEL CODE OPERATION

This section describes the operation of the computer code at the Naval Postgraduate School on the IBM 3033 computer under VMS using the VS FORTRAN compiler.

The propellant longevity model must be compiled in the VM mode using the automatic precision increase option. If the propellant longevity code is in filename SDI and filetype FORTRAN (the filetype must be FORTRAN), the correct form for the compilation command is:

```
FORTVS SDI (AUTODBL(DBLPAD4))
```

The listing generated by this compilation takes up about 20 percent of the user's "A" disk.

Prior to program execution, the input and output files must be specified. If the input file is in filename PLEP01 and filetype DATA2, then the correct form of the command is:

#### FILEDEF 5 DISK PLEP01 DATA2 A1

This informs the computer where to look for input during execution of the model code. If hard copy of the output is desired, it can be written to a file instead of the screen by using the FILEDEF command. If the file name is SDI and the desired type is DATA, the correct command is:

#### FILEDEF 6 DISK SDI DATA A1

After execution of the propellant longevity code, the results will be in SDI DATA on the user's "A" disk.

To execute the model listing generated upon compilation, the command RUN SDI is typed (this assumes that SDI is the filename of the propellant longevity program).

This program can have very long execution times. A general rule of thumb is that execution time takes less than  $PSIZE * ITER1 / 10,000$  minutes. Roughly, the computation takes 100 microseconds for each revolution. For example, if PSIZE is 100 and ITER1 is 10,000 (corresponding to a five year lifetime) then the IBM 3033 will take 200 minutes to complete the calculations. The user must carefully choose small values of PSIZE and ITER1 on the initial investigation of elements.

The simplest graphical routine to construct plots of tabular data is EASYPLOT. The EASYPLOT routine was used to generate all the plots shown in Chapter IV.

In summary, the steps of program operation are:

- (1) Compile the program using the automatic precision increase option.

- (2) Select the mode of operation and input element values by manipulation of the input file.
- (3) Define input and output files.
- (4) Execute the program by typing the file name.

The next chapter presents the results of the input element sensitivity analysis performed to test the model reasonableness during verification.



#### IV. MODEL VERIFICATION

This chapter presents the results of the propellant longevity model verification at the Naval Postgraduate School. Standard model verification tests the model against three questions. First, does the model address the problem? Second, are the model predictions reasonable? Third, how do the model predictions compare to real-world observations?

This verification addresses only the first two criteria. Observational data for comparison with the model predictions is not available in an unclassified state. The quantitative analysis of model predictions is thus not addressed in this verification.

The model does address the initial problem. It predicts the fuel mass decrement of a low-earth-orbit satellite doing intrack micro-thrusting to overcome atmospheric drag.

The reasonableness test is the subject of the remainder of this chapter. An effective way to test the model performance is to examine model predictions resulting from the full "intended use" range of the input variables. Furthermore, if a plot is made of predicted results as a selected input element is incremented through its range, prediction trends can be found and examined. This procedure provides a qualitative analysis of model sensitivity to the selected input element.

To aid in these tests and trend studies, a sensitivity analysis feature was incorporated into the program code of the model, as previously described. Graphical results of each single variable sensitivity analysis are presented for the input elements.

The format of the following figures are all related. They represent plots of satellite mission life in modified Julian days (here after referred to simply as "days") versus a specified input element. All figures have the Y-axis as mission life and the X-axis as the variable selected for analysis. In each case the range of values for the input element is selected to remain within reasonable values of the input variable, as discussed in Chapter III. The granularity in most cases is 1/25 (PSIZE = 25). In some cases it is necessary to decrease the granularity to 1/100 (PSIZE = 100) to see the actual trends.

The default values discussed in Chapter III are used for all input elements not selected for analysis (except where noted). They correspond to a near-polar, retrograde orbit of an actual satellite supplied as sample input by NSWC. The model predicted propellant longevity using all default conditions and 10 kilograms of fuel is 13.74 days. When the default values and 100 kilograms of fuel are used, the resulting propellant longevity is 150.21 days. An \* symbol on the plotted curves indicates the default value of the

analyzed input element. The default value names are again summarized here. The units can be found in Chapter III.

Satellite physical parameters:

SPI (motor specific impulse)	230
WT (satellite initial mass)	9100
W (initial fuel mass)	100 and 10
CD (drag coefficient)	2.2 and 3.0
A (cross-sectional area)	.00005

Atmospheric specific parameters:

D (atm. rotation factor)	1.0
F107 (decimetric solar flux)	100
FBAR (average F107)	100
AKP (geomagnetic index)	2.0
TVE (time of vernal equinox)	43222.7382

NAVSPASUR orbital elements:

UJD (time of epoch)	44619.98716775
ETU (mean anomaly)	150.0000
H0 (R.A. of ascending node)	95.0000
G0 (argument of perigee)	200.0000
ES (eccentricity)	.0100000
XI (inclination)	95.0000
RND (time rate of mean motion)	.000783912
ESD (eccentricity decay rate)	-.239590000
A0 (semi-major axis)	1.06
ADOT (semi-major axis decay)	-701.8652

The input element sensitivity analyses are divided into related sets. All the sets are discussed in the same basic format. Each analysis is single-variable and arranged as follows:

- (1) The expected trend of real-world mission life resulting from the selected variable incrementing through its range.
- (2) The expected mission life trend predicted by the model as a result of the selected variable incrementing through its range.
- (3) The actual mission life results of the selected variable incrementing through its range.
- (4) A discussion of the selected variable sensitivity analysis.

The explanations for the plotted trends are based on expected behavior in agreement with current theory. An understanding of the actual mechanisms producing the observed trends will be improved with further research.

For a given set of satellite-orbital configurations, the satellite mission life will be shortest for satellites traveling through the most dense atmosphere. Thus for a given input variable sensitivity analysis, the range of values corresponding to satellite travel through the most dense atmospheric conditions will produce the shortest mission life. The range of values of the same input variable corresponding to satellite travel through the least dense atmosphere will likewise produce the longest mission life. The orbital-perigee atmospheric-density-bulge



encounter geometry is thus critical in mission life analysis.

The initial sensitivity plot of an input variable is accomplished with 10 kilograms of fuel. In many cases, true geopotential-induced orbital-drift trends are not seen with small amounts of drag-compensating fuel. To verify trends caused by geopotential-induced orbital drift, the initial compensating fuel is increased to 100 kilograms. The differences in the 10 kilogram and 100 kilogram mission life plot trends can then be attributed to geopotential effects and the movement of the center of most direct solar heating during the mission.

The 133.14 day nominal mission life resulting from the default values of the input elements and 100 kilograms of drag compensating fuel is almost a half-year. During this half-year, the earth is revolving around the sun causing the noon-sun atmospheric position to increase in longitude by about one degree per day. This greatly complicates trend analysis when using the 100 kilogram fuel case alone. It is thus necessary to include the 10 kilogram fuel case. The 13.74 nominal mission life of the 10 kilogram fuel case is short enough so that it shows little longitudinal movement of the most-direct-sun atmospheric position.

In many of the sensitivity analysis plots, the predicted mission life curve has a "knee." This "knee" corresponds to the range of the selected input variable that produces



changing behavior in the mission life curve. The location of these ranges has significance to design research.

The input variables are divided into four categories based upon their effect on mission life. The first category contains the input variables that affect the atmospheric-bulge orbital-perigee encounter geometry. The second category contains the input variables that affect the slowing effectiveness of the atmospheric density bulge on the particular satellite configuration. The third category contains the input variables that affect the depth of penetration of the satellite into the atmosphere at perigee. Finally, the fourth category contains the input variables that have no affect at all on mission life. As will be seen, predicted mission life is most sensitive to the third category (factors affecting atmospheric penetration at perigee).

Factors affecting the atmospheric-density-bulge orbital-perigee encounter geometry are: the time of vernal equinox passage TVE, the time of epoch UJD, the argument of perigee  $G_0$ , the right ascension of the ascending node  $H_0$ , and the inclination  $XI$ . The time of vernal equinox provides a real time reference for earth in its orbit relative to the sun. When combined with the time of epoch (sometimes called the time of perigee passage), these two factors determine the position of the noon sun in right ascension and declination relative to the atmosphere. The default values used in the

model verification position the initial noon sun at approximately 300 degrees longitude and 20 degrees south latitude relative to the celestial meridian containing the first point of aries. The right ascension of the ascending node and the argument of perigee combine to position the point of perigee in longitude relative to the first point of aries. The orbital inclination positions the point of perigee in latitude (or declination). Actual positioning of the satellite in the above orbit is accomplished by specifying the mean anomaly. All these orbital mechanics terms have been explained in Chapter II.A.

The expected real-world behavior of satellite mission life as a result of varying the time of vernal equinox or time of epoch is discussed next. The time of vernal equinox TVE serves to set a real-time reference for positioning of the earth in its orbit relative to the sun. When the time of epoch UJD is specified, the position of the point of the most direct atmospheric heating (noon sun) in the atmosphere is set. The atmospheric density-bulge follows the location of the most direct solar heating. The result of TVE and UJD varying in relation to each other is a seasonal positioning of the earth in its orbit around the sun at the time of initial perigee passage. Due to the earth's rotational-axis tilt, the point of most direct solar heating moves in longitude and latitude as the earth moves in its orbit

around the sun. Figures 3 and 4 in Chapter II.A aid this visualization.

The earth and solar cycles effecting the atmospheric density-bulge combine to define its size and shape. These cycles are discussed in Chapter II.B, and stated again here. They are: diurnal, semi-annual, seasonal-latitudinal, solar rotational, and solar activity related. The Jacchia J60 model atmosphere, as used in the propellant longevity model, incorporates only the diurnal cycle.

Once the position, size, and shape of the atmosphere is set, the mission life of a drag compensating satellite orbiting within it can be developed. For such a satellite in a specific initial orbit, the following real-world trend in mission life (propellant longevity) should be observed. The trend should be cyclic, resulting from the superposition of all the atmospheric heating cycles. Mission lives will be shortest for orbits having their perigee in the most dense atmospheric bulges. The longer mission lives will be observed for satellites having their orbits farthest away from the density-bulge. Thus the plots of satellite mission life will show peaks and valleys consistent with the above discussion.

In the propellant longevity model, the diurnal cycle is the only atmospheric heating cycle that is incorporated. Positioning of the earth in its orbit is accomplished by the combination of the time of vernal equinox and time of epoch

in the subroutine SOLOC. As discussed in Chapter III, the subroutine SOLOC positions the sun by right ascension and declination over the earth's atmosphere. The routine DRAG considers the diurnal density bulge to be centered under the solar position. The density profile of the atmospheric density-bulge is generated in the routine JAC60 based on the value of the input element F107.

The propellant longevity model considers the atmosphere to be oblate, diurnal, and revolving around the sun with a 23.5 degree rotational-axis tilt. The expected model-predicted-mission-life trend as is cyclic as TVE and UJD are varied. Every year should be an exact replica of every other year. Two peaks and two valleys in the yearly mission-life plot should be observed. The deepest valley occurs when the point of perigee is most closely centered in the atmospheric density bulge. With a low eccentricity ( $e = .01$ ) orbit considered, a much shallower valley will occur about six months later. This shallower valley corresponds to the point of apogee being most closely centered in the atmospheric density-bulge.

Two peaks in plotted mission life should occur corresponding to the orbital plane being most perpendicular to the earth-sun line. The peaks should be six months apart, of approximately equal magnitude, and interspaced between the mission-life valleys. As the eccentricity of the orbit is increased, the apogee-associated valley will



become shallower while the perigee-associated valley becomes deeper.

Figures 12, 13, 14, and 15 present the plots of the sensitivity analysis of TVE. In Figure 12, TVE has a range of 1000 days, from 38422 to 39422 days. The initial fuel is 10 kg. The resultant predicted mission life ranges cyclically between 11 and 18 days.

Figure 13 has an incremented range for TVE of 38422 to 38522, or 100 days. Initial fuel is 10 kg. The resulting predicted mission life again ranges cyclically between 11 and 18 days.

In Figure 14 the width of the incremented range is raised to 10,000 days (about 27 years). The minimum value of TVE is 38422 and the maximum is 49422. Again 10 kg of fuel is used. The results are cyclic between 11 and 18 days until TVE becomes greater than time of epoch UJD. The results at the high end of TVE in this plot are thus unreasonable. The time of vernal equinox passage chosen must occur before the satellite is launched requiring TVE to be less than UJD.

The TVE is again incremented through a small range of 20 days in Figure 15. Initial fuel is 100 kg. The resulting range of mission life predicted is from 150 to 153 days. Note the absence of the cyclic trend.

Figures 16 and 17 present the results of the sensitivity analysis plots of the time of epoch UJD with a range of 1000



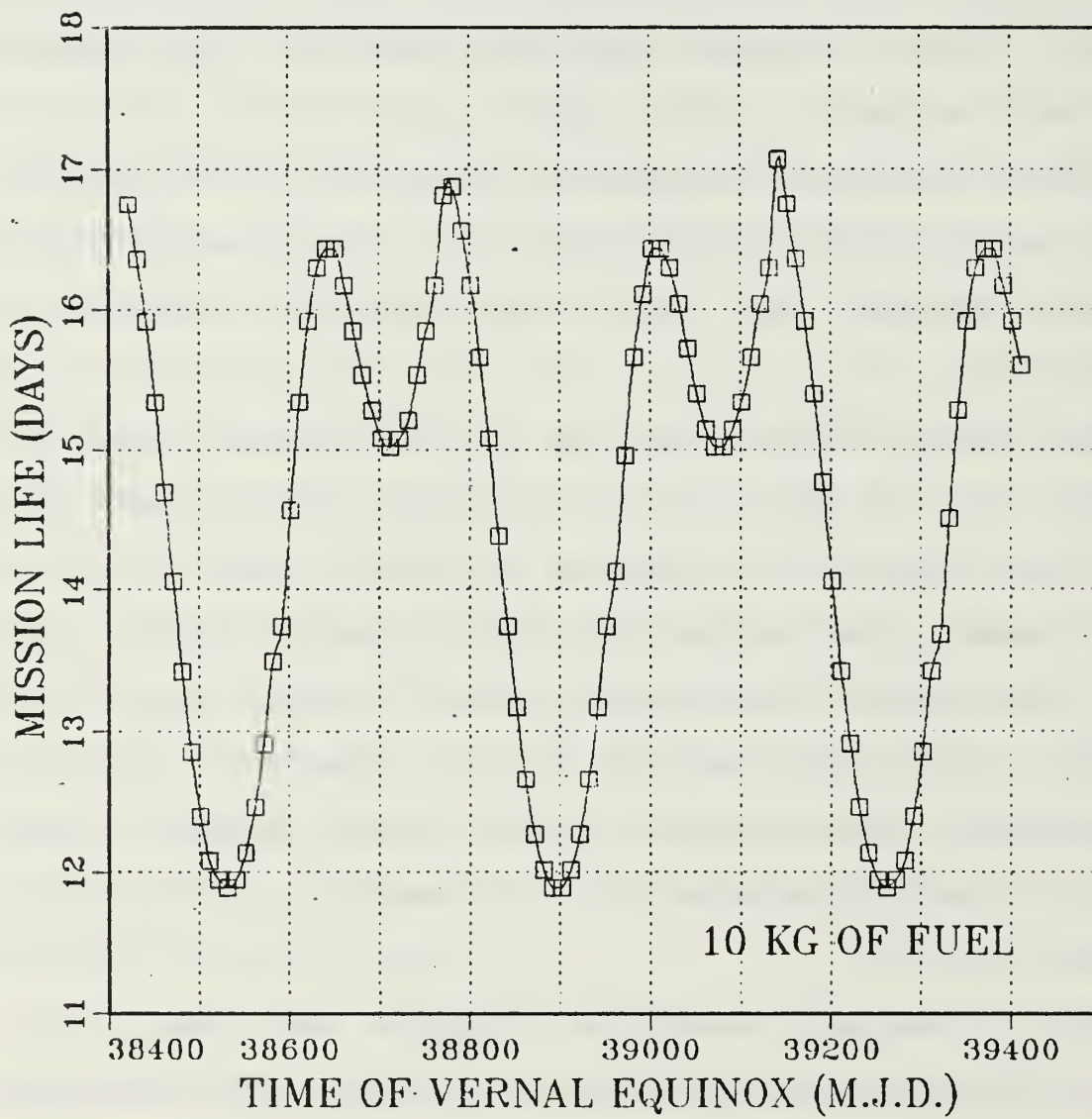


Figure 12. Mission Life versus Time of Vernal Equinox (1000 Days)

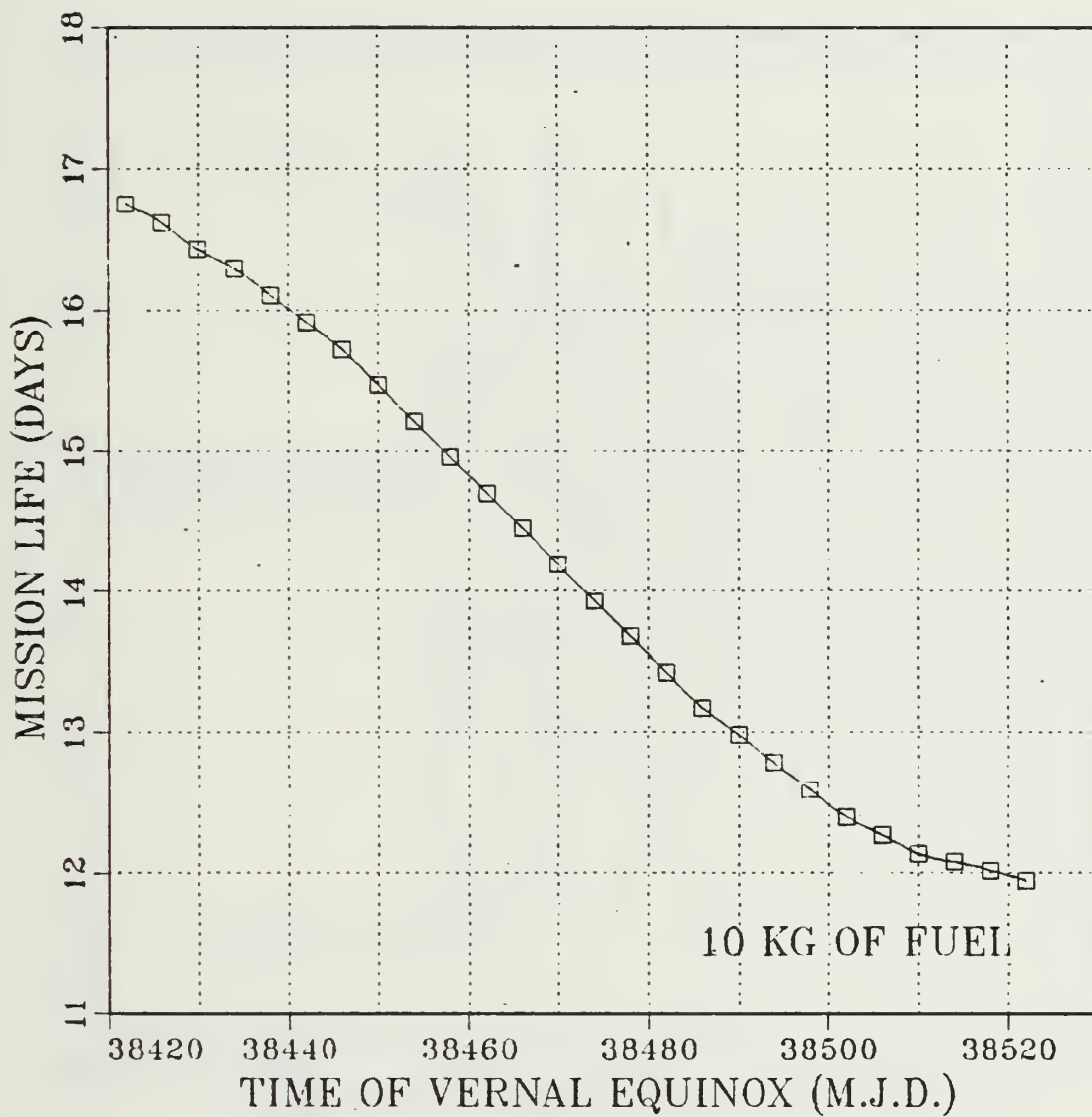


Figure 13. Mission Life versus Time of Vernal Equinox (100 Days)

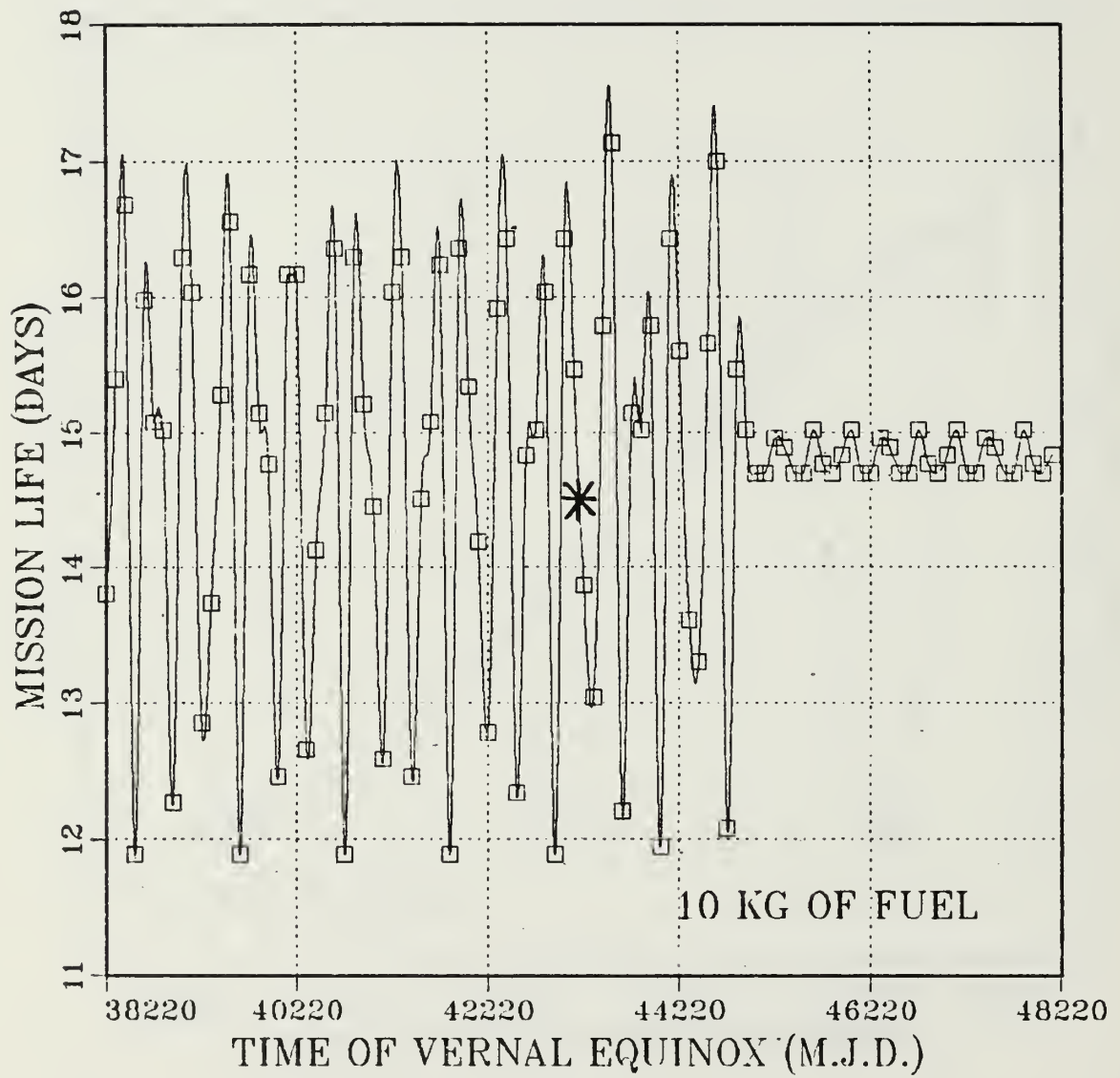


Figure 14. Mission Life versus Time of Vernal Equinox (10,000 Days)

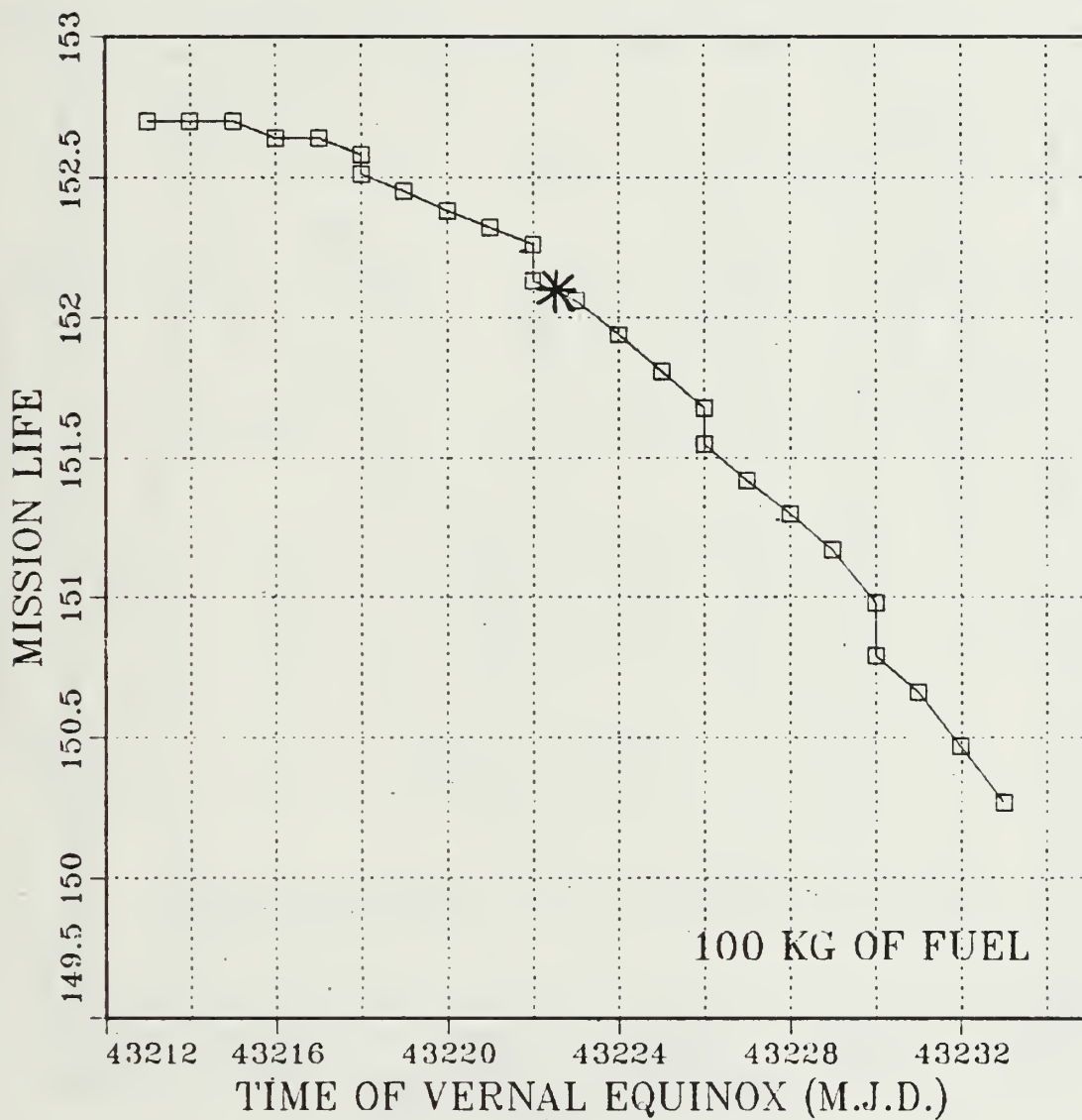


Figure 15. Mission Life versus Time of Vernal Equinox (20 Days)

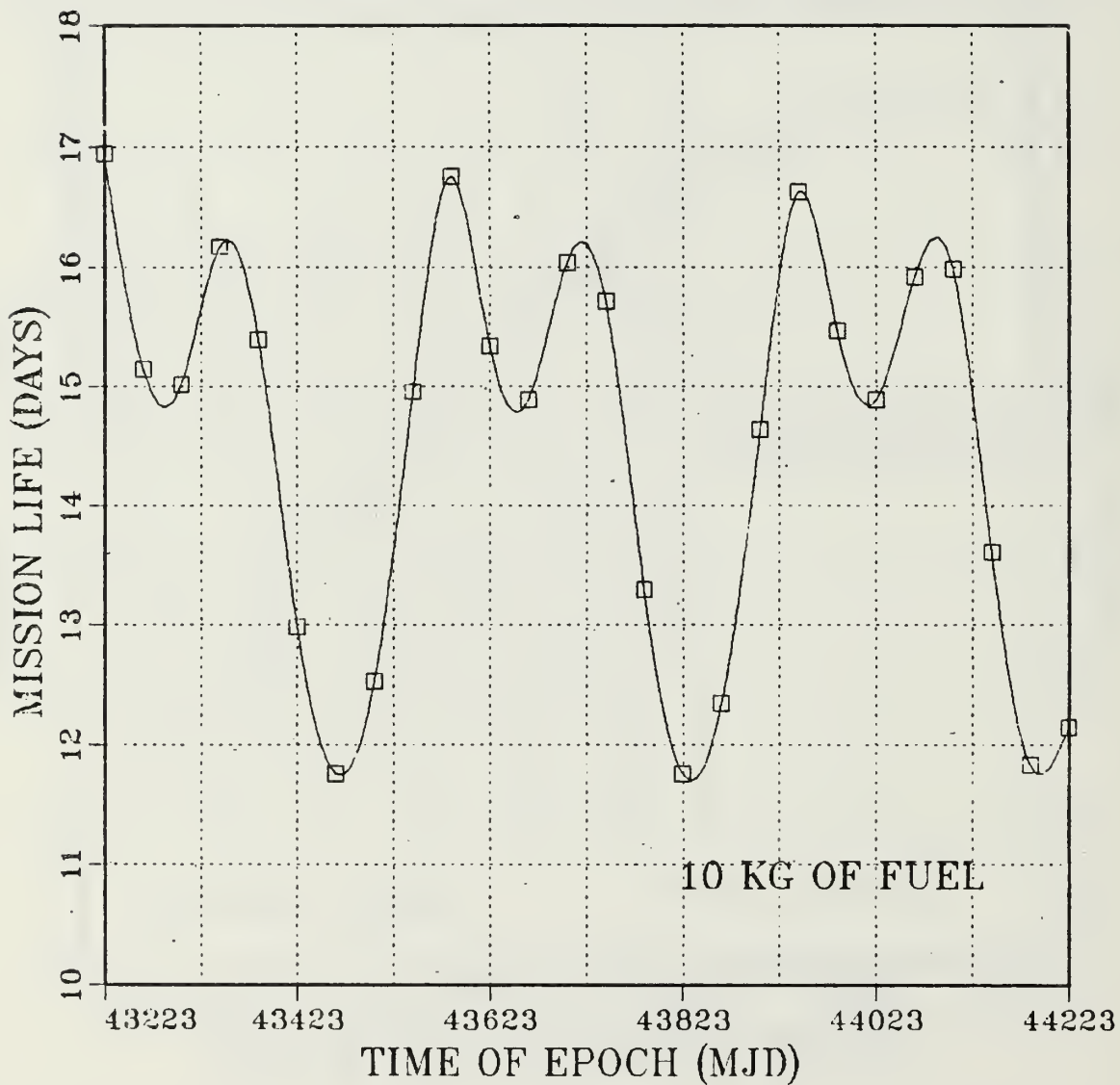


Figure 16. Mission Life versus Time of Epoch  
(1000 Days and 10 kg of Fuel)



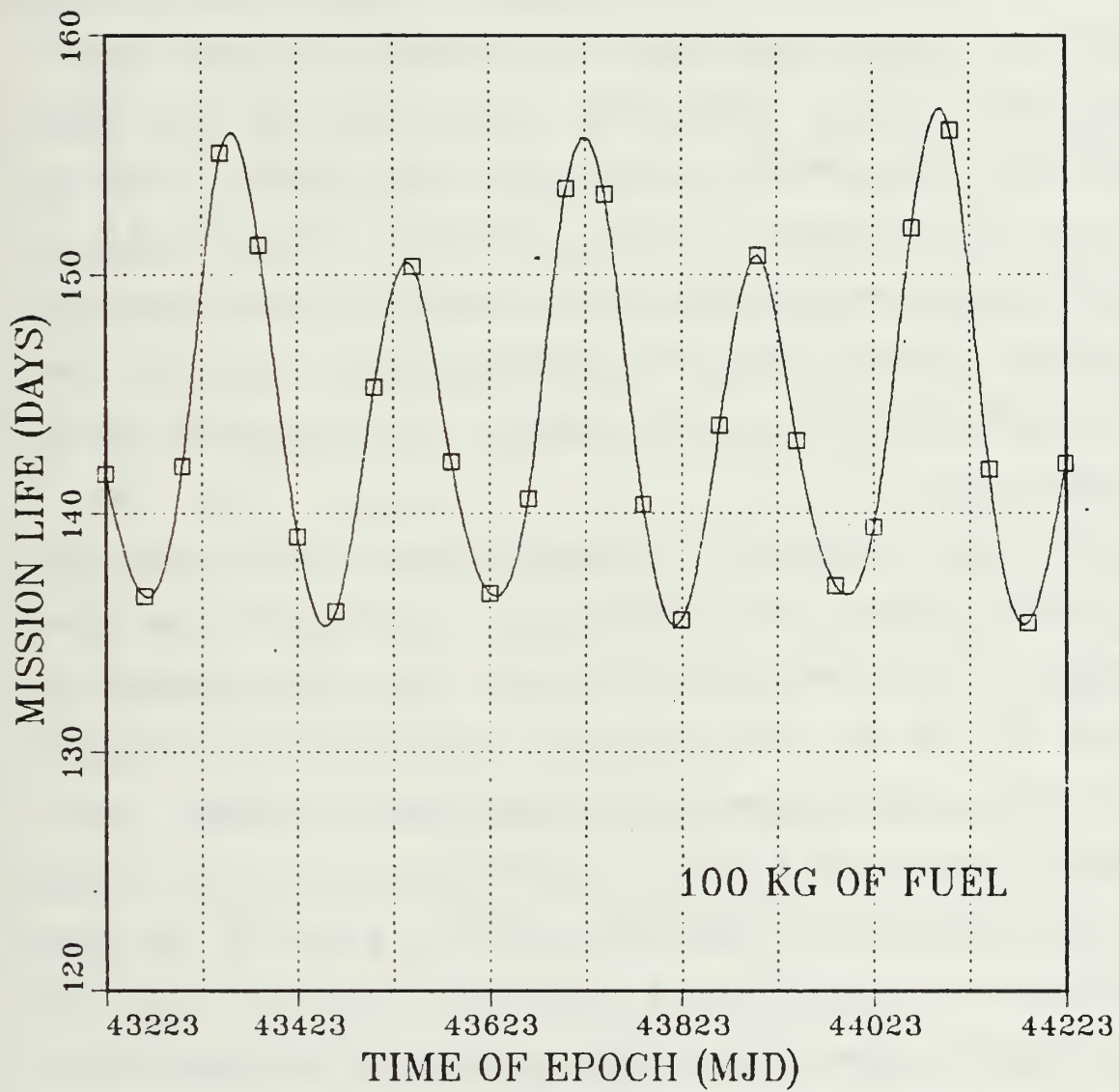


Figure 17. Mission Life versus Time of Epoch  
(100 Days and 100 kg of Fuel)

days. Note the similarity to the TVE plots, as theoretically expected. Figure 16 shows the 10 kg fuel case, and Figure 17 the 100 kg fuel case.

The trends observed in Figures 12 through 17 are in agreement with expected model predictions. The plotted trends may have significant differences from real-world trends due to the limitations of the Jacchia J60 model atmosphere. It should be noted that the default values of TVE and UJD produce a solar location approximately 30 degrees longitude past the winter solstice in the southern hemisphere heading toward the spring (vernal) equinox. The approximate latitude of the default solar position is 20 degrees south.

The right ascension of the ascending node  $H_0$  positions the orbital plane with reference to the celestial meridian containing the first point of aries. When the argument of perigee  $G_0$  and the inclination  $XI$  are specified, the point of perigee is positioned in longitude and latitude. This geometry is shown on Figure 4 in Chapter II.A.

The real-world trend in mission life of a drag compensating satellite, as a result of varying  $H_0$ ,  $G_0$ , and  $XI$  is cyclic. The cycle repeats every 360 degrees for  $H_0$  and  $G_0$ , and every 180 degrees for  $XI$ . The observed pattern of peaks and valleys will be highly variable, depending on the values of these three factors.

Model predicted mission life trends due to varying  $H_0$ ,  $G_0$ , and  $XI$  through their ranges should closely parallel real-world expectations. This close parallel between model predictions and observation assumes the atmospheric density-bulge has been properly positioned and described.

The default values of 95 and 200 degrees for the inclination and the argument of perigee combine to produce a point of perigee that is very nearly 20 degrees below the descending node in the southern hemisphere of the earth's atmosphere. The results of the sensitivity analysis plots for the right ascension of the ascending node and the argument of perigee are shown in Figures 18 through 21.

The right ascension of the ascending node  $H_0$  is incremented from 0 to 360 degrees. Figure 18 presents the 10 kg fuel case and Figure 19 the 100 kg fuel case. Predicted mission life ranges are 11 to 18 days in Figure 18, and 135 to 160 days in Figure 19.

The argument of perigee  $G_0$  is incremented from 0 to 360 degrees with a 10 kg fuel case in Figure 20, and a 100 kg fuel case in Figure 21. The predicted mission life are 13 to 18 days, and 148 to 160 days, respectively.

In Figure 18 two approximately equal mission life peaks and valleys are observed. The valleys correspond to the points of perigee and apogee closely approaching the atmospheric density bulge. The peaks occur when the orbital plane is most nearly perpendicular to the earth-sun line

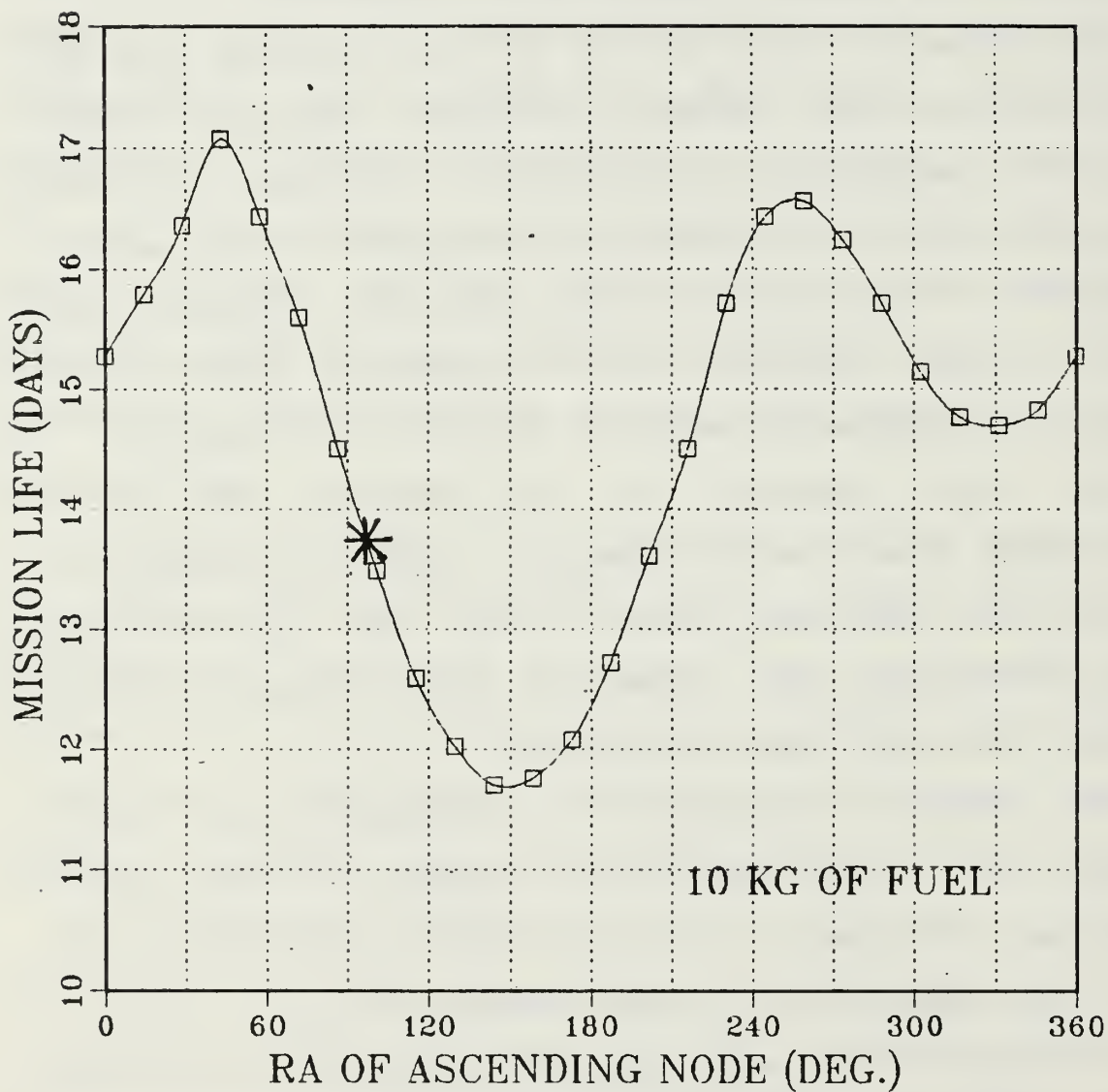


Figure 18. Mission Life versus Right Ascension of the Ascending Node (10 kg of Fuel)

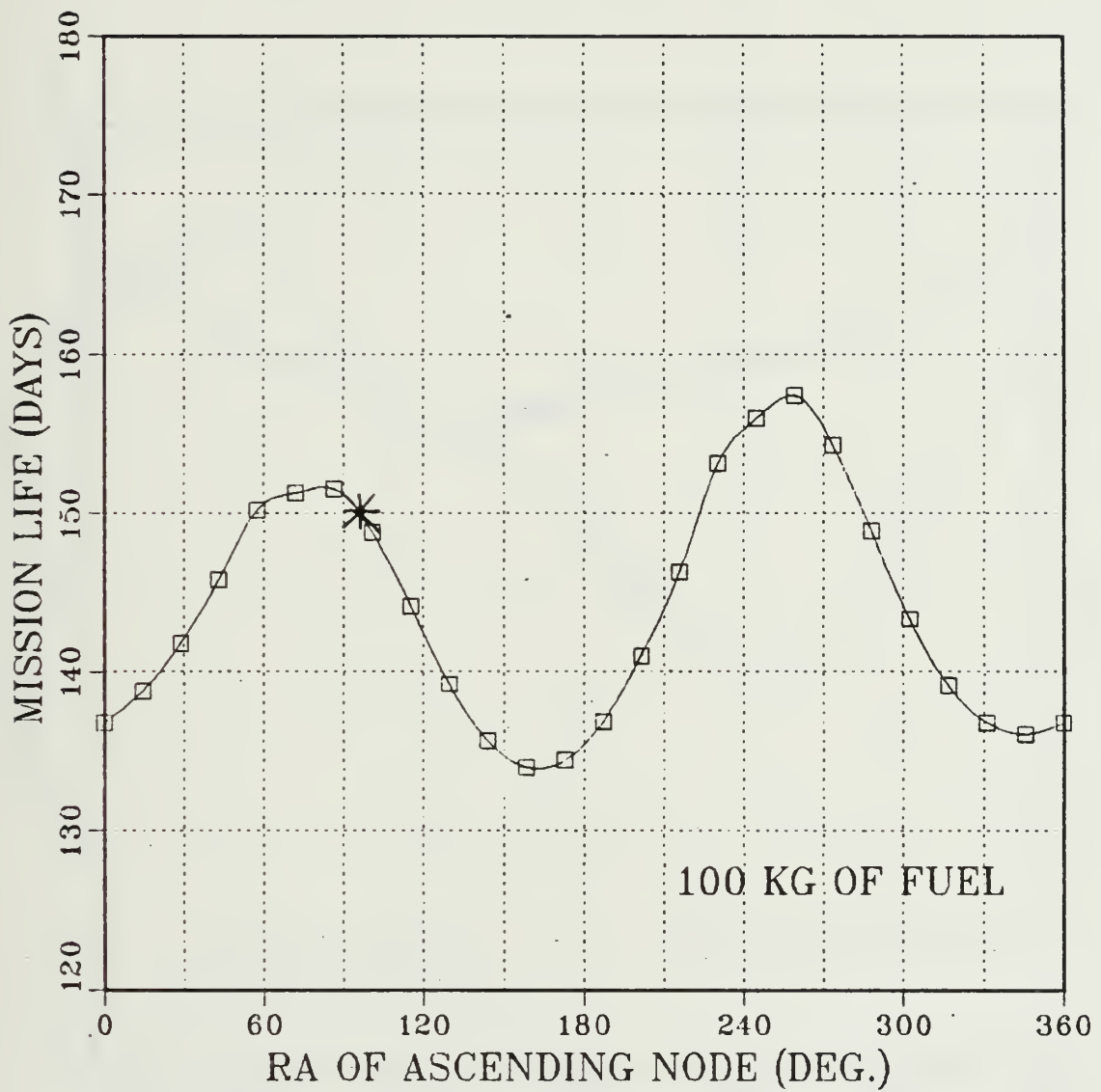


Figure 19. Mission Life versus Right Ascension of the Ascending Node (100 kg of Fuel)



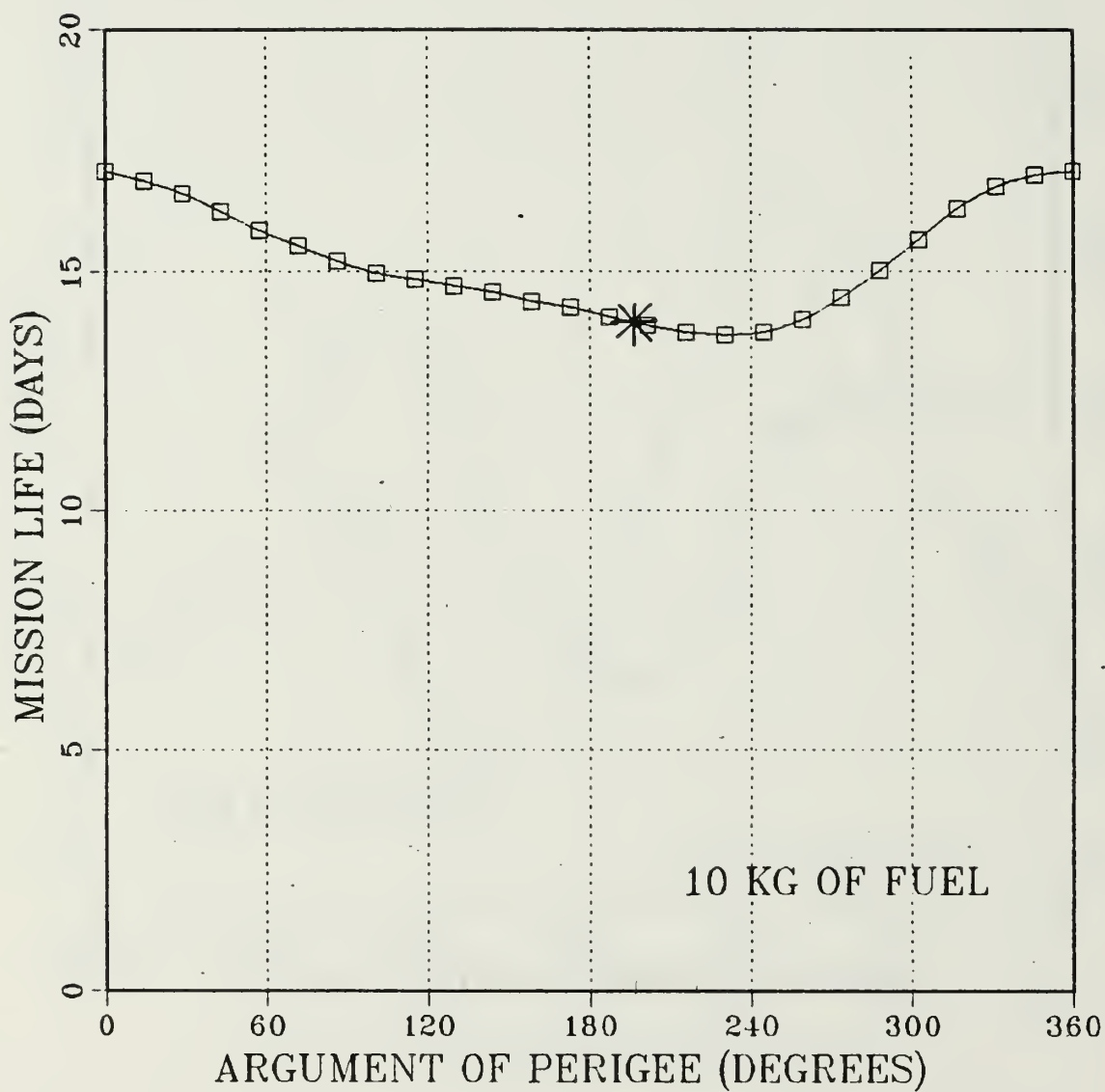


Figure 20. Mission Life versus Argument of Perigee (10 kg of Fuel)

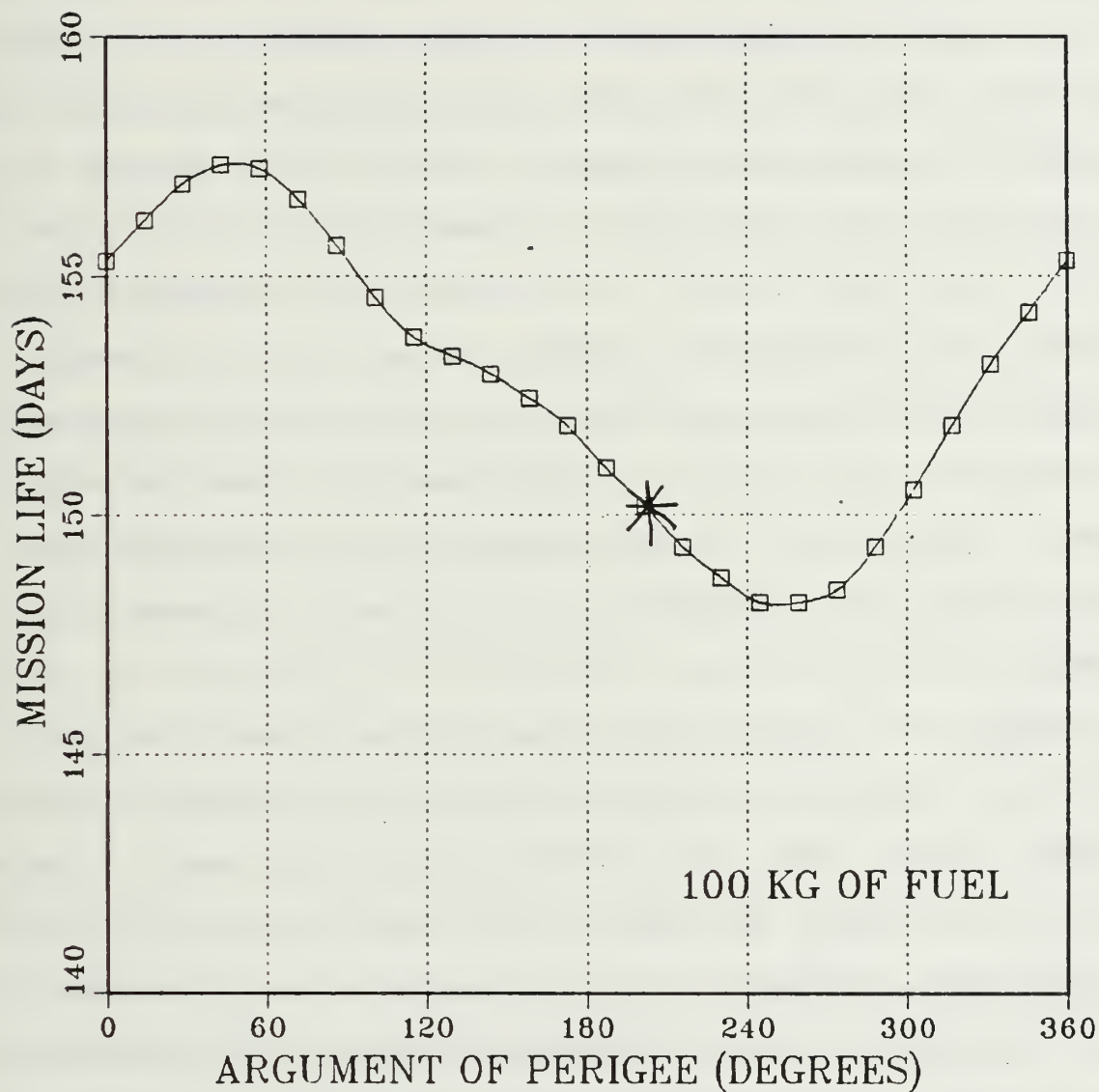


Figure 21. Mission Life versus Argument of Perigee (100 kg of Fuel)

which contains the atmospheric density bulge center. The change in shape of the 10 and 100 kilogram curves (Figures 18 and 19) is due to the movement of the atmospheric density bulge during mission life and to geopotential-induced orbital drift.

With default values of 95 degrees for both the right ascension of the ascending node and inclination, the effect of varying the argument of perigee from 0 to 360 degrees is to move the point of perigee around the initially fixed orbital plane (see Figure 4 in Chapter II). The plot of mission life corresponding to this motion should be cyclic showing one peak and one valley. The valley corresponds to the perigee point closest to the atmospheric density-bulge center. The peak in plotted mission life occurs when the apogee point is closest to the atmospheric density-bulge center.

Figures 20 and 21 show the plotted results of the sensitivity analysis of the argument of perigee  $G_0$ . The expected single peak and single valley are seen. The difference in the 10 kilogram case in Figure 20 and the 100 kilogram case in Figure 21 is due to the seasonal movement of the atmospheric density-bulge and geopotential-induced orbital drift. The magnitude of the mission life variations is less than that produced by varying the right ascension of the ascending node. This effect is due to low eccentricity

orbit ( $e = 0.01$ ) and the position of the orbital plane with reference to the earth-sun line.

Factors which primarily move the orbital plane in relation to the atmospheric density-bulge center will show two peaks and two valleys in their single-cycle mission-life range. Factors which primarily move the point of perigee in an initially specified orbital plane will show one peak and one valley in their single-cycle range. These considerations assume that only low eccentricity orbits are being considered.

Based on the above discussion, Figures 18 through 21 appear to agree with expected real-world and model-predicted mission life trends.

The analysis of predicted mission life trends due to varying the inclination  $XI$  is more complex. Several factors must be considered in addition to the orbital-perigee atmospheric density-bulge encounter geometry. First, the diurnal atmosphere model used by the propellant longevity model is also oblate, and is thus more dense at the equator than at the poles. This fact means that satellites in near polar orbits travel through an overall less dense atmosphere than those in a near equatorial orbit. Second, the atmosphere rotates in the same direction as the earth. Hence prograde orbital satellites experience less satellite-to-atmosphere relative velocity than satellites in retrograde orbits. If the satellite altitude is low enough,

a near-equatorial prograde orbit satellite has a longer mission life than the same satellite in a near-equatorial retrograde orbit. These additional effects complicate the analysis of mission life resulting from varying the orbital inclination.

The default value position of the center of the atmospheric density-bulge is 300 degrees longitude and 20 degrees south latitude. The bulge is moving at a rate of about one degree longitude per day toward the vernal equinox. The point of perigee is default positioned at approximately 275 degrees longitude and 20 degrees south latitude. As can be seen, the point of perigee is quite close to the center of the atmospheric density-bulge. The motion of the point of perigee, as the inclination is increased from near 0 degrees to near 180 degrees, describes a semicircle 20 degrees in radius around the descending node. The point of perigee remains quite close to the initial position of the center of the atmospheric density-bulge.

Figures 22, 23, 24, and 25 are the predictions of the sensitivity analysis plots of orbital inclination XI. The incremented range is from 22.5 to 157.5 degrees. Nearer equatorial inclinations are prohibited by the available arithmetic precision on the IBM 3033. Figure 22 shows the 10 kg fuel case, Figure 23 the 100 kg fuel case, and Figure 24 the 100 kg fuel case with a granularity of 1/100 and a



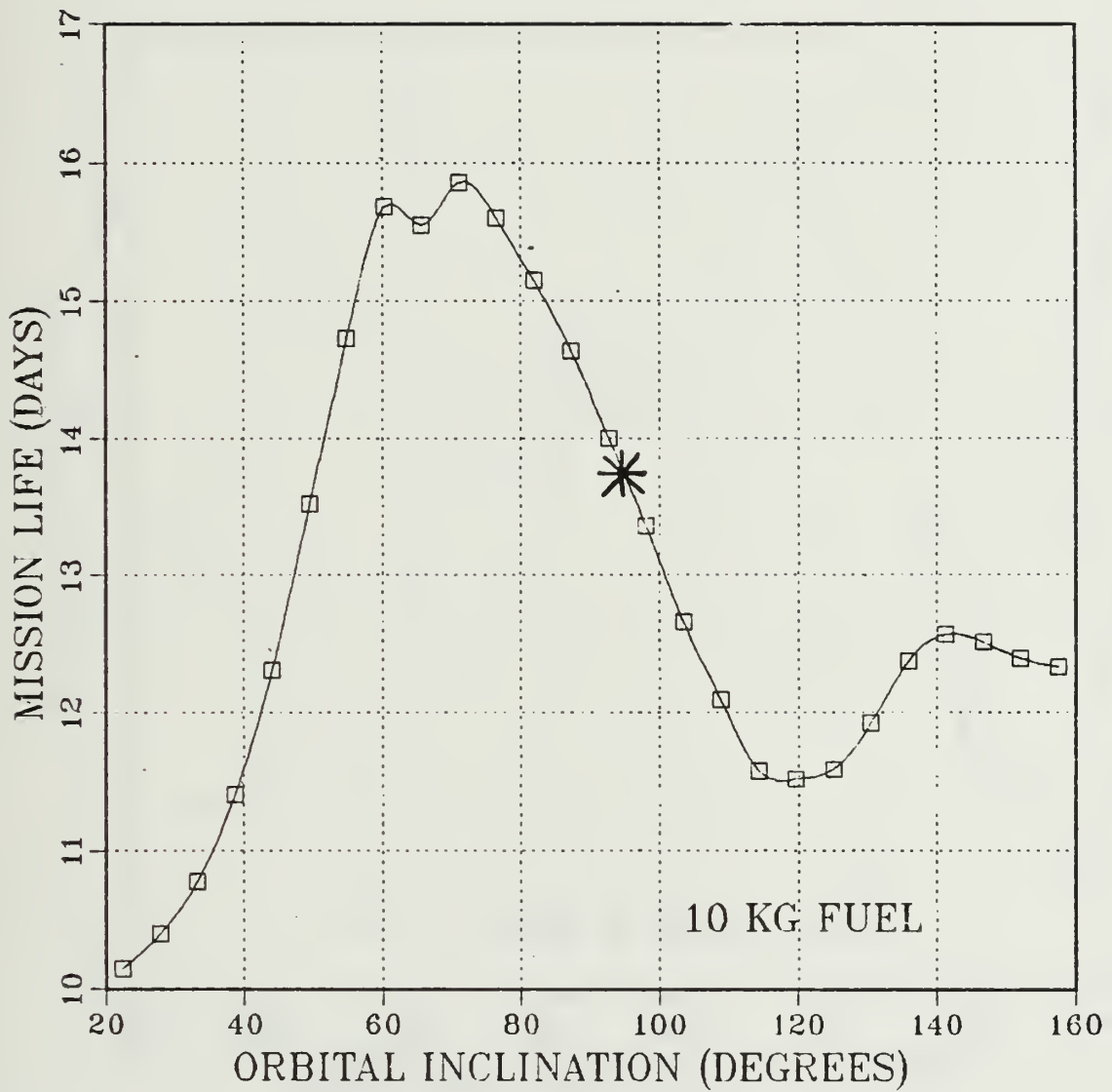


Figure 22. Mission Life versus Orbital Inclination (10 kg of Fuel)

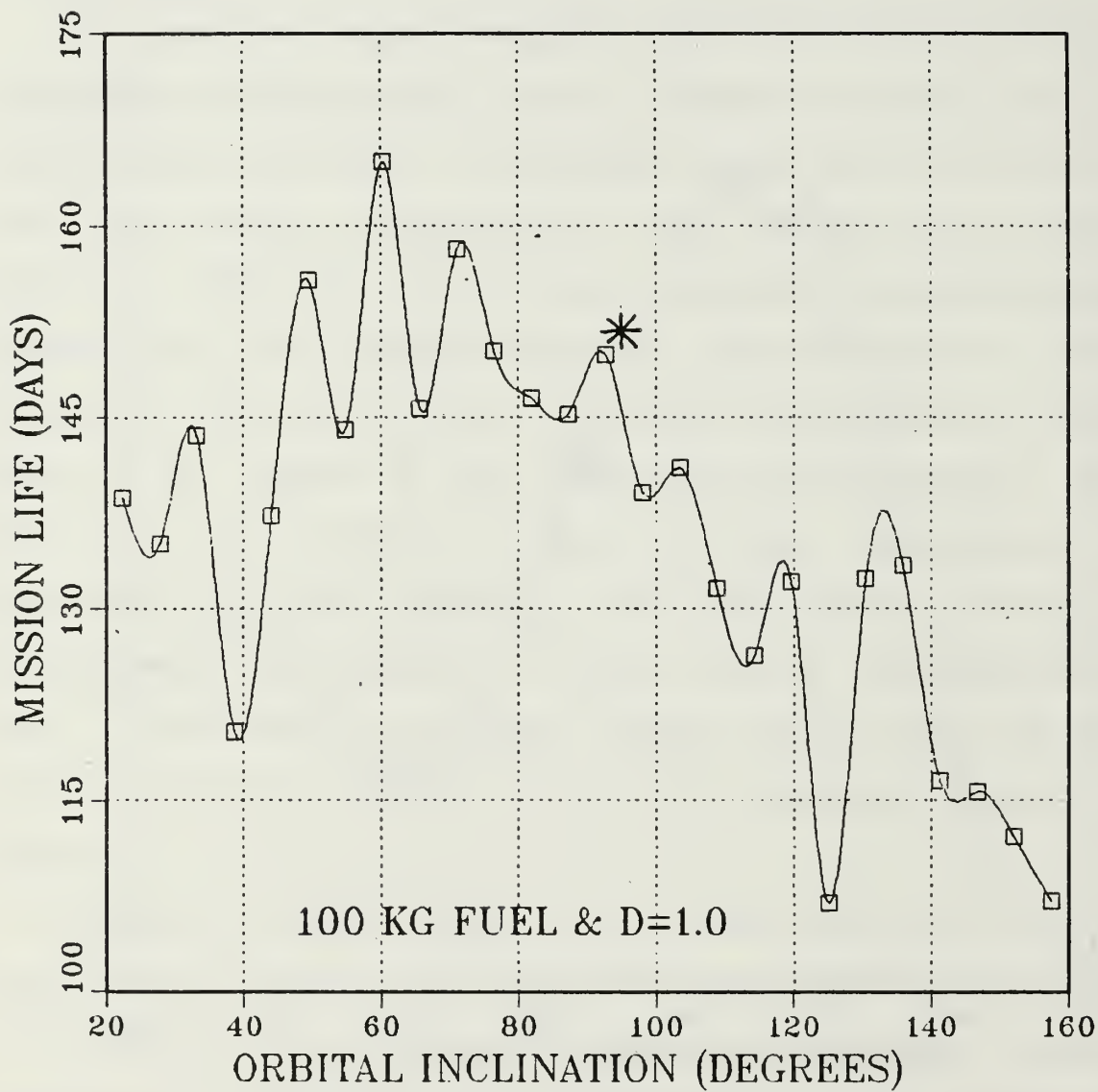


Figure 23. Mission Life versus Orbital Inclination (100 kg of Fuel)

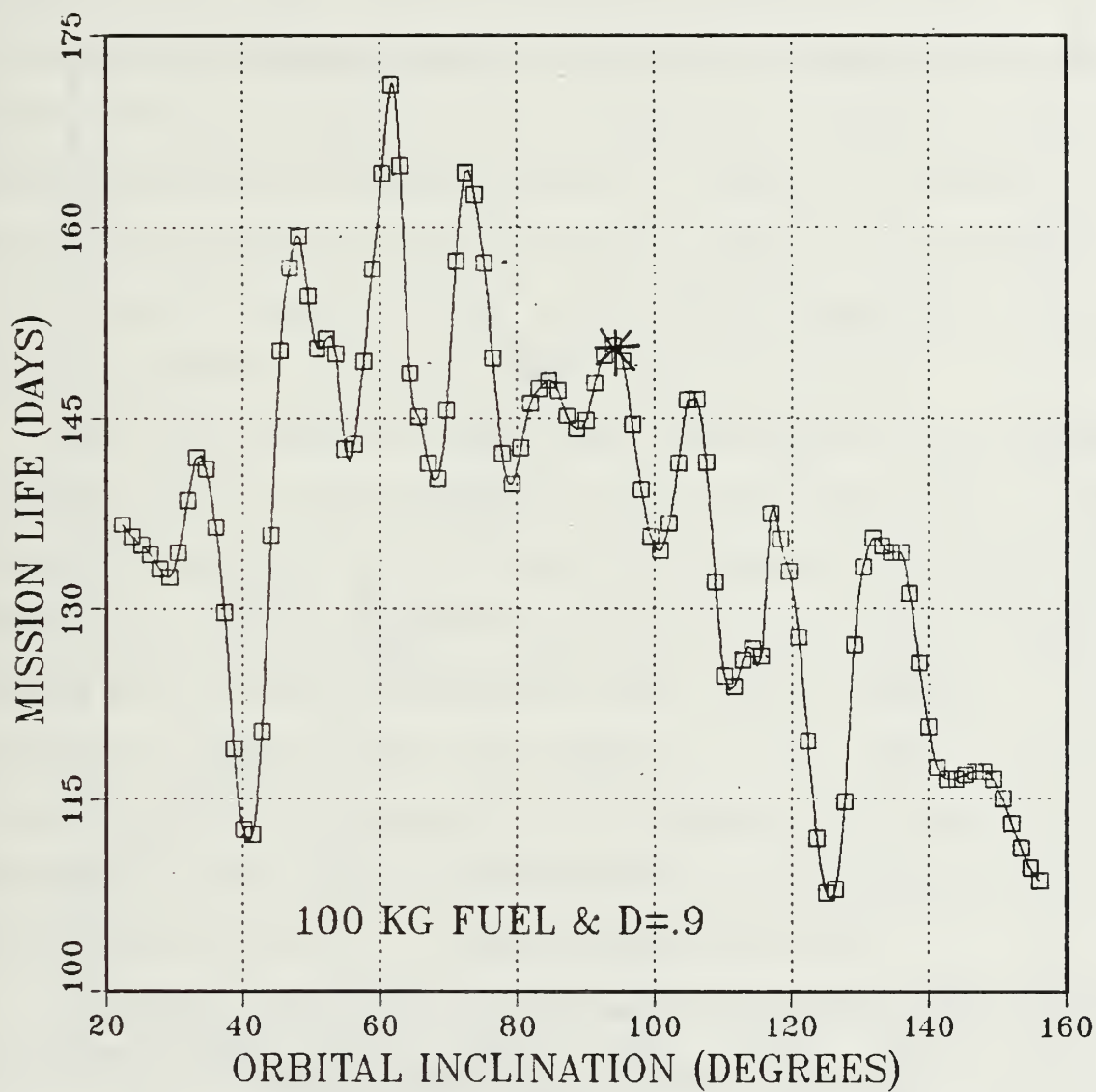


Figure 24. Mission Life versus Orbital Inclination  
(100 kg of Fuel and PSIZE = 100)

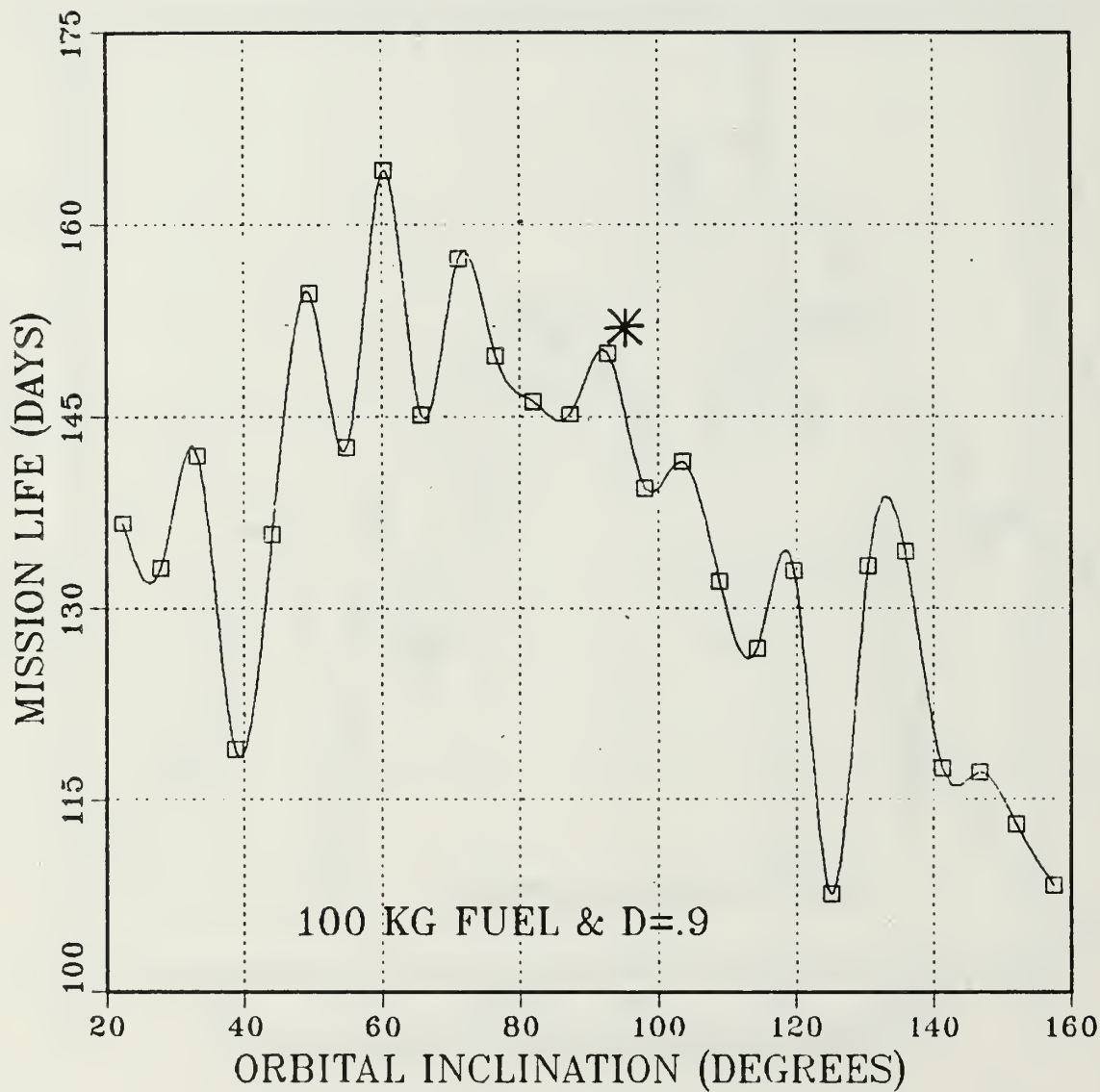


Figure 25. Mission Life versus Orbital Inclination  
(100 kg of Fuel, PSIZE = 100, and D = 0.9)

rotation factor of 0.9. Predicted mission life ranges are 7.8 to 13.7 days in Figure 22, and 90 to 138 days in Figures 23 and 25.

Figure 25 shows the effect of the using 100 kilograms of compensating fuel and a rotation factor of 0.9. This situation is compared to 100 kilograms of compensating fuel and a rotation factor of 1.0 in Figure 23. Only very slight differences occur between Figures 23 and 25. Mission life is a little longer in the retrograde orbits using a rotation factor of 0.9 and a little shorter in the prograde orbits using a rotation factor of 0.9.

When the satellite orbit is lowered to an altitude at perigee of 200 kilometers ( $AO = 1.03$ ) with 1000 kg of fuel, mission life is reduced in the retrograde-equatorial orbit below that of the prograde-equatorial orbit. The observed peaks at 70 and 140 degrees also shift leftward. The observed dimple seen in Figure 22 at the critical inclination of 63 degrees may be geopotential-induced or an artifact of the Kozai approximations as discussed by Taff [Ref. 2:pp 332-342].

A further explanation of the plot of mission life versus inclination shown in Figure 22 is presented here. A more detailed study of this input variable is worthy of a complete paper itself.

The low mission life found at low values of inclination is due to the combination of the point of perigee position



and oblate-atmosphere effects. The low inclination orbits travel through the "fat part" of the oblate atmosphere near the equator. As the inclination increases, the point of perigee moves away from the center of the atmospheric density-bulge and the satellite's orbit moves up out of the thick equatorial atmosphere. These two factors combine to produce the observed rapid rise in mission life seen in Figure 22. Beyond near-polar values of the inclination, the predicted mission life again falls. The mission life valley seen at 120 degrees is probably due to maximum orbital time near the atmospheric density-bulge center.

Figure 23 shows the effect of starting with 100 kilograms of initial drag-compensating fuel. Note the many peaks and valleys. To confirm that these peaks and valleys represent actual predicted mission life trends and not simply data scatter, the granularity was decreased to 1/100. Figure 24 is a plot of these results, and confirms the trends outlined in Figure 23. The many peaks and valleys superimposed over the general trend of mission life seen in Figure 22 are probably due to geopotential-induced orbital drift.

The results of the sensitivity and trend analysis of the orbital inclination XI have been discussed with reference to in Figures 22 through 25. Future investigation of the plotted data may reveal more insight toward understanding

the underlying mechanisms. The sensitivity analysis plots show no trends that appear unreasonable.

The sensitivity analysis for the input variables effecting the orbital-perigee atmospheric density-bulge encounter geometry (category one) have now been presented. The next set of analyses are those of the second category, which contains the input variables affecting the slowing power of the atmosphere. These variables are: decimetric solar flux F107, drag coefficient CD, cross-sectional area A, specific impulse SPI, and the atmospheric rotation factor D. The initial mass of drag-compensating fuel is also included in this category because it improves satellite mission-life resistance to atmospheric drag.

The real-world expected effect on mission life as a result of varying the decimetric solar flux F107 is to vary the heating effectiveness of the sun. As the decimetric solar flux increases, the density of the atmosphere will increase.

The Jacchia J60 model atmosphere used in the propellant longevity model subroutine JAC60 uses the F107 flux as a multiplier for the exponential density term. The expected model predictions of mission life as the F107 flux is varied through its range of 50 to 300 is a multiplicatively decreasing plot.

The results of the sensitivity analysis for predicted mission life as the decimetric solar flux is varied are

presented in Figures 26 and 27. Figure 26 is the result of 10 kg of initial maneuvering fuel, and Figure 27 is the result with 100 kg of fuel. The predicted mission life in Figure 26 ranges from 24.99 to 3.96 days. The 100 kg fuel case in Figure 27 predicts a mission life ranging from 270.12 to 43.07 days. These results are in agreement with expectations.

The next set of analyses consider effects of the drag coefficient, satellite cross-sectional area, and specific impulse. All of these factors are multipliers acting to change the resistance of the satellite to atmospheric drag. The drag coefficient  $C_D$  is a proportionality constant in the drag force model. The satellite cross-sectional area  $A$  changes the size of the satellite that the atmosphere actually acts against. As satellite cross-sectional area increases it will take multiplicatively more energy to compensate for the orbital energy lost by the satellite working against the drag force. The specific impulse  $SPI$  is a multiplier that expresses the effectiveness of the expelled fuel mass in overcoming the drag force.

The rotation factor  $D$  is the ratio of the atmospheric rotation rate to the earth's rotation rate. Its effect is to change the satellite to atmospheric relative velocity as the inclination changes. A logical range of  $D$  is between the values 0.9 and 1.0. The sensitivity analysis range of 0.1 to 10.0 was chosen to show model sensitivity for a wide

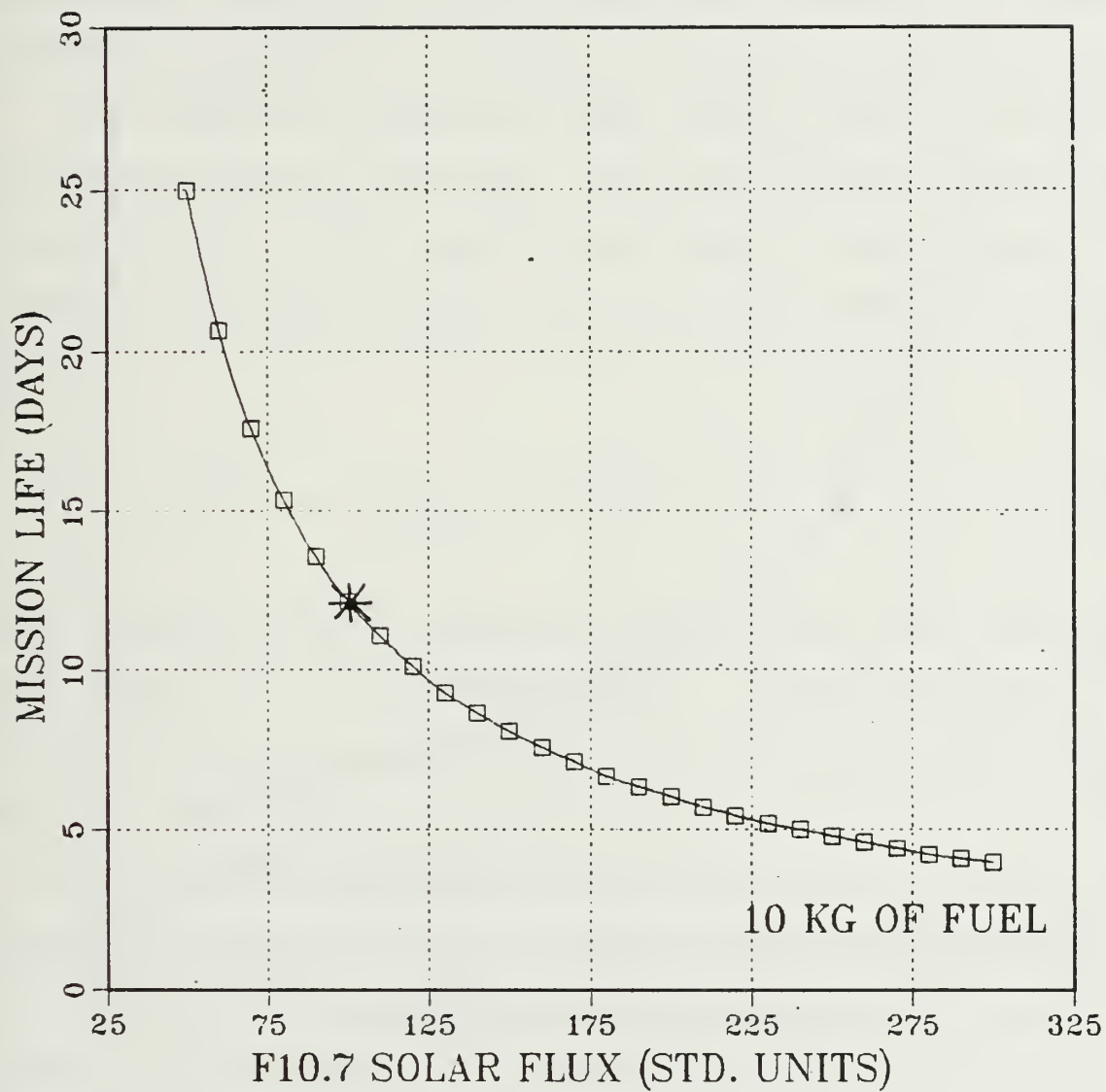


Figure 26. Mission Life versus F10.7 Flux (10 kg of Fuel)

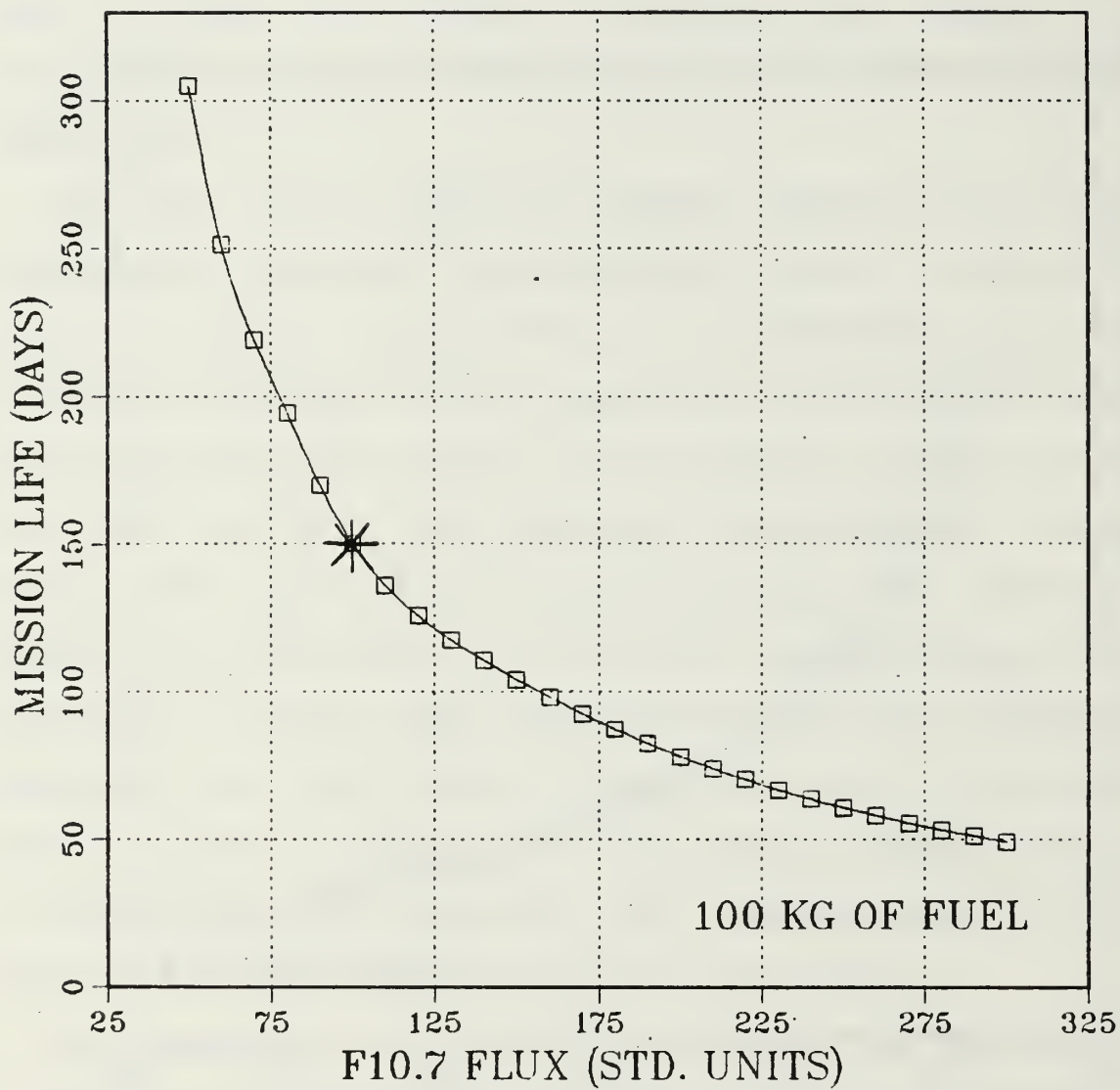


Figure 27. Mission Life versus F10.7 Flux (100 kg of Fuel)



range of D. As presented in Chapter II Equation 12, the D factor is combined with the inclination and the ratio of the radius-at-perigee to the velocity-at-perigee producing the  $\delta$  factor. This factor is used to convert the satellite tangential velocity into the satellite-to-atmospheric relative velocity.

The propellant longevity model uses A, CD,  $\delta$ , and SPI as proportionality constants, multiplicatively changing the effectiveness of the expelled fuel mass. The routine PLEP combines these four factors into a single constant DEL given by:

$$\text{DEL} = A * \text{CD} * \delta * 3.14159/\text{SPI} \quad (14)$$

This constant DEL is passed to the routine KOZAI which in turn passes it to the routine DRAG. In the routine DRAG, DEL is used as the final multiplier in determining required fuel for each orbit.

The expected model-predicted mission-life as a result of changing these factors is a multiplicative increase when A, CD, or  $\delta$  are increased linearly. A multiplicative decrease should occur when SPI is increased linearly.

Expected results of varying D from 0.1 to 10.0 in the near-polar retrograde orbit are shown in Figure 28. Note that a very slight lowering of mission life is seen when the rotation factor increases. Figures 29 and 30 show the

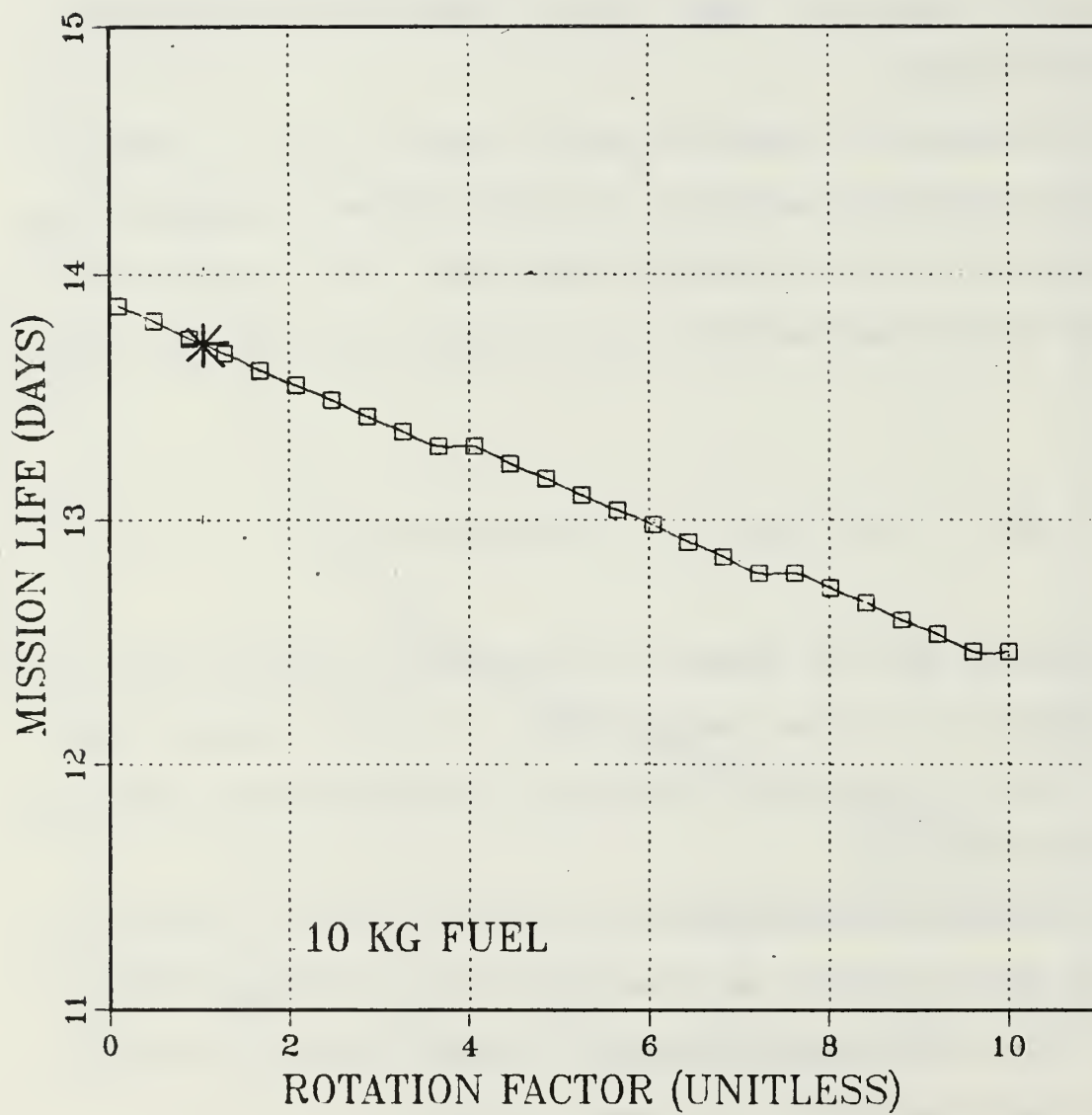


Figure 28. Mission Life versus Rotation Parameter (10 kg of Fuel and Default Inclination)

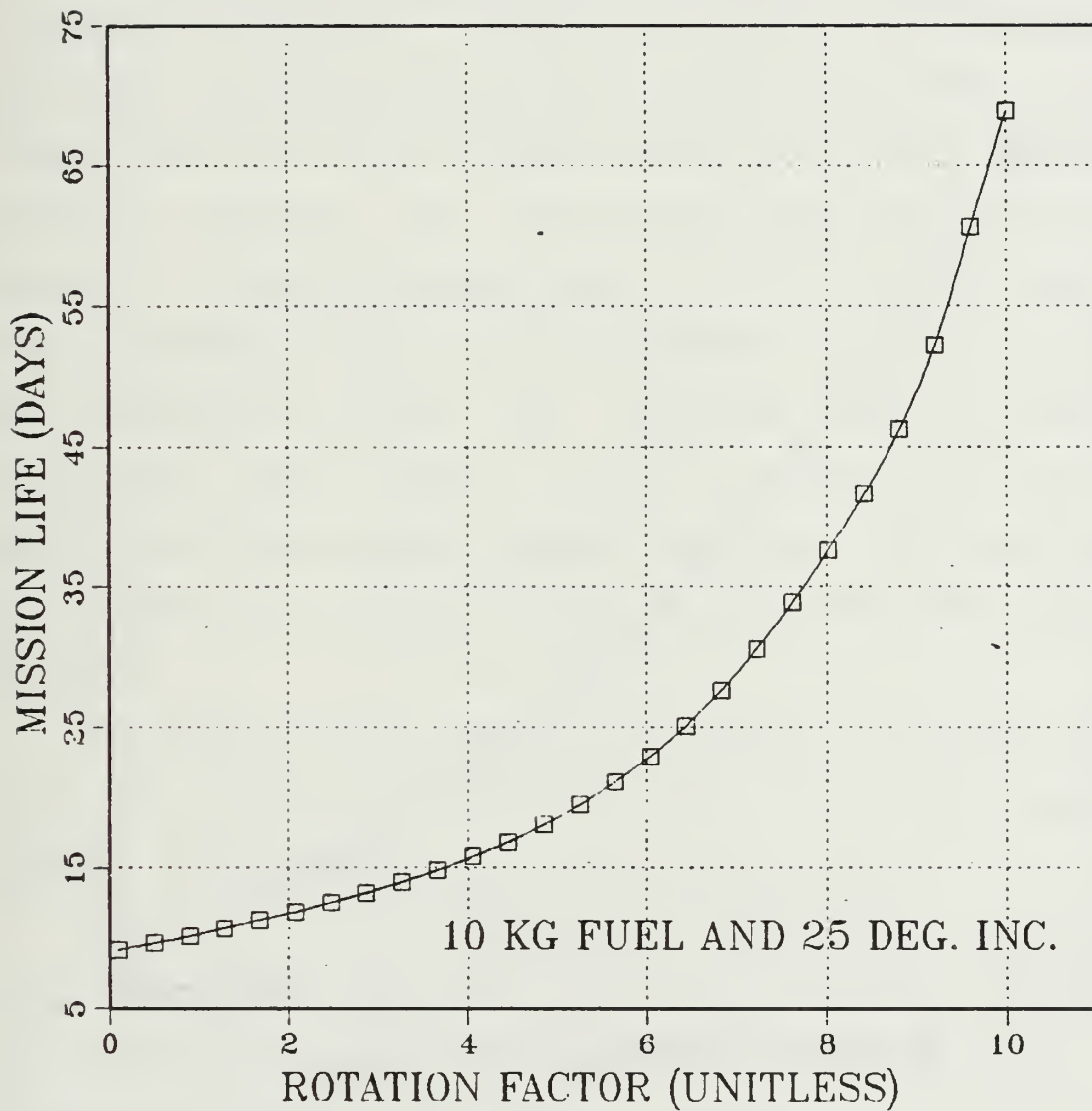


Figure 29. Mission Life versus Rotation Parameter  
(10 kg of Fuel and Prograde Orbit)

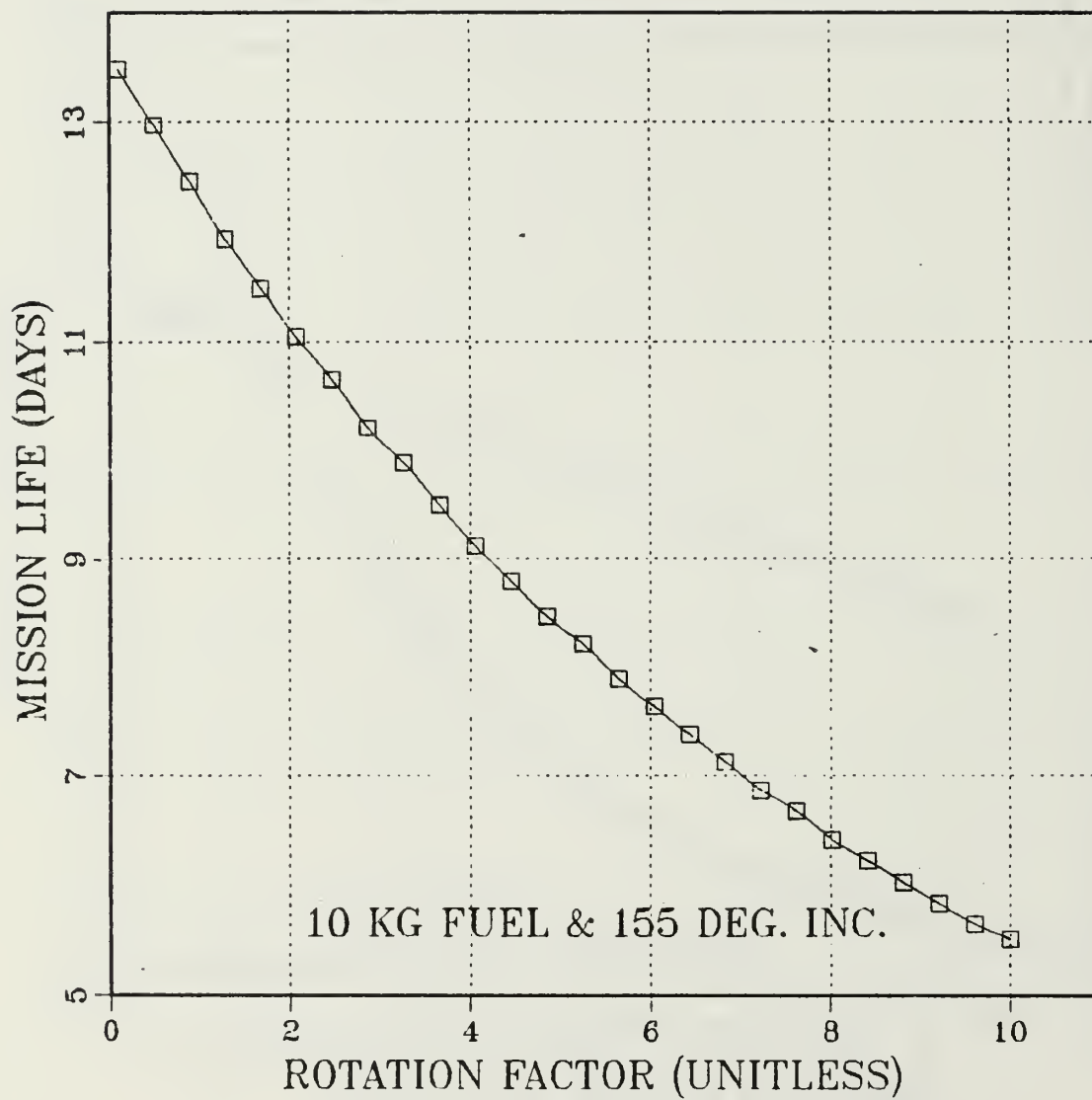


Figure 30. Mission Life versus Rotation Parameter  
(10 kg of Fuel and Retrograde Orbit)

plotted result of varying  $D$  through the same range of 0.1 to 10.0. However, in Figure 29 an inclination of 25 degrees is used instead of the default 95 degrees, and in Figure 30 an inclination of 155 degrees is used. In Figure 29 it is seen that the mission life multiplicatively increases as  $D$  is linearly increased. Figure 30 shows a multiplicative decrease in mission life as  $D$  is linearly increased. These trends are due to the change in the satellite-to-atmosphere relative velocity. The increasing mission life expectancy within a strongly prograde orbit (Figure 29) is a result of the decreasing satellite-to-atmosphere relative velocity. The decreasing mission life expectancy within a strongly retrograde orbit (Figure 30) is a result of increasing satellite-to-atmosphere relative velocity. The plots shown in Figures 28, 29 and 30 are in agreement with expected results.

The results of the sensitivity analysis plots on mission life as a result of varying  $CD$ ,  $A$ , and  $SPI$  are shown in Figures 31 through 35.

Figures 31 and 32 result from varying the satellite drag coefficient  $CD$  from 1.0 to 3.5. Figure 31 represents the 10 kg fuel case and Figure 32 the 100 kg case. The predicted mission life range in Figure 31 is 31.18 to 8.63 days, and in Figure 32 from 308 to 99.58 days.

The sensitivity analysis mission-life trend plots of satellite cross-sectional area  $A$  are shown in Figures 33 and



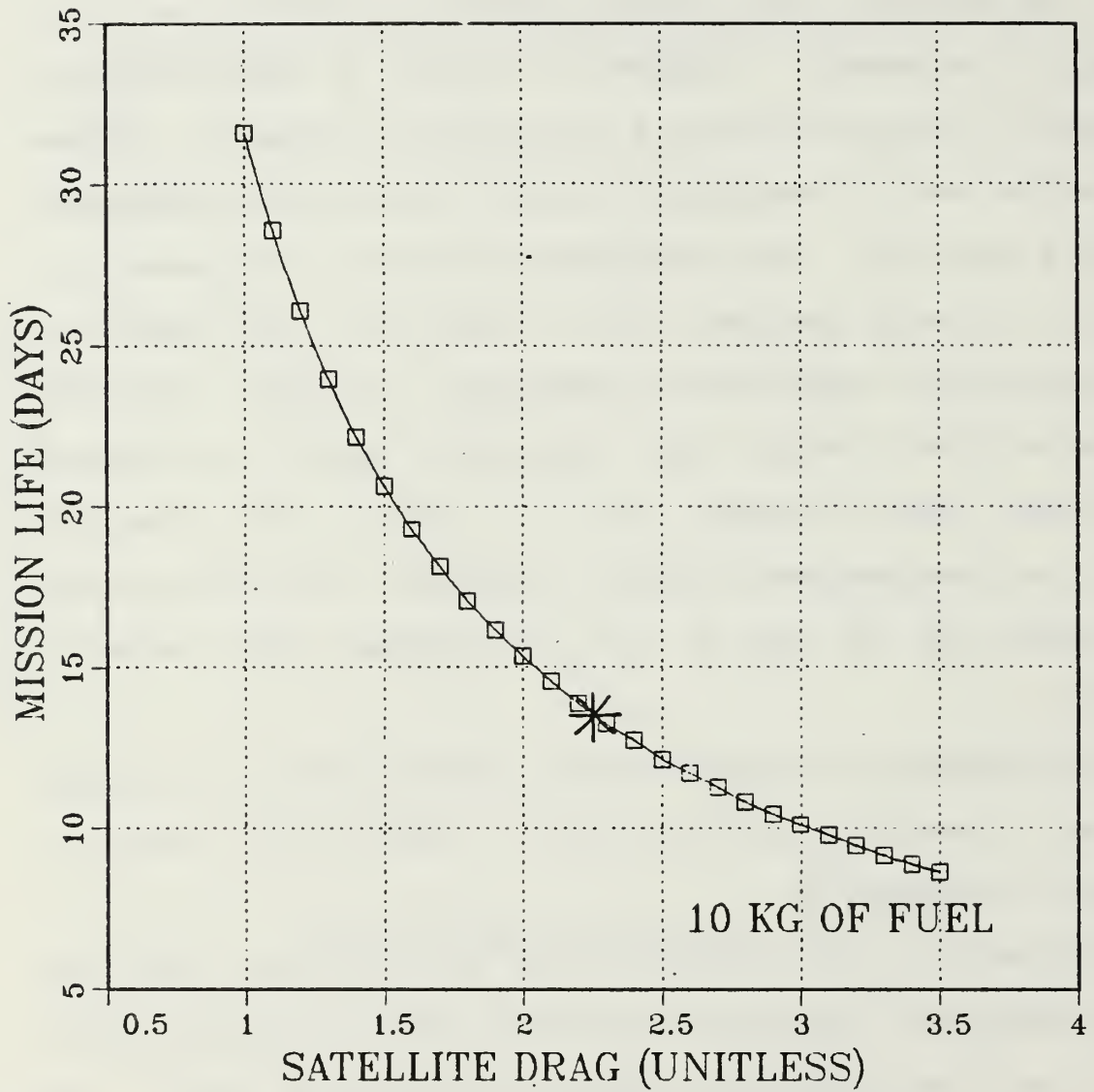


Figure 31. Mission Life versus Drag Coefficient (10 kg of Fuel)

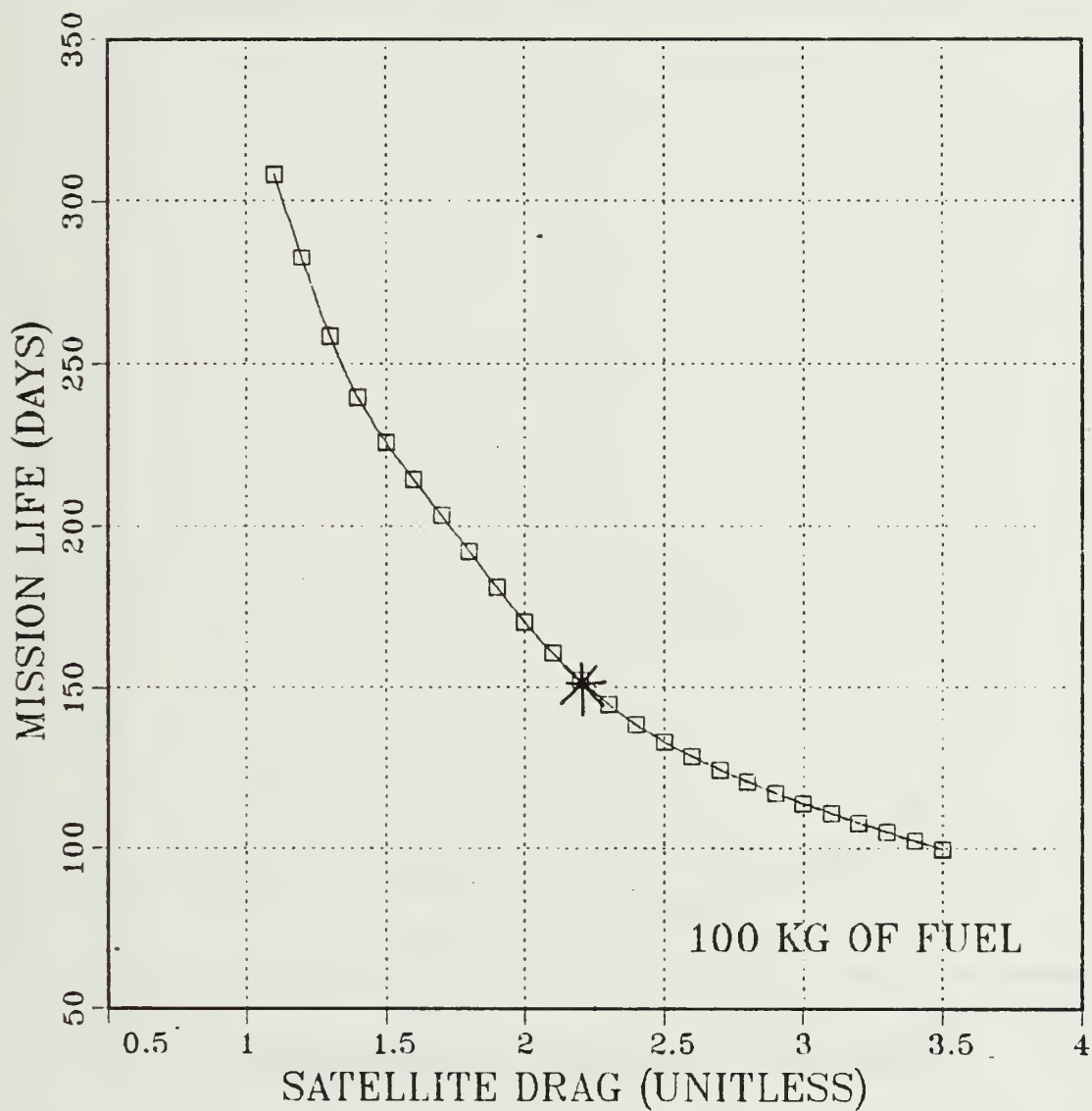


Figure 32. Mission Life versus Drag Coefficient (100 kg of Fuel)

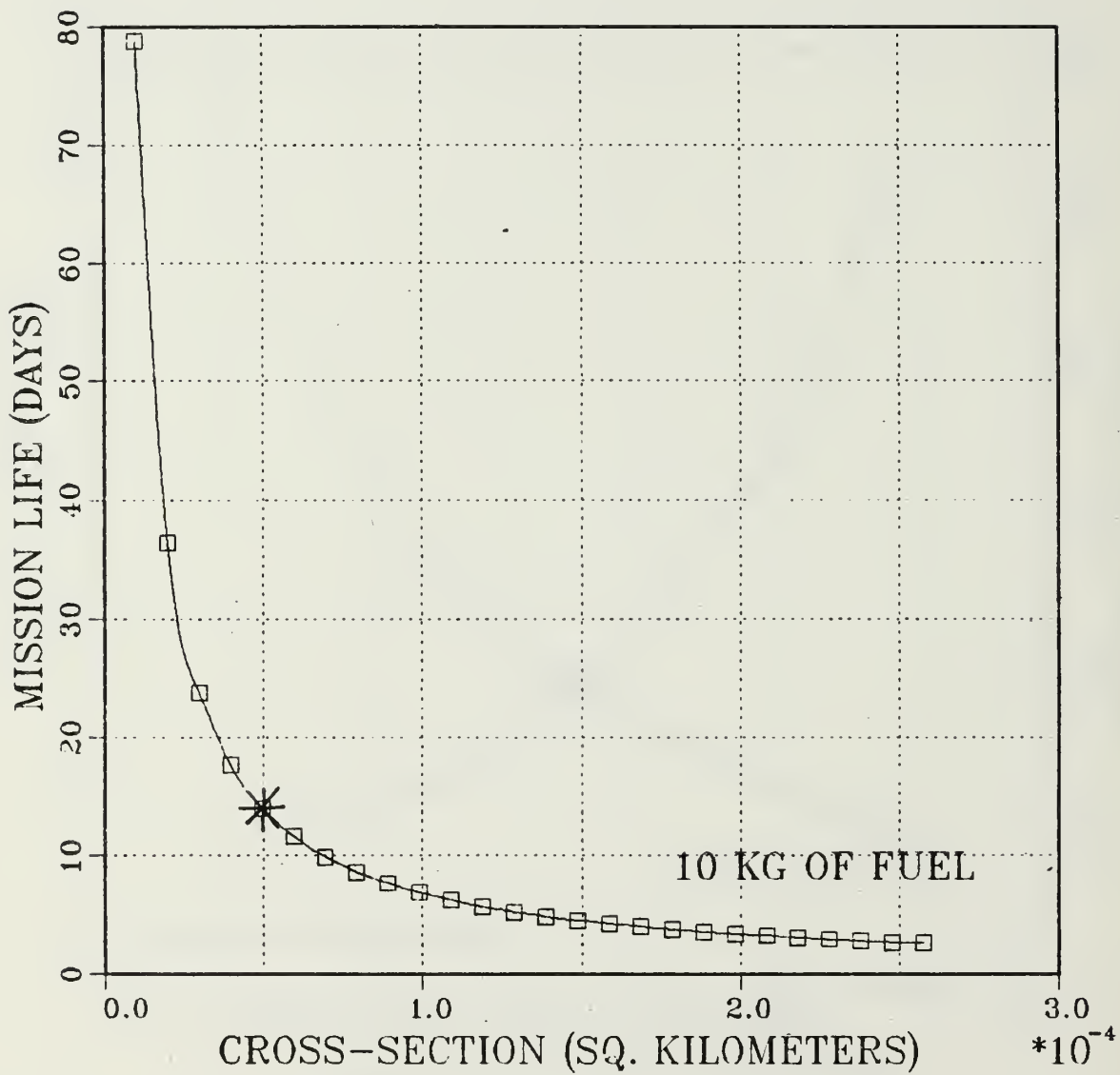


Figure 33. Mission Life versus Cross-Sectional Area (10 kg of Fuel)

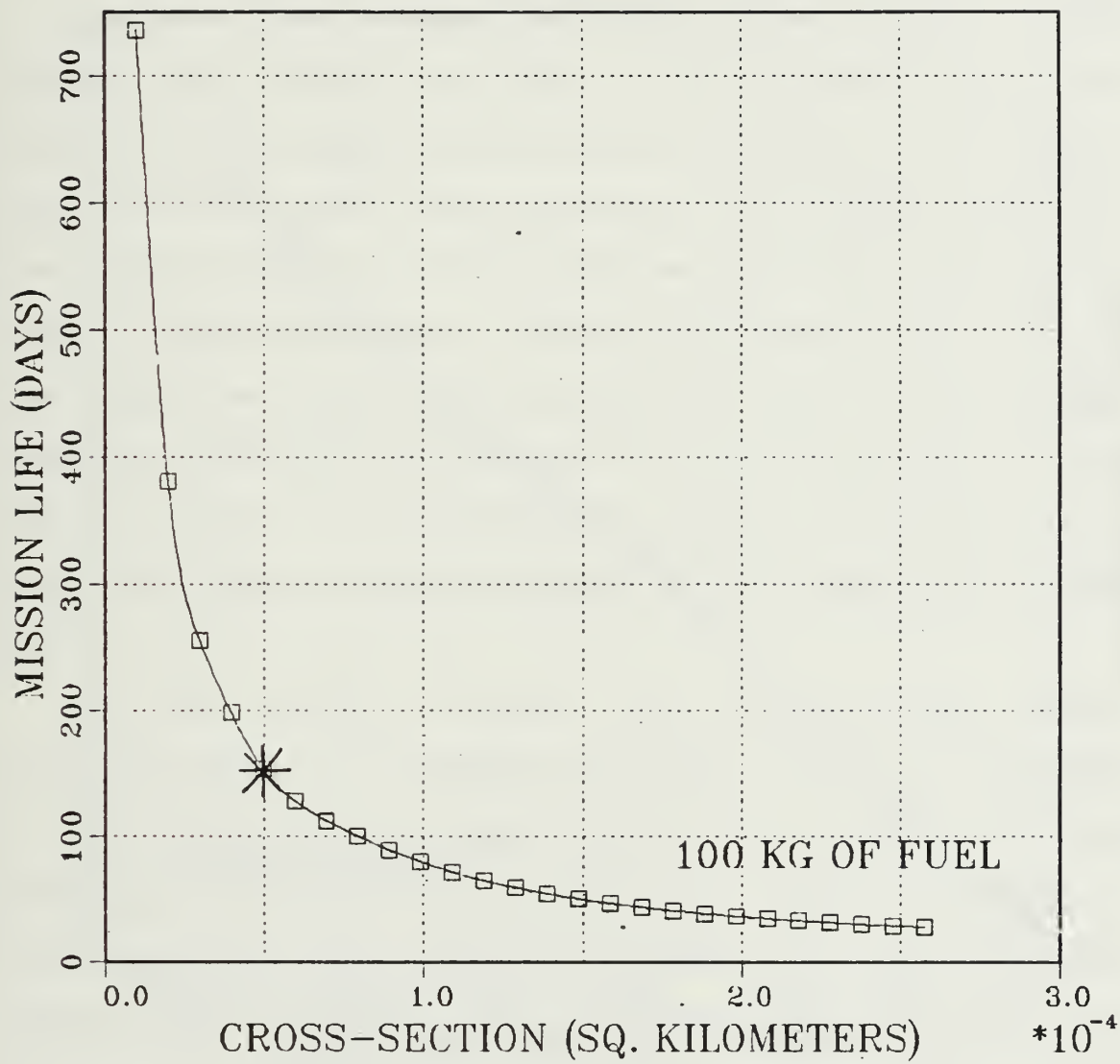


Figure 34. Mission Life versus Cross-Sectional Area (100 kg of Fuel)

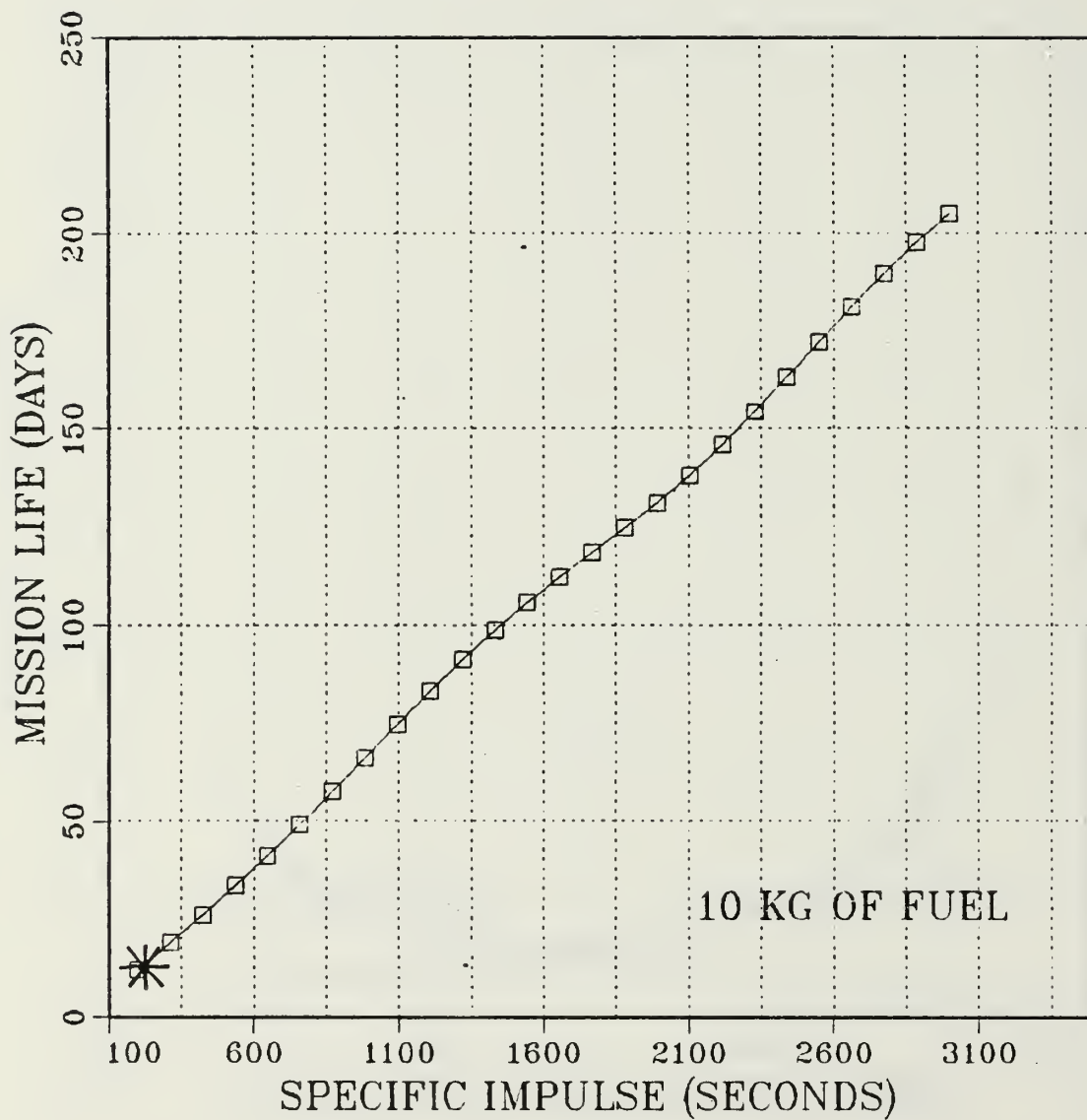


Figure 35. Mission Life versus Specific Impulse (10 kg of Fuel)



34. Figure 33 is the 10 kg fuel case and Figure 34 the 100 kg case. In both cases, A was varied from 0.000010 to 0.0001000 square kilometers. The ranges mapped by these plots are 80 to 0.64 days and 736.29 to 108.7 days, respectively.

Figure 35 is the analysis of motor specific impulse SPI varying from 200 to 3000 with 10 kg of initial fuel. The apparent linear shape of the SPI plot is due to its inverse multiplicative action and the range of the constant DEL (14) over which it acts. As SPI increases, the drag compensating fuel is more effective. Linearly increasing SPI has the same effect as starting at the default value \* on the cross-sectional plots and moving along the plot to the left. Note that the shape of cross-sectional mission life plot in this range is closer to the expected mirror image of the SPI plot.

As noted earlier, mission life plots showing "knees" have significance to research and design studies. The knees in the cross-sectional area mission life plots are very pronounced. Less distinctive knees are seen in the mission-life plots of the decimetric solar flux and the drag coefficient. The default value of the cross-sectional area is right in the knee range of the predicted mission-life plots, as seen in Figures 34 and 35.

The final input variable in the second category is the initial propellant mass W. The expected mission life of a

drag compensating satellite as fuel is increased linearly should be a linear increase in the predicted mission life. A given amount of fuel produces a certain mission life. Twice that amount of fuel in the same general configuration should produce about twice the mission life. The expected shape of the sensitivity analysis plot of predicted mission life for linearly increasing initial propellant mass is a approximately straight line. Figure 36 is the result of varying  $W$  on mission life. The plot is approximates a straight line as expected. The ripples are probably due to geopotential-induced orbital-drift or to movement of the atmospheric density-bulge during mission life.

The results of the sensitivity and trend analysis mission-life plots for  $CD$ ,  $A$ ,  $D$ ,  $SPI$ , and  $W$  agree with expectations. All input variables in the second category have been examined. The next input variables to be examined are in the third category.

Consider now the input variables that affecting the depth of penetration of the satellite into the atmosphere at perigee. The variables that affect the satellite altitude at perigee are the semi-major axis and the orbital eccentricity. These variables show the most pronounced effects on mission life. The real-world effect on mission life when linearly changing the altitude at perigee is an exponential increase in mission life. The effect of varying

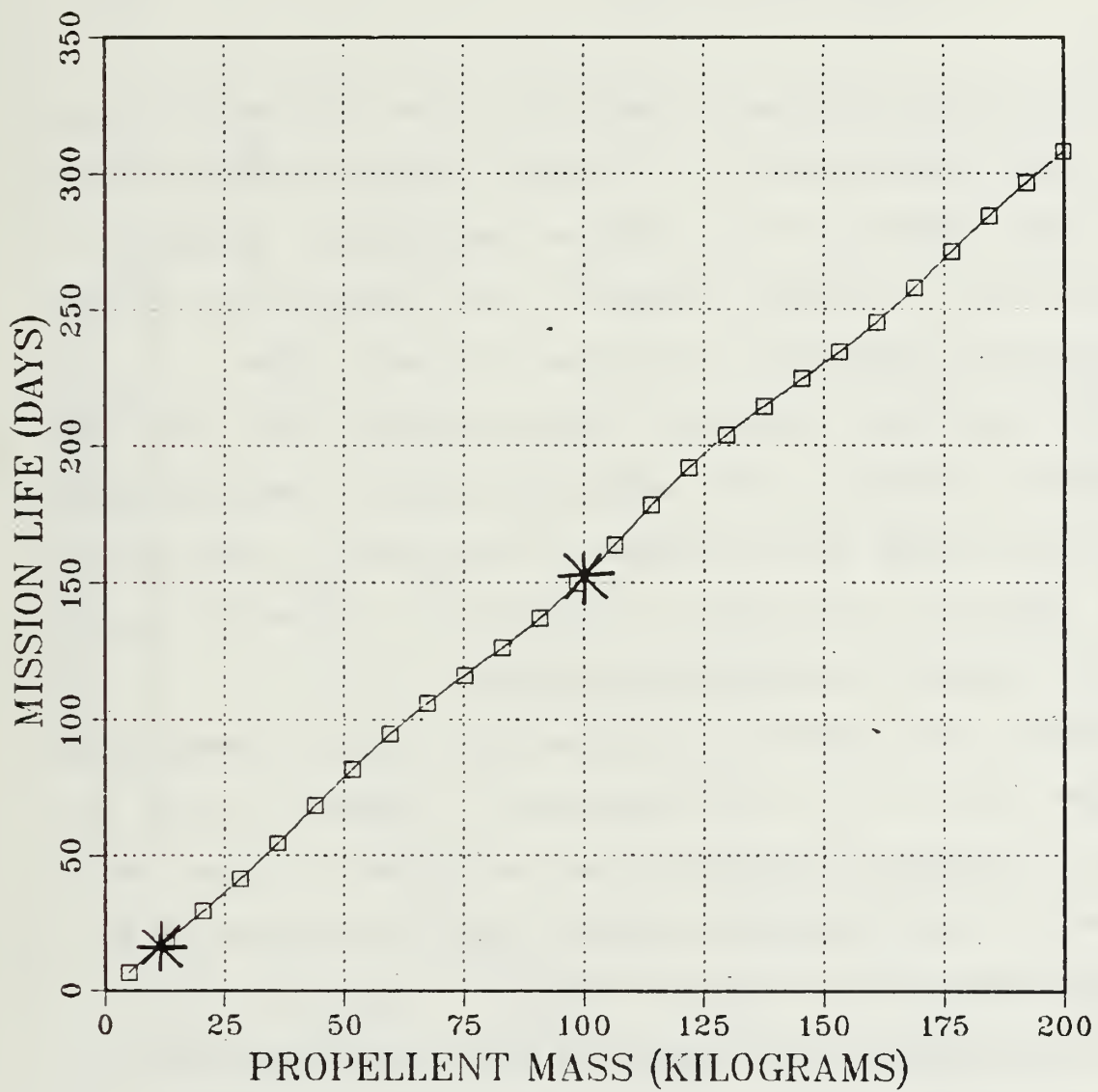


Figure 36. Mission Life versus  
Initial Propellant Mass

the eccentricity and the semi-major axis on the altitude at perigee is summarized by

$$r_p = a * (1 - e) \quad (15)$$

Here,  $r_p$  is the radius at perigee,  $a$  the semi-major axis, and  $e$  the eccentricity. A linear increase in the semi-major axis results in a modified exponential increase in mission life. A linear increase of the eccentricity results in a modified exponential decrease in mission life.

The propellant longevity model computes the satellite altitude at perigee in the subroutine SALT. The subroutine DRAG then passes the altitude at perigee to the routine JAC60 where it is used to develop an exponent for an empirical model of atmospheric density.

Mission life results of varying the orbital eccentricity ES from 0.01 to 0.1 are presented in Figures 37 and 38. Figure 37 is the 10 kg fuel case, and Figure 38 the 100 kg fuel case. The predicted mission life ranges from 14 to 0 days in Figure 37, and 150 to 0 days in Figure 38.

An analysis of the semi-major axis A0 is presented in Figure 39 with a range of 1.025 to 1.175 earth radii. In this case, 1 kg of fuel is allocated initially. The resulting mission life is from 0 to 384 days.

The plots of mission life resulting from varying the semi-major axis A0 and the orbital eccentricity ES, show

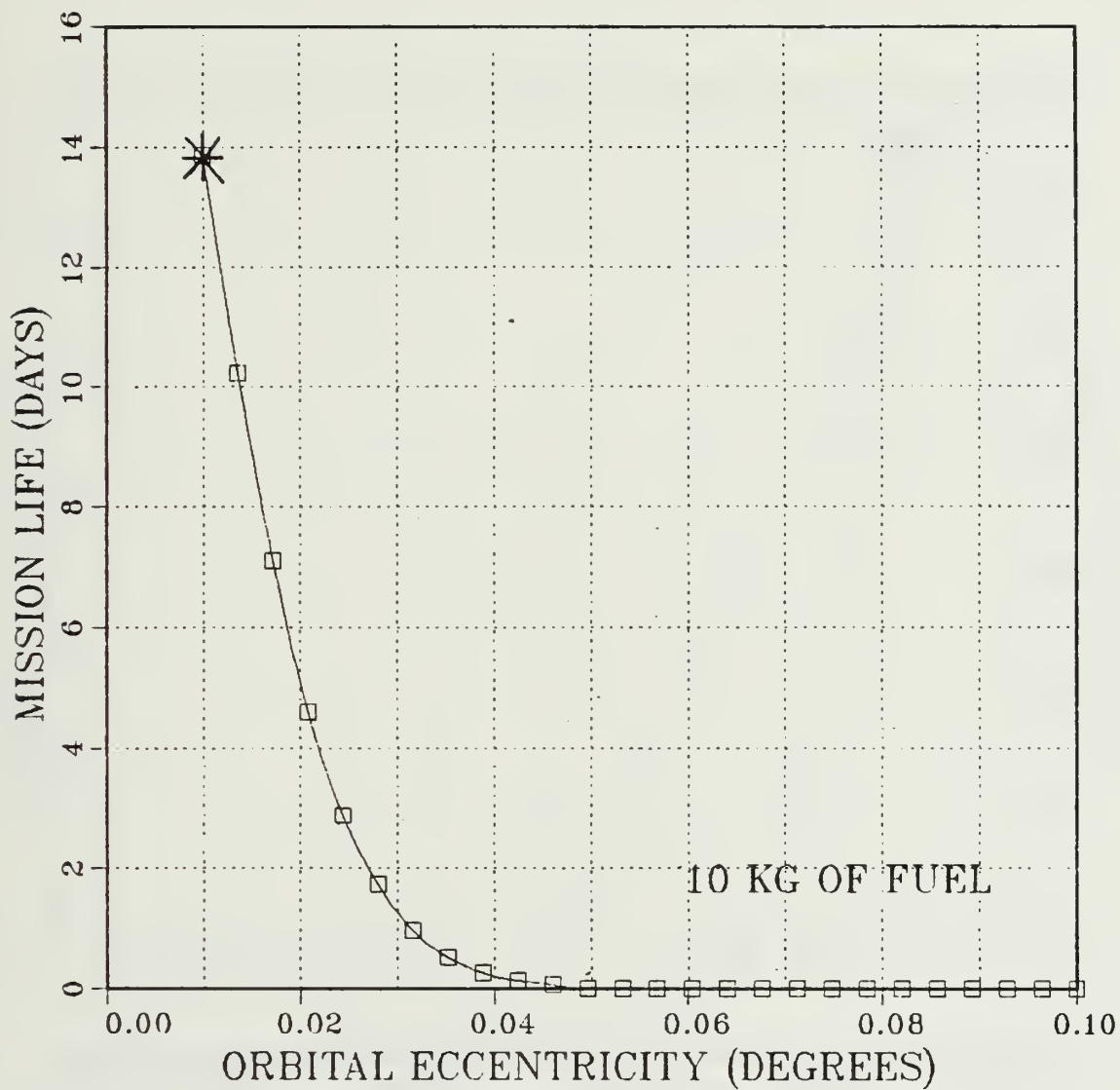


Figure 37. Mission Life versus Orbit Eccentricity (10 kg of Fuel)



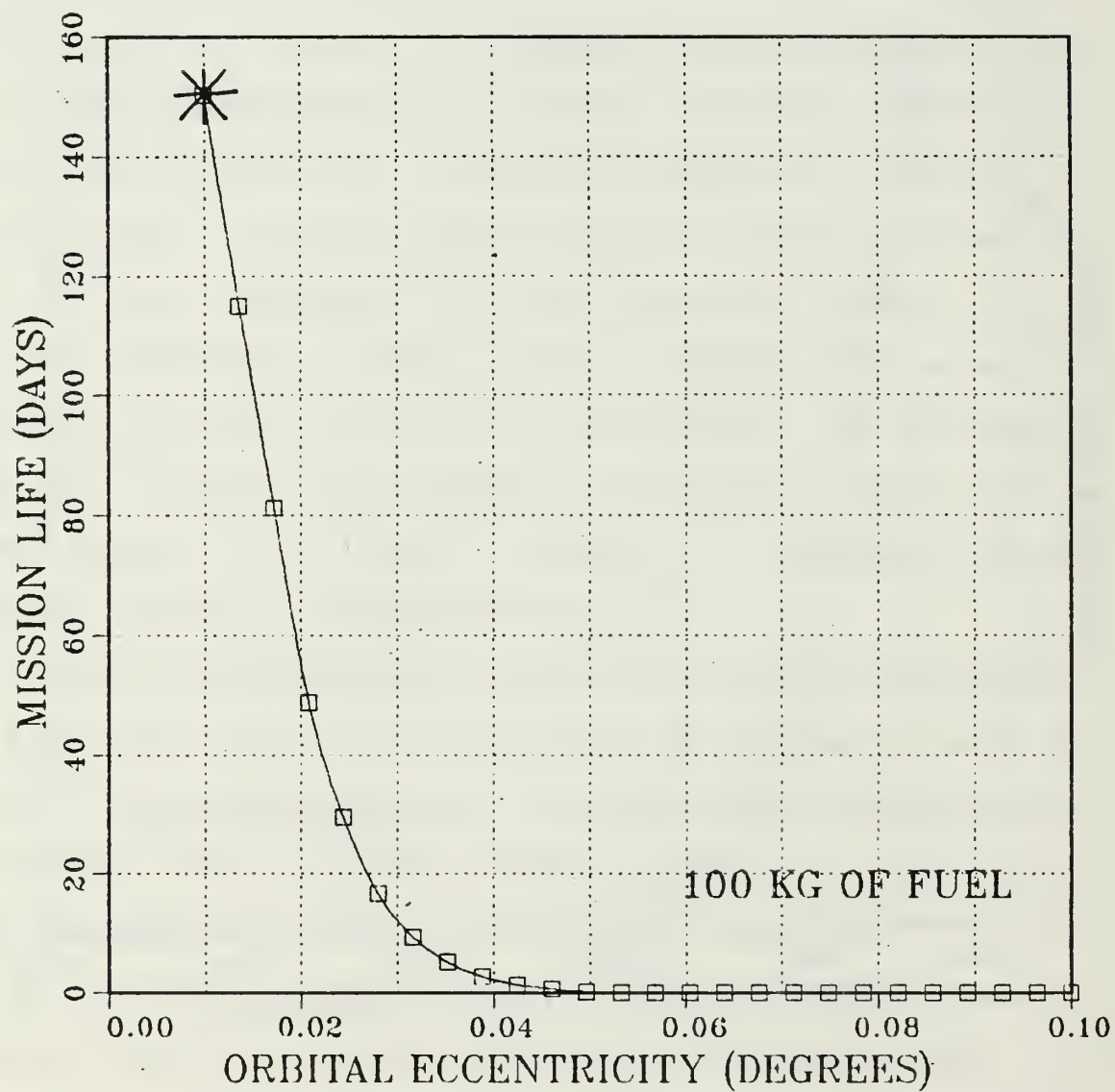


Figure 38. Mission Life versus Orbit Eccentricity (100 kg of Fuel)

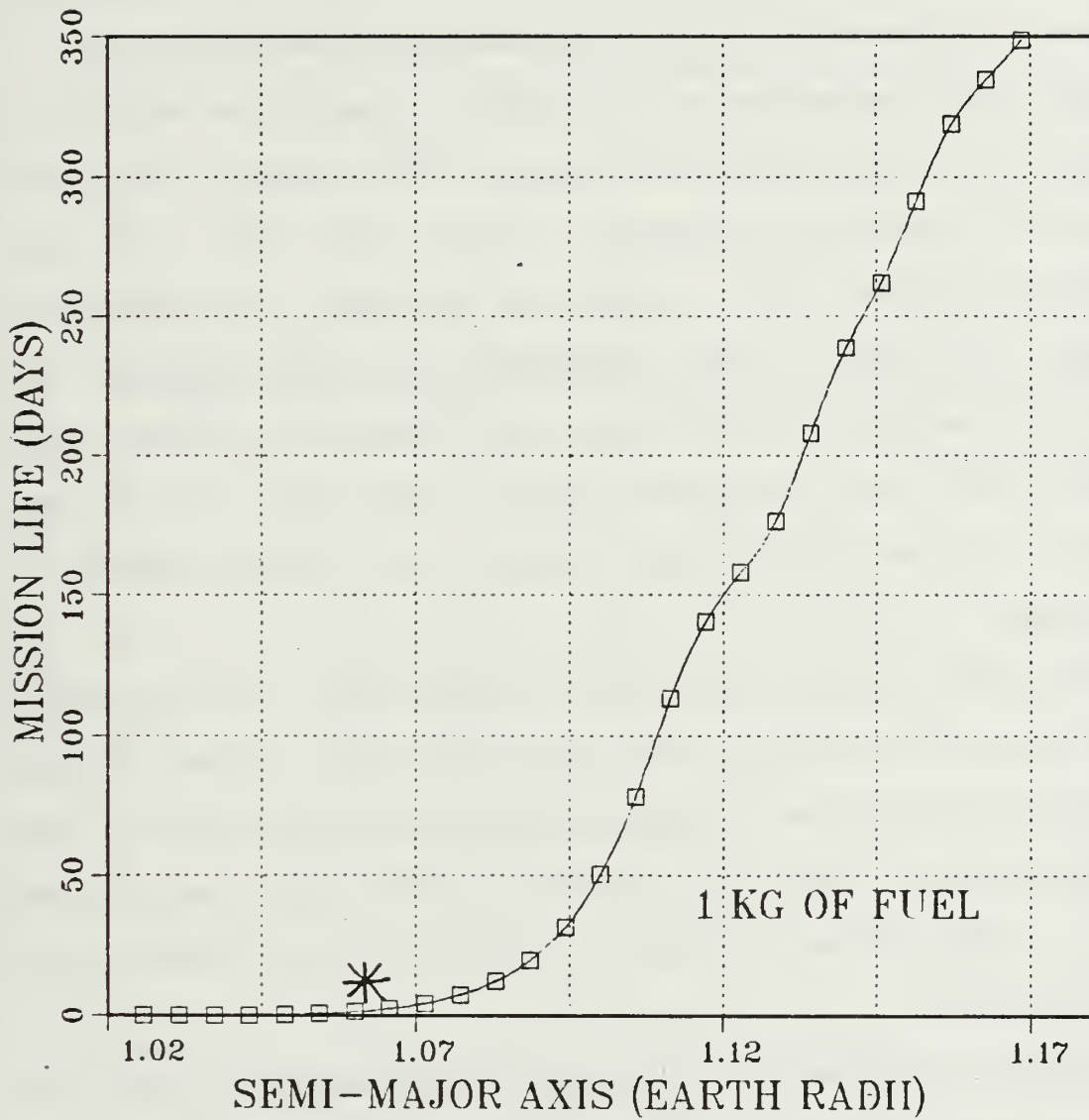


Figure 39. Mission Life versus Semi-Major Axis (1 kg of Fuel)

major knees in their curves. The \* symbol indicates the default value of the varied element. Note that the amount of fuel used in the analysis of the semi-major axis is 1 kg. The use of the usual 10 kg produces a plot that exceeding the reasonable range of mission life. The results shown in Figures 37 through 39 are in agreement with expectations.

The input variables in the fourth category (no effect on mission life) are the mean anomaly ETU, initial satellite weight WT, average decimetric solar flux FBAR, and the geomagnetic index AKP. FBAR and AKP have no effect on mission life due to the limitations of the Jacchia J60 atmosphere model. In the real world these two factors may combine with the decimetric solar flux F107 to produce changes in the atmospheric density of three orders of magnitude.

The model theory used by Dr. Parks [Ref. 1] to predict the propellant longevity of a satellite doing intrack micro-thrusting to overcome atmospheric drag is independent of the satellite mass. The fuel required to overcome drag-induced orbital energy loss is based strictly on the satellite's shape and size.

Figure 40 presents the sensitivity analysis plot of predicted mission life as a result of varying the satellite initial mass WT. The plot is a straight horizontal line, as expected.

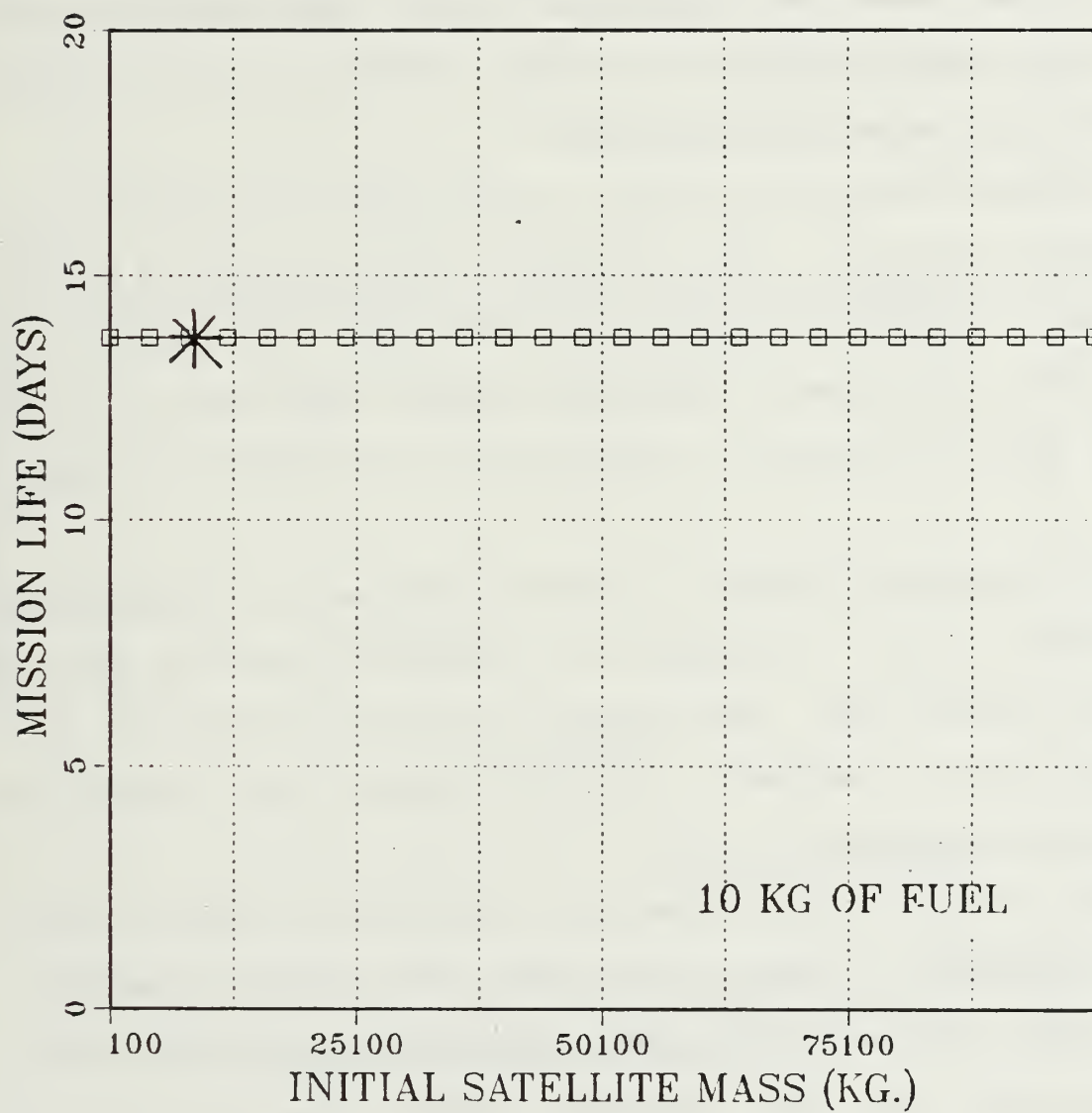


Figure 40. Mission Life versus Satellite Mass (10 kg of Fuel)

The final analysis is concerned with the mean anomaly. In the near-circular default orbit, the mean anomaly and the eccentric anomaly are nearly the same. The Keplerian mean anomaly functions to position the satellite in its designated orbit. For a mission life lasting several days, it should make no difference where the satellite is initially positioned in its orbit. Rather, it's the orbit itself that makes the difference.

Analysis plots of the mean anomaly ETU are presented in Figures 41 and 42. The incremented range is from 0 to 179 degrees. Figure 41 is the 10 kg fuel case and Figure 42 is the 100 kg fuel case. Predicted results range from 13.74 to 13.87 days in Figure 41, and from 149 to 154 days in Figure 42.

The results in Figure 41 are as expected, an approximate horizontal line. In Figure 42, a valley is seen in the 40 to 120 degree range. The valley is only four days deep, but is difficult to explain. Further research may reveal its underlying mechanism.

The results of the trend and sensitivity analysis have been presented. Mission life has been found to be most sensitive to those factors that affecting the orbital radius at perigee. The main unexpected results are found in the analysis of the inclination and the mean anomaly. The pattern of many peaks and valleys found in the 100 kilogram fuel case (Figures 23, 24 and 25) warrants further research.



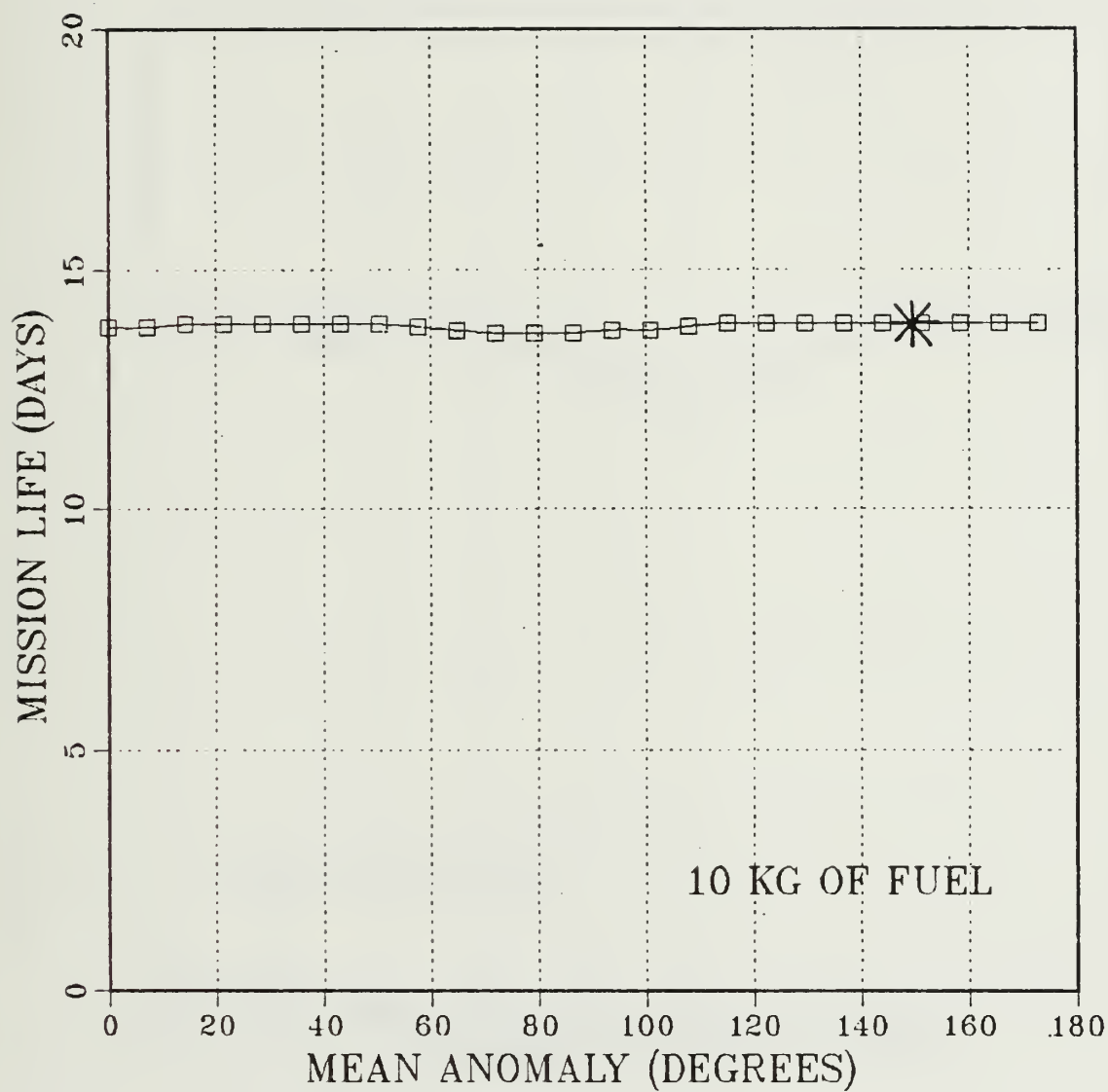


Figure 41. Mission Life versus Mean Anomaly (10 kg of Fuel)

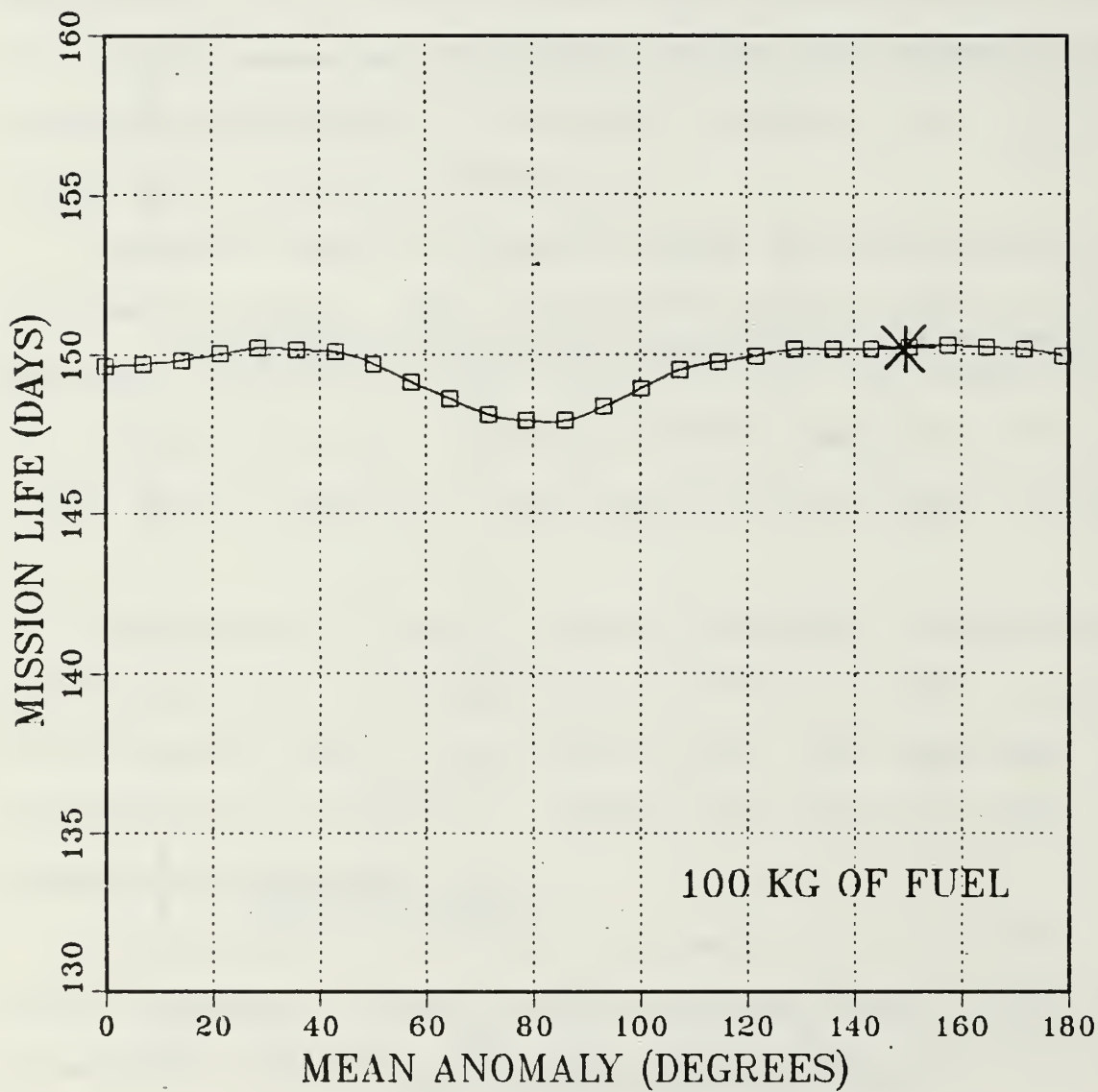


Figure 42. Mission Life versus Mean Anomaly (100 kg of Fuel)

The four day dimple seen in the mean anomaly plot (Figure 41) also warrants further study.

## V. SUMMARY

This final chapter presents the summary and conclusions of the thesis. Recommendations for model use are also given.

The low-earth-orbit satellite propellant longevity model has been tested in a sensitivity analysis. Based on the results of the sensitivity analysis the model reasonableness is confirmed. The first chapter presented a model overview, model motivation, and the process employed to verify the model. Chapter I also discusses some changes made to the model computer program for the IBM 3033 at the Naval Postgraduate School. Chapter II presents the orbital mechanics and atmospheric concepts as background for model understanding and it's operation. In Chapter III the model and its computer program were discussed. Operating instructions specific for the computer program use at the Naval Postgraduate School are also presented there. The sensitivity analysis results are presented in Chapter IV.

The propellant longevity model predicts how long the fuel of a low-earth-orbital satellite thrusting to overcome atmospheric drag will last before starting uncontrolled decay into the atmosphere. Model verification reasonableness tests reveal no inconsistencies with the established theory. The results of the sensitivity analysis are

therefore in agreement with the expectations. The irregularities in the model predictions (occurring with inclinations of less than 22.5 degrees) are due to computer round off error, not the model itself.

The propellant longevity model currently uses the Jacchia J60 model atmosphere. This atmosphere model may significantly reduce the real-world accuracy of predicted mission lifetimes.

The short term confidence factor in predicted mission life might be increased by the employment of the Jacchia J77 model atmosphere. One drawback to the use of the Jacchia J77 model atmosphere is that it may double the computer run time.

One solution to the trade-off of increased accuracy of the Jacchia J77 model versus the shorter computation time of the Jacchia J60 model, would be to allow the user to select an atmosphere option.

Transportation of the computer program of the model to an IBM AT could provide more flexibility in preliminary design analysis.

This model is a tool for the low-earth-orbit satellite system planner in designing and managing satellite systems that have precise orbital element control requirements. These systems are those with SDI and reconnaissance missions.



This model, with the addition of the Jacchia J77 model atmosphere and a subroutine to calculate fuel required to compensate for aspherical geopotential forces, could be used to optimize SDI defensive satellite constellation design.

Existing real-world data to compare with the model predictions is limited to a very classified system. The final step in verifying the propellant longevity model would be to make this comparison test.

[illegible]

REFERENCE 8 FLEAGLE, R.G., "AN INTRODUCTION TO ATMOSPHERIC PHYSICS", ACADEMIC PRESS, 1980.

MODULE	FUNCTION
PLEP	SYSTEM INITIALIZATION AND CONTROL. CALLED BY: CALLS: (SUBROUTINES) TIMES CALLED ****              SNALYS              1 KOZAI              1/ITERATION
SNALYS	SENSITIVITY MODE SCANNED ELEMENT GENERATOR. CALLED BY: CALLS: (SUBROUTINES) TIMES CALLED PLEP              ****              ****
KOZAI	SYSTEM WORKHORSE, DRIVER AND RECORD KEEPER. NSWC TR 83-135. CALLED BY: CALLS: (SUBROUTINES) TIMES CALLED PLEP              BRAUER              1 PERIOD             1 MEAN               1 THRST              1/(SAT.REV.) GEOP               1/(SAT.REV.) DRAG               1/(SAT.REV.)
BRAUER	CONVERTS NAVSPASUR BROUWER MEAN ORBITAL ELEMENT SET INTO A BROUWER OSCULATING ORBITAL SET. A CODING OF THE BROUWER-LYDDANE THEORY. NSWC TR 83-107, 83-135, BROUWER (REF. 1). CALLED BY: CALLS: (SUBROUTINES) TIMES CALLED KOZAI             ****             ****
POSVEL	COMPUTES SATELLITES POSITION AND VELOCITY IN INERTIAL SPACE FROM THE OSCULATING ORBITAL ELEMENTS. NSWC TR 82-387 PP. 24-25. CALLED BY: CALLS: (SUBROUTINES) TIMES CALLED SATLOC             NWTRPH             1
NWTRPH	A NEWTON-RAPHSON SOLUTION TO KEPLERS EQUATION. NSWC TR 82 387 P 23. CALLED BY: CALLS: (SUBROUTINES) TIMES CALLED POSVEL             ****             ****
FUNCTIONS XSPA-XSPR	COMPUTES SHORT PERIODIC EFFECTS ON ORBITAL ELEMENTS. CALLED BY SUBROUTINE MEAN. NSWC 81-456 PAGES 9-11 AND NSWC TR 83 243 REF 3. CALLED BY: CALLS: (SUBROUTINES) TIMES CALLED MEAN               ****             ****
MEAN	USES THE WALTER METHOD TO CONVERT OSCULATING ORBITAL ELEMENTS TO KOZAI LIKE MEAN ELEMENTS USING FIRST ORDER PERIODIC VARIATIONS. SIMILAR TO THE METHOD IN NSWC TR 83 135 PP 16-18. CALLED BY: CALLS: (FUNCTIONS) TIMES CALLED KOZAI              XSPA-XSPR          1
GEOP	COMPUTES AVERAGED SECULAR CHANGES IN KOZAI MEAN ELEMENTS INDUCED BY GRAVITATIONAL FIELD THROUGH FOURTH ZONAL HARMONIC (J2-J4 TERMS). NSWC TR 81- 456. EQS.(2.5). CALLED BY: CALLS: (SUBROUTINES) TIMES CALLED KOZAI             ****             ****
SOLOC	COMPUTES THE RIGHT ASCENSION AND THE DECLINATION

```

*      OF THE SUN FOR THE MODEL ATMOSPHERE. NSWC TR 81-
*      456 PP. 20-21.
*      CALLED BY:      CALLS:
*                      (SUBROUTINES)  TIMES CALLED
*                      ****          ****
*      DRAG
*
* PERIOD      COMPUTES THE ANOMALISTIC PERIOD.
*      CALLED BY:      CALLS:
*                      (SUBROUTINES)  TIMES CALLED
*                      ****          ****
*      KOZAI
*
* DRAG      COMPUTES DRAG EFFECTS AND FUEL MASS DECREMENT
*           REQUIRED TO MAINTAIN THE SEMIMAJOR AXIS VIA
*           IN TRACK MICROTHRUSTING. NSWC TR 82-243 EQ.
*           58. THIS ONE EQUATION IS THE HEART OF THE MODEL.
*      CALLED BY:      CALLS:
*                      (SUBROUTINES)  TIMES CALLED
*                      ****          ****
*      KOZAI      SOLOC      1
*                  SATLOC     3
*                  SALT       1
*                  JAC60      3
*                      (FUNCTIONS)
*                      MMBSIR   1
*                      XSPM     1
*
* JAC60      COMPUTES ATMOSPHERIC DENSITY BASED ON THE JACCHIA
*           (60) MODEL ATMOSPHERE. CALLED THREE TIMES TO
*           COMPUTE DIFFERENT VALUES FOR THE DENSITY FOR EACH
*           REVOLUTION: MAX, MIN AND OP.
*      CALLED BY:      CALLS:
*                      (SUBROUTINES)  TIMES CALLED
*                      ****          ****
*      DRAG
*
* THRST      CALCULATES CHANGES TO KOZAI ORBITAL ELEMENTS IF
*           AN ORBITAL ADJUST IS SCHEDULED. CALCULATES THE
*           MASS OF FUEL USED TO PERFORM THE ADJUST.
*           NSWC TR 83-31 EQ. 16, AND NSWC TR 81-456 EQ. 2-26
*      CALLED BY:      CALLS:
*                      (SUBROUTINES)  TIMES CALLED
*                      ****          ****
*      KOZAI
*
* SALT      COMPUTES SATELLITE ALTITUDE. NSWC TR 81-456 EQ.
*           4.34.
*      CALLED BY:      CALLS:
*                      (SUBROUTINES)  TIMES CALLED
*                      ****          ****
*      DRAG
*
* SATLOC     COMPUTES SATELLITE LOCATION. RIGHT ASCENSION,
*           DECLINATION AND ITS GEOMAGNETIC LATITUDE.
*      CALLED BY:      CALLS:
*                      (SUBROUTINES)  TIMES CALLED
*                      ****          ****
*      DRAG      POSVEL      1
*
* FUNCTION   COMPUTES BESSEL FUNCTIONS. AN IMSL ROUTINE
* (MMBSIR)   RESIDENT ON THE IBM 3800. THIS WILL VARY WITH
*           LOCAL INSTALLATIONS.
*      CALLED BY:      CALLS:
*                      (SUBROUTINES)  TIMES CALLED
*                      ****          ****
*      DRAG

```

\*\*\*\*\*

```

*
* *****
* *****
* **                                **
* **      PROGRAM PLEP              **
* **                                **
* *****
* *****

```



# PROGRAM PLEP

```

*
*****
* THIS MODULE IS THE INPUT, CONTROL AND INITIALIZATION SECTION FOR THE
* REST OF THE SYSTEM. IT ACCEPTS THE 'FIVE CARD' FORMAT OF NAVSPASUR
* AS THE BROUWER MEAN ORBITAL ELEMENT SET. THE SPECIFIC SATELLITE
* PARAMETERS ARE ENTERED. ATMOSPHERIC MODEL ELEMENTS ARE INITIALIZED.
* FINALLY, SYSTEM CONTROL CONSTANTS ARE SET TO GENERATE THE OUTPUT. A
* FURTHER DESCRIPTION OF THE ABOVE FUNCTIONS IS CONTAINED IN THE
* DESCRIPTION OF ARGUMENTS.
*****

```

## DESCRIPTION OF ARGUMENTS

### INPUT ARGUMENTS

#### PROGRAM CONTROLS

```

ITER1_____ INTEGER, MAXIMUM NUMBER OF REVOLUTIONS DESIRED
              FOR CONSIDERATION. A CONTROL PARAMETER.
ITER2_____ INTEGER, ORBITAL PRINT FREQUENCY. A CONTROL
              PARAMETER. SETTING ITER2 = TO 100 WILL REDUCE
              TABULAR OUTPUT BY ONLY PRINTING OUTPUT EVERY 100
              ORBITS.
PSENS_____ INTEGER, CONTROL PARAMETER. PSENS=1 SPECIFIES
              SENSITIVITY ANALYSIS MODE. PSENS=0 SPECIFIES
              STANDARD PROPELLANT LONGEVITY MODE.
IET_____   INTEGER, CONTROL PARAMETER. IET=1 PRINTS THE
              INITIAL ANOMALISTIC PERIOD. IET=0 SUPPRESSES PRINT.
NOA_____   INTEGER, NUMBER OF SCHEDULED ORBIT ADJUSTS. THIS
              IS A CONTROL PARAMETER WITH ALLOWED VALUES FROM
              ZERO TO TEN. THE ONLY ORBIT ADJUSTS CURRENTLY
              SUPPORTED ARE CHANGES TO THE SEMI-MAJOR AXIS.
IRV(K)_____ INTEGER ARRAY. (K=10 MAX). THE ELEMENTS OF THE
              ARRAY SPECIFY THE REVOLUTION NUMBER DURING WHICH
              EACH OF THE ORBITAL ADJUSTS ARE PERFORMED. K MUST
              EQUAL NOA.
DA(K)_____ INTEGER ARRAY. (K=10 MAX) THE ELEMENTS OF THE
              ARRAY SPECIFY THE CHANGE IN KILOMETERS OF THE
              SEMIMAJOR AXIS. K MUST EQUAL NOA.
PSIZE_____ INTEGER, CONTROL PARAMETER THE NUMBER OF INTERVALS
              IN THE SENSITIVITY ANALYSIS.

```

#### SATELLITE PHYSICAL PARAMETERS

```

SPI_____ REAL, MOTOR SPECIFIC IMPULSE IN SECONDS. AGRAWAL
              (REF. 2:PP. 163-166) GIVES SAMPLE VALUES.
WT_____ REAL, INITIAL MASS OF THE SATELLITE IN KILOGRAMS.
              (INCLUDING THE FUEL MASS)
W_____ REAL, INITIAL MASS OF FUEL IN KILOGRAMS.
CD_____ REAL, DRAG COEFFICIENT OF THE SATELLITE.
              DIMENSIONLESS. NORMALLY VARIES FROM ONE TO
              AROUND THREE, DEPENDING ON VELOCITY, DENSITY,
              COMPOSITION OF ATMOSPHERE AND PHYSICAL DESIGN.
              IS MOST OFTEN SET AT 2.20 FOR ALTITUDES BETWEEN
              200 AND 400 KM. FOR ALTITUDES OF 1000 KM CD IS
              SET AT JUST ABOVE 3.0. JACCHIA (REF. 3:P 2).
A_____ REAL, SATELLITE CROSSESECTIONAL AREA IN SQUARE
              KILOMETERS.

```

#### ATMOSPHERIC SPECIFIC PARAMETERS

```

D_____ REAL, RATIO OF ATMOSPHERIC TO EARTH ANGULAR
              ROTATION RATES. A CONSTANT IN EQUATION 11 OF
              NSWC TR 83-243. UNITLESS. THE ACTUAL VALUE WILL
              DEPEND ON LATITUDE AND ALTITUDE. RANGE .8 TO 1.0.
F107_____ REAL, DECIMETRIC SOLAR FLUX. JACCHIA (REF 4 & 5).
              THIS VALUE IS USED BY THE INDUSTRY TO REPRESENT
              THE XUV FLUX IN THE THERMOSPHERE. THE XUV FLUX

```



\* IS THE FACTOR CREATING THE SUN FACING DIURNAL \*  
 \* DENSITY AND TEMPERATURE BULGE IN THE THERMOSPHERE. \*  
 \* IT IS DIRECTLY RELATED TO SOLAR ACTIVITY. IT \*  
 \* VARIES WITH THE 27 DAY SLOAR ROTATION AND 11 YEAR \*  
 \* SUNSPOT ACTIVITY CYCLE. ORR (REF. 6:APPENDIX B) \*  
 \* INDICATES RANGES OF 73.3 TO 242.9. XUV FLUX AND \*  
 \* THE GEOMAGNETIC HEATING EFFECTS CAN CAUSE \*  
 \* DENSITY TO CHANGE BY THREE ORDERS OF MAGNITUDE AT \*  
 \* 600 KILOMETERS. THE 10.7 CM FLUX IS DECTABLE FROM \*  
 \* THE GROUND AND THEORETICALLY PARELLELS THE XUV \*  
 \* FLUX. THE XUV FLUX IS NOT MEASUREABLE FROM THE \*  
 \* GROUND DUE TO NEAR COMPLETE UPPER ATMOSPHERE \*  
 \* ABSORPTION. \*  
 \* FBAR\_\_\_\_\_ REAL, THE AVERAGE 10.7 CM FLUX. THE EFFECTS OF THE \*  
 \* XUV HEATING DO NOT RETURN TO THE ORIGINAL UNHEATED \*  
 \* CONDITION IN AN EARTH ROTATION. A HIGH HEATING \*  
 \* CONDITION WILL HAVE SOME LONGER TERM EFFECTS. \*  
 \* THESE LONGER TERM EFFECTS ARE MODELED HERE BY \*  
 \* TAKING A MOVING 90 DAY 10.7 CM AVERAGE. \*  
 \* FBAR RANGES FROM A LOW OF 73 TO A HIGH OF 230. \*  
 \* AKP\_\_\_\_\_ REAL, GEOMAGNETIC ACTIVITY INDEX, JACCHIA (REF. 4 \*  
 \* AND 5). GEOMAGNETIC ACTIVITY ALSO CAUSES HEATING \*  
 \* IN THE THERMOSPHERE. THE EXACT MECHANISM IS NOT \*  
 \* UNDERSTOOD. IDEALLY QUEIT MAGNETIC CONDITIONS \*  
 \* CORRESPOND TO AN INDEX OF 0. MAXIMUM ACTIVITY FOR \*  
 \* WHICH SIGNIFICANT DATA EXISTS ARE RELATED TO AN \*  
 \* INDEX OF BETWEEN 6 AND 7. NORMAL ACTIVITY \*  
 \* INDICATES AN INDEX OF BETWEEN 1 AND 2. \*  
 \* TVE\_\_\_\_\_ REAL, TIME OF VERNAL EQUINOX PASSAGE. USED TO \*  
 \* TRANSFORM TIME FROM INERTIAL TO EARTH FIXED \*  
 \* REFERENCE FRAMES. FOUND IN THE ASTRONOMICAL ALMANAC \*  
 \* FOR THE YEAR OF CHOICE. (MODIFIED JULIAN DAYS). \*  
 \* A DESCRIPTION IS IN TAFF (REF. 7:PP. 103-104). \*  
 \*  
 \* NAVSPASUR ORBITAL ELEMENTS \*  
 \*  
 \* THE NAVSPASUR ORBITAL ELEMENT SET IS THE BROUWER MEAN \*  
 \* ELEMENT SET. BROUWER (REF. 1) IS THE BEST DESCRIPTION FOR \*  
 \* THIS ELEMENT SET. \*  
 \* UJD\_\_\_\_\_ REAL, TIME OF EPOCH IN MODIFIED JULIAN DAYS. \*  
 \* THIS IS THE TO IN THE EQUATION FOR THE MEAN ANOMALY \*  
 \* M. (  $M = M_0 + N * (T - T_0)$  ). TAFF (REF. 7). \*  
 \* ETU\_\_\_\_\_ REAL, INITIAL MEAN ANOMALY M0. MEASURED IN DEGREES \*  
 \* HAS A RANGE OF 0 TO 360. \*  
 \* GO\_\_\_\_\_ REAL, MEAN ARGUMENT OF PERIGEE. RANGES FROM 0 TO \*  
 \* 360 DEGREES. NOT DEFINED FOR CIRCULAR ORBITS. \*  
 \* HO\_\_\_\_\_ REAL, MEAN RIGHT ASCENSION OF THE ASCENDING NODE. \*  
 \* RANGES FROM 0 TO 360 DEGREES. NOT DEFINED FOR \*  
 \* EQUITORIAL ORBITS \*  
 \* ES\_\_\_\_\_ REAL, MEAN ECCENTRIY. FOR THIS THEORY RANGES FROM \*  
 \* 0.01 TO 0.1. THESE ARE LOW ECCENTRICITY ORBITS. \*  
 \* XI\_\_\_\_\_ REAL, MEAN INCLINATION. RANGES FROM 0 TO 180 \*  
 \* DEGREES. VALUES OF 0 AND 180 ARE IN EQUITORIAL \*  
 \* ORBITS. INCLINATION OF 90 IS A POLAR ORBIT. RANGES \*  
 \* OF 0 TO 90 ARE IN PROGRADE ORBITS. INCLINATIONS \*  
 \* 90 TO 180 ARE IN RETROGRADE ORBITS. FOR AN \*  
 \* INCLINATION OF 0 OR 180 HO IS NOT DEFINED. THERE \*  
 \* IS NO ASCENDING NODE IN EQUITORIAL ORBITS. \*  
 \* RND\_\_\_\_\_ REAL, RATE OF CHANGE OF MEAN MOTION. MEASURED IN \*  
 \* REVOLUTIONS PER (DAY SQUARED). VALUES OF .00001 \*  
 \* AND ABOVE ARE CONSIDERED SIGNIFICANT WHEN \*  
 \* ATMOSPHERE INDUCED. REFERENCE (TAFF) P137 \*  
 \* ESD\_\_\_\_\_ REAL, ECCENTRICITY DECAY RATE MEASURED IN \*  
 \* INVERSE SECONDS. \*  
 \* AO\_\_\_\_\_ REAL, KAULA SEMIMAJOR AXIS. MEASURED IN \*  
 \* MEAN EQUITORIAL EARTH RADII (6378.165 KM). RANGES \*  
 \* FROM 1.02594 TO 1.16847 TO MAINTAIN AN ALTITUDE OF \*  
 \* 100 TO 1000 KM FOR RADIUS AT PERIGEE. THIS MUST BE \*  
 \* CAREFULLY SCALED TO ECCENTRICITY TO PREVENT \*  
 \* CRASHING THE SATELLITE. PERIGEE ALTITUDES ABOVE \*

```

*           600 KM ARE ESSENTIALLY ABOVE THE ATMOSPHERE.
* ADOT_____REAL, SEMIMAJOR AXIS DECAY RATE.
*
*
*
*
*
*****
*
* DIMENSION SNSAR(20), SNSMIN(20), IRV(10), DA(10), SNSDEL(20)
*
*****
* THE SET OADJ IS COMMON TO PLEP, KOZAI, THRST AND SNALYS.
*
*****
* COMMON / OADJ / NOA, IRV, DA, SPI, WT, PSENS
*
*****
* THE SET XXXX IS COMMON TO PLEP AND PERIOD.
*
*****
* COMMON / XXXX / IET
*
*****
* THE SET SOLAR IS COMMON TO PLEP AND DRAG.
*
*****
* COMMON / SOLAR / F107 , FBAR , AKP , TVE
* INTEGER PSIZE, PSENS, PSYNS
* REAL MINSN
*
*****
* INITIALIZING CONSTANTS.
*
*****
* DATA R2 / 541.15E-06 / , DEG / 57.295779513D0 / , ROE / 6378.165D0 /
*
*****
* INPUTTING CONTROL PARAMETERS.
*
*****
* READ *, ITER1, ITER2, NOA, PSENS, IET, PSIZE
*
*****
* INPUTTING SATELITE SPECIFIC PARAMETERS.
*
*****
* READ *, CD, A, D, SPI, W, WT
*
*****
* INPUTTING EARTH AND ATMOSPHERIC PARAMETERS.
*
*****
* READ * , F107 , FBAR , AKP , TVE
*
*****
* INITIALIZING BROUWER MEAN ORBITAL ELEMENTS FROM THE NAVSPASUR
* FIVE CARD FORMAT ORBITAL DATA SET.
*
*****
* READ 5 , UJD , ETU , H0 , G0 , ES , XI
* 5 FORMAT ( / 8X, F14.8, 5(1X, F8.4) )
* READ 10 , RND , ESD
* 10 FORMAT ( 20X, F11.9, 19X, E12.5 )
* READ 15 , A0 , ADOT
* 15 FORMAT ( / 8X, F11.5, 1X, E14.7 )
*
*****
* INPUTTING THE REVOLUTION NUMBER AND CORRESPONDING CHANGE IN
* SEMIMAJOR AXIS
*
*****
* IF ( NOA .EQ. 0 ) GO TO 30

```

```

DO 20 K = 1, NOA
  READ *, IRV(K) , DA(K)
20 CONTINUE

```

```

*****
* THIS NEXT SERIES OF CODE SETS THE INITIAL VALUES FOR THE SCANNING *
* ARRAY MATRIX SO AS TO ALLOW THE RECOVERY OF THE ORIGINAL INPUT *
* ELEMENTS IF SENSITIVITY MODE IS NOT SELECTED. *
*****

```

```

30 DO 90 ICN = 1,20
  SNSDEL(ICN) = 1.0
  SNSMIN(ICN) = 0.0
  SNSAR(ICN) = 0.0
90 CONTINUE

```

```

*****
* THE NEXT SERIES OF WRITE STATEMENTS OUTPUTS THE ORIGINAL INPUT *
* PARAMETERS. UNITS ARE SUPPLIED FOR CLARIFICATION. *
*****

```

```

  WRITE(6,98)
  WRITE(6,99)
  WRITE(6,103)
  WRITE(6,99)
  WRITE(6,104) D, F107, FBAR, AKP, TVE
  WRITE(6,105) CD, A, SPI, W, WT
  WRITE(6,106) UJD, ETU, H0, G0, XI
  WRITE(6,107) RND, ES, ESD, A0, ADOT
  WRITE(6,108) ITER1, NOA
  IF(NOA .GT. 0) THEN
    WRITE(6,109)
    DO 27 NN = 1, NOA
      WRITE(6,110) IRV(NN), DA(NN)
27    CONTINUE
  END IF
  WRITE(6,99)

```

```

*****
* THIS NEXT CODE SETS THE INITIAL INPUT PARAMETERS TO SOME RETAINER *
* VARIABLES THAT ALLOW RETURNING TO THE ORIGINAL VALUES IF THE *
* SENSITIVITY MODE IS SELECTED. THIS PREVENTS HAVING TO REREAD ALL *
* THE INPUT PARAMETERS BACK IN FOR EACH RUN OF THE SENSITIVITY SCAN. *
*****

```

```

V1=CD
V2=A
V3=D
V4=SPI
V5=W
V6=WT
V7=F107
V8=FBAR
V9=AKP
V10=TVE
V11=UJD
V12=ETU
V13=H0
V14=G0
V15=ES
V16=XI
V17=RND
V18=ESD
V19=A0
V20=ADOT

```

```

*****
* THIS IS THE ITERATIVE SCANNING ROUTINE. ARGUMENTS ARE INCREMENTED *
* FRACTIONALLY THROUGH THEIR SPECIFIED RANGE AS SPECIFIED IN THE *
* INPUT TO THE SUBROUTINE SNALYS (PSIZE ITERATIONS OF PLEP). *
* IF SENSITIVITY MODE IS NOT SELECTED PSIZE=1. *
*****

```



```

      IF(PSENS .EQ. 0) THEN
        PSIZE=0
      END IF
      DO 40 PSYNS = 0, PSIZE
*
*****
* THIS NEXT SET OF CODE IS ENVOCKED WHEN PSENS IS EQUAL TO ONE.
* IT SETS UP FOR AND CALLS THE SENSITIVITY ARGUMENT ARRAY SNALYS FOR*
* SUBSEQUENT SCANNING. (PSENS = 1 SELECTS SENSITIVITY MODE
*****

      IF (PSENS .EQ. 1) THEN
        IET=0
*
*****
* THE SUBROUTINE SNALYS INITIALIZES THE SCANNED INPUT PARAMETERS TO *
* BE INCLUDED IN THE STUDY. IT ALSO PRINTS THE SENSITIVITY MATRIX. *
*****
*
        IF(PSYNS .EQ. 0) THEN
          CALL SNALYS( PSIZE, SNSAR, SNSMIN, SNSDEL, SUMCK, DELSN,
1             MINSN)
        ELSE
          CD = V1

*****
* RECOVERY OF THE ORIGINAL INPUT PARAMETERS AFTER THE FIRST RUN OF *
* A SENSITIVITY ANALYSIS.
*****
*
          A = V2
          D = V3
          SPI= V4
          W = V5
          WT = V6
          F107= V7
          FBAR= V8
          AKP= V9
          TVE=V10
          UJD=V11
          ETU=V12
          H0 =V13
          G0 =V14
          ES =V15
          XI =V16
          RND=V17
          ESD=V18
          A0 =V19
          ADOT=V20
        END IF
      END IF
      ASYNS=REAL(PSYNS)
      ASIZE=REAL(PSIZE)
      IF(PSENS .EQ. 1) THEN
        IF(SUMCK .EQ. 1.0) THEN
          SCNFRC = ASYNS*DELSN + MINSN
        ELSE
          SCNFRC = ASYNS/ASIZE
        END IF
      END IF

*****
* THIS NEXT CODE CREATES THE CURRENT VALUE FOR THE SCANNED INPUTS. *
* IF SENSITIVITY IS SELECTED THE PARAMETER WILL SCAN FROM MIN TO MAX*
* WITH A GRANULARITY OF 1/PSIZE PER SCAN
*****

      CD = SNSAR(1)*(SNSMIN(1)+ASYNS*SNSDEL(1))-CD*(SNSAR(1)-1.0)
      A = SNSAR(2)*(SNSMIN(2)+ASYNS*SNSDEL(2))-A *(SNSAR(2)-1.0)
      D = SNSAR(3)*(SNSMIN(3)+ASYNS*SNSDEL(3))-D *(SNSAR(3)-1.0)
      SPI= SNSAR(4)*(SNSMIN(4)+ASYNS*SNSDEL(4))-SPI*(SNSAR(4)-1.0)

```

```

W = SNSAR(5)*(SNSMIN(5)+ASYNS*SNSDEL(5))-W*(SNSAR(5)-1.0)
WT = SNSAR(6)*(SNSMIN(6)+ASYNS*SNSDEL(6))-WT*(SNSAR(6)-1.0)
F107= SNSAR(7)*(SNSMIN(7)+ASYNS*SNSDEL(7))-F107*(SNSAR(7)-1.0)
FBAR= SNSAR(8)*(SNSMIN(8)+ASYNS*SNSDEL(8))-FBAR*(SNSAR(8)-1.0)
AKP= SNSAR(9)*(SNSMIN(9)+ASYNS*SNSDEL(9))-AKP*(SNSAR(9)-1.0)
TVE= SNSAR(10)*(SNSMIN(10)+ASYNS*SNSDEL(10))-TVE*(SNSAR(10)-1.0)
UJD= SNSAR(11)*(SNSMIN(11)+ASYNS*SNSDEL(11))-UJD*(SNSAR(11)-1.0)
ETU= SNSAR(12)*(SNSMIN(12)+ASYNS*SNSDEL(12))-ETU*(SNSAR(12)-1.0)
HO = SNSAR(13)*(SNSMIN(13)+ASYNS*SNSDEL(13))-HO*(SNSAR(13)-1.0)
GO = SNSAR(14)*(SNSMIN(14)+ASYNS*SNSDEL(14))-GO*(SNSAR(14)-1.0)
ES = SNSAR(15)*(SNSMIN(15)+ASYNS*SNSDEL(15))-ES*(SNSAR(15)-1.0)
XI = SNSAR(16)*(SNSMIN(16)+ASYNS*SNSDEL(16))-XI*(SNSAR(16)-1.0)
RND= SNSAR(17)*(SNSMIN(17)+ASYNS*SNSDEL(17))-RND*(SNSAR(17)-1.0)
ESD= SNSAR(18)*(SNSMIN(18)+ASYNS*SNSDEL(18))-ESD*(SNSAR(18)-1.0)
AO = SNSAR(19)*(SNSMIN(19)+ASYNS*SNSDEL(19))-AO*(SNSAR(19)-1.0)
ADOT= SNSAR(20)*(SNSMIN(20)+ASYNS*SNSDEL(20))-ADOT*(SNSAR(20)-1.0)

```

```

*****
* DEL IS THE CONSTANT MULTIPLIER FOR THE INTEGRAL IN EQUATION 33 OF *
* NSWC TR 83-243 *
*****

```

```

DEL = CD*A*3.14159D0/SPI

```

```

*
*****
* IF THE SENSITIVITY ANALYSIS MODE IS NOT SELECTED, THEN THE SYSTEM *
* PRINTS STANDARD MISSION LIFE TIME TABULAR DATA. *
*****
*

```

```

IF (PSENS .EQ. 0) THEN
    BCOF = CD * A
    WRITE (6,98)
    WRITE (6,99)
    WRITE (6,100)
    WRITE (6,99)
    WRITE (6,101) BCOF, SPI, W
    WRITE (6,102) F107, FBAR, TVE
END IF

```

```

*
*****
* CONVERTING DEGREES TO RADIANS *
*****
*

```

```

XI = XI / DEG
GO = GO / DEG
HO = HO / DEG
FLO = ETU / DEG

```

```

*
*****
* THIS NEXT CODE SEQUENCE CONDITIONS THE ELEMENTS AS PER NSWC TR 82-387
* PAGE 7. IT CONVERTS THE KAULA SEMIMAJOR AXIS AO IN EARTH RADII TO *
* BROUWER MEAN SEMIMAJOR AXIS VIA EQNS 2.1 AND 2.2. THE SEMIMAJOR AXIS*
* DECAY RATE ADOT IS CONVERTED IN A LIKE MANNER VIA 2.3, 2.4, AND 2.5 *
*****
*

```

```

FN = 1. / ( 1. - ES * ES )**1.5D0
TA = SIN ( XI )
TB = TA * TA
TE = 1. - (3.*TB) / 2.
TAD = (( 3.*R2) / (2.*AO*AO))*TE*FN
AK = AO
AO = (AO*((1. + 2.*TAD) / (1. - TAD))**0.66666667D0)*ROE
XDOT = TAD*(3.*ESD*(ES/(1.-ES*ES)) - 2.*(ADOT/AK))
ADT = (ADOT/AK)*AO + 2.*AK*ROE*XDOT*((1. + 2.*TAD)*
1      ((1. - TAD)** 5))*(-0.333333333D0)

```

```

*****
* TIME IS NOW CONVERTED FROM SECONDS TO DAYS *
*****

```

```

ADT = ADT / 86400.D0
ESD = ESD / 86400.D0

```





```

DIMENSION SNSAR(20), SNSMIN(20), SNSMAX(20), SNSDEL(20)
CHARACTER*4 SNSCAR
INTEGER N, PSIZE
REAL SNSAR, SNSMIN, SNSMAX, SNSDEL, SUMCK, DELSN, MINSN
WRITE (6,98)
WRITE(6,120)
WRITE(6,100)
WRITE(6,120)
WRITE(6,200) PSIZE
ASIZE=REAL(PSIZE)
READ(5,102)
SUMCK = 0.0
DO 20 N = 1, 20

    READ 101, SNSCAR, SNSAR(N), SNSMIN(N), SNSMAX(N)
    SNSDEL(N) = (SNSMAX(N)-SNSMIN(N))/ASIZE
    IF (SNSAR(N) .EQ. 1.0) THEN
        SUMCK = SUMCK + 1.0
        DELSN = SNSDEL(N)
        MINSN = SNSMIN(N)
        WRITE(6,300) SNSCAR, SNSMIN(N), SNSMAX(N),
            SNSDEL(N)
1    END IF
20 CONTINUE
    IF (SUMCK .GT. 1.0) THEN
        DELSN = 0.0
        MINSN = 0.0
    END IF
    WRITE(6,120)
    WRITE(6,400)

98 FORMAT ( 1H1 )
120 FORMAT(//5X, '-----',//)
100 FORMAT(//17X, 'SENSITIVITY ANALYSIS FOR',/16X, 'LOW EARTH ORBIT ',
X 'SATELLITES',/19X, 'PROPELLENT LONGEVITY',//)

200 FORMAT (5X, ' TABLE OF INPUT PARAMETERS SCANNED FROM MINIMUM TO',
X /5X, ' MAXIMUM WITH THE INDICATED INCREMENT PER RUN. ',/5X,
X ' THE GRANULARITY IS 1/',I4,'./5X, ' ALL OTHER INPUT PARAMETERS
X ARE RETURNED TO THEIR',/5X, ' INITIAL VALUES AT EACH INCREMENT.'
X ///'INPUT PARAMETER',8X, 'MINIMUM',13X, 'MAXIMUM',13X, 'INCREMENT'//)

102 FORMAT (1X)
101 FORMAT ( A4, 1X, F3.1, F16.9, 4X, F16.9)
300 FORMAT (5X, A4, 6X, 3(3X, F16.9))
400 FORMAT(//, 10X, ' SENSITIVITY SCAN RESULTS FOR ABOVE SPECIFICS'//
15X, 'REV NUMBER',8X, 'TIME(DAYS)',15X, 'FRACTION OF SCAN')

RETURN
END

```

```

*
*
*
*
*
*
*
*
*

```

```

*****
*****
**
**      SUBROUTINE KOZAI      **
**
**

```

```

*
*
*
*
*****
*****
*
*
*****
*
* SUBROUTINE KOZAI IS THE SYSTEM WORKHOUSE. IT CALLS BRAUER TO CON-
* VERT THE BROUWER MEAN ORBITAL ELEMENTS OF THE NAVPASUR INPUT TO
* BROUWER OSCULATING ELEMENTS. THESE OSCULATING ELEMENTS ARE CON-
* VERTED TO KOZAI-LIKE MEAN ELEMENTS IN THE SUBROUTINE MEAN. THE
* SUBROUTINE PERIOD COMPUTES THE INITIAL ANOMALISTIC PERIOD. THE
* SUBROUTINE GEOP COMPUTES THE EFFECTS OF THE OBLATE GEOID ON THE
* ORBITAL ELEMENTS (THROUGH THE J4 TERM). SUBROUTINE THRST COMPUTES
* THE EFFECTS ON THE ELEMENTS DUE TO PERIGEE BURNS TO CHANGE
* THE SEMIMAJOR AXIS DURING IRV(K) BY THE AMOUNT DA(K). FINALLY,
* SUBROUTINE DRAG COMPUTES THE THE AMOUNT OF FUEL NEEDED TO OVERCOME
* THE DRAG EFFECTS BY CONTINUOUS INTRACK MICROTHRUSTING.
* KOZAI KEEPS TRACK OF THE FUEL USED AND ORBITAL ELEMENT CHANGES.
* WHEN THE FUEL IS EXHAUSTED KOZAI RETURNS SYSTEM CONTROL TO PLEP.
*
*****
*
SUBROUTINE KOZAI(ADT,A0,ES,XI,FL0,G0,H0,UJD,W,DEL,ITER1,ITER2,
1 SCNFRC,D)
  DIMENSION XOSC(6), XM(6), DXDT(6), XDD(6), IRV(10), DA(10)
  DIMENSION DXM(6)
  COMMON / OADJ/ NOA, IRV, DA, SPI, WT, PSENS
  DATA B0,B2,B3,B4,B5,B6 / .398603254E+06,-.1755528999E+11,
1 .26386647738E+12,.1063073996E+16,.805605022E+18,
1 .7292115856E-04/
  DATA DEG/57.295779513D0/,CN2/0.0/,A1,E1,RN1/0.0,0.0,0.0/,DT/0.0/
  DATA PI / 3.14159D0 /
  DATA NPL0T / 0 /
  IRC = 0
  PCOUNT=0
  KK = 0
  PI2 = 2.D0* PI
  CALL BRAUER (B0,B2,B3,B4,B5,DT,A0,ES,XI,FL0,G0,H0,CN2,A,CE,CI,CL,
1 G,H,A1,E1,RN1 )

  IF (PSENS.EQ. 0) THEN
    WRITE(6,100) ITER1
100  FORMAT(/5X,'MAXIMUM NUMBER OF ORBITAL REVOLUTIONS=',I10)
    WRITE(6,101) ITER2
101  FORMAT(/5X,'DATA PRINTED EVERY ',I3,' ORBITAL REVOLUTIONS')
    SCNFRC = 0.0
  END IF
  CALL PERIOD ( A0, ES, XI, PA )
  XOSC(1) = A
  XOSC(2) = CE
  XOSC(3) = CI
  XOSC(4) = G
  XOSC(5) = H
  XOSC(6) = CL
  CALL MEAN (XOSC,XM)
  ILINE = 0
  CIW = XM(3)*DEG
  GW = XM(4)*DEG
  HW = XM(5)*DEG
  CLW = XM(6)*DEG
  IF (PSENS.EQ. 0) THEN
    WRITE(6,102)
    WRITE(6,103) (XM(K),K=1,2),CIW,GW,HW,CLW
  END IF
103 FORMAT(/5X,'SEMIMAJOR AXIS=',E22.14,' KM'/
X 5X,'ECCENTRICITY=',E22.14/
X 5X,'INCLINATION=',E22.14,' DEG'/
X 5X,'ARGUMENT OF PERIGEE=',E22.14,' DEG'/
X 5X,'ASCENDING NODE=',E22.14,' DEG'/
X 5X,'MEAN ANOMALY=',E22.14,' DEG')

```

```

102 FORMAT(/5X,'KOZAI MEAN ELEMENT SET')
DELT = PA
CALL THRST ( XM, DXM, IRC, KK, PA, DWOA)
DO 10 I = 1, ITER1
  T = ( I - 1 ) * DELT / 86400.
  TT = UJD + T
15  CALL GEOP (XM,DXDT)
16  DO 20 JJ = 1,6
      XM(JJ) = XM(JJ) + DXDT(JJ)*DELT + DXM(JJ)
      IF ( JJ .LT. 4 ) GO TO 20
      XM( JJ ) = AMOD ( XM(JJ), PI2 )
20  CONTINUE
  IRC = 0
  DO 30 II = 1, NOA
      IF ( I.EQ. IRV(II)) IRC = 1
      IF ( IRC .EQ. 1) KK = II
30  CONTINUE
  CALL THRST(XM, DXM, IRC, KK, PA, DWOA)
*
*****
* CALCULATING THE DEL1 IN NSWC TR 83-243 EQN 11.
*****
*
  RP=XM(1)*(1.0-XM(2))
  VP=SQRT((B0/XM(1))*((1.0+XM(2))/(1.0-XM(2))))
  DEL1=(1.0-(RP/VP)*D*B6*COS(XM(3)))*2
  DDELT=DEL*DEL1

  CALL DRAG ( XM, DDELT, TT, DELMG )
  W = W + DELMG - DWOA
  WT = WT + DELMG - DWOA
  IF (PSENS .EQ. 0) THEN
    IF (PCOUNT.NE.(ITER2-1)) THEN
      PCOUNT=PCOUNT+1
      GO TO 10
    ELSE
      PCOUNT=0
    END IF
    IF ( ILINE .GE. 50 ) ILINE = 0
    ILINE = ILINE + 1
    IF ( ILINE .EQ. 1 ) WRITE ( 6,104)
    IF ( ILINE .EQ. 1 ) WRITE ( 6,105)
    WRITE ( 6, 106) I, TT, T, W
  END IF
  IF ( W.LE. 0.00) THEN
    IF (NPLOT .EQ. 1) THEN
      PRINT *, T, SCNFRC
    ELSE
      WRITE(6,107) I, T, SCNFRC
    END IF
    RETURN
  END IF
10 CONTINUE
  IF (NPLOT .EQ. 1) THEN
    PRINT *, T, SCNFRC
  ELSE
    WRITE(6,107) I,T,SCNFRC
  END IF
104 FORMAT(1H1)
105 FORMAT(/5X,'REV NUMBER',3X,'TIME(MJD)',8X,'TIME(DAYS)',8X,
  X 'PROPELLANT REMAINING(KG)',/)
106 FORMAT(5X,I10,3X,F9.2,8X,F10.2,15X,F8.2)
107 FORMAT(5X,I10, 8X,F10.2,15X,F16.9)
  RETURN
  END
*
*
*
*
*
*
*****
*****
**          SUBROUTINE BRAUER          **
**                                          **
**                                          **

```



\*  
\*  
\*  
\*

\*\*\*\*\*  
\*\*\*\*\*

```

SUBROUTINE BRAUER(B0,B2,B3,B4,B5,DT,A2P,E2P,CI2P,CL02P,G02P,H02P,
1004 1CN2,A,CE,CI,CL,G,H,ADT,RND,ESD)
A2P2=A2P**2
A2P4=A2P2**2
CN0=SQRT(B0/(A2P2*A2P))
E2P2=E2P**2
ETA=SQRT(1.-E2P2)
SINEI=SIN(CI2P)
THETA=COS(CI2P)
THETA2=THETA**2
THETA4=THETA2**2
THETA6=THETA4*THETA2
CJ2=-B2/(2.*B0*A2P2)
ETA2=ETA**2
ETA3=ETA2*ETA
ETA4=ETA2**2
CJ21P=CJ2/ETA4
CJ31P=B3/(B0*A2P2*A2P*ETA4*ETA2)
CJ41P=(3.*B4)/(8.*B0*A2P4*ETA4*ETA4)
CJ51P=B5/(B0*A2P4*A2P*ETA4**2*ETA2)
FUN1=3.*THETA2-1.
FUN2=1.-5.*THETA2
SINEI2=SINEI**2
A1=A2P*CJ2*FUN1
A0=-A1/ETA3
A2=3.*A2P*CJ2*SINEI2
FUN5=1.-11.*THETA2-(40.*THETA4)/FUN2
FUN6=-FUN1-(8.*THETA4)/FUN2
FUN4=THETA2/SINEI2
FUN22=FUN2**2
CJ21P2=CJ21P**2
E01P=((E2P*ETA2)*(3.*CJ21P2*FUN5-10.*
1CJ41P*FUN6))/(24.*CJ21P)
E21P=-2.*E01P
E31P=((35.*CJ51P*E2P2*ETA2*SINEI)*(FUN2-(16.*THETA4)/FUN2))/(96.*
1CJ21P)
E11P=-.75D0*E31P+((.25D0*ETA2*SINEI)*(CJ31P+.3125D0*CJ51P
1*(4.+3.*E2P2)*
2(1.-9.*THETA2-(24.*THETA4)/FUN2)))/CJ21P
CI0=-(E2P*THETA)/(ETA2*SINEI)
CI2=CJ21P*THETA*SINEI*1.5D0
CI1=E2P*CI2*.66666667D0
FUN7=(-.5D0*ETA3*CJ21P)/E2P
CL21P=(ETA3/CJ21P)*(.25D0*CJ21P2*FUN5-.83333333D0*CJ41P*FUN6)
CL12P=CN0*(1.+1.5D0*CJ21P*ETA*FUN1+.09375D0*CJ21P2*ETA*(-15.+16.
1*ETA+25.*ETA2+(30.-96.*ETA-90.*ETA2)*THETA2+(105.+144.*ETA+25.
2*ETA2)*THETA4)+.9375D0*CJ41P*ETA*E2P2*(3.-30.*THETA2+35.*THETA4))
CL22P=.5D0*CN0*CN2
G21P=(1./(24.*CJ21P))*(-3.*CJ21P2*(2.+E2P2-11.*(2.+3.*E2P2)*THETA2
1-40.*(2.+5.*E2P2)*THETA4/FUN2-400.*E2P2*THETA6/FUN22)+10.*CJ41P*
2(2.
3+E2P2-3.*(2.+3.*E2P2)*THETA2-8.*(2.+5.*E2P2)*THETA4/FUN2-80.*E2P2*
4THETA6/FUN22))
G12P=CN0*(-1.5D0*CJ21P*FUN2+.09375D0*CJ21P2*(-35.+24.*ETA+25.
1*ETA+
2(90.-192.*ETA-126.*ETA2)*THETA2+(385.+360.*ETA+45.*ETA2)*THETA4)+
3.3125D0*CJ41P*(21.-9.*ETA2+(-270.+126.*ETA2)*THETA2+(385.-189.
4*ETA2)*THETA4))
H2=1.5D0*CJ21P*THETA
H3=-2.*H2
H1=.66666667D0*E2P*H2
H31P=((35.*CJ51P*E2P2*E2P*THETA)/(144.*CJ21P))*(.5D0/SINEI*(FUN2-(
116.*THETA4)/FUN2)+SINEI*(5.+(32.*THETA2)/FUN2+80.*THETA4/FUN22))
H11P=-.25*
1H31P+((.25D0*E2P*THETA)/(CJ21P*SINEI))*(CJ31P+.3125D0*CJ51P*
2(4.+3.*E2P2)*(1.-9.*THETA2-(24.*THETA4)/FUN2)+1.875D0*CJ51P
3*SINEI2*
4(4.+3.*E2P2)*(3.+(16.*THETA2)/FUN2+(40.*THETA4)/FUN22))

```



```

H21P=(E2P2*THETA)/(12.*CJ21P)*(-3.*CJ21P2*(11.+(30.*THETA2)/FUN2+
1(200.*THETA4)/FUN22)+10.*CJ41P*(3.+(16.*THETA2)/FUN2+(40.*THETA4)/
2FUN22))
H12P=CN0*THETA*(-3.*CJ21P+.375D0*CJ21P2*(-5.+12.*ETA+9.*ETA2+
1(-35.-
236.*ETA-5.*ETA2)*THETA2)+1.25D0*CJ41P*(5.-3.*ETA2)*(3.-7.*THETA2))
AID=CJ51P/CJ21P
AID2=FUN2-(16.*THETA4)/FUN2
C1=35./384.*AID*ETA3*E2P*SINEI*AID2
AID3=THETA2/SINEI
AID4=THETA2*SINEI
E2P3=E2P2*E2P
C2=35./1152.*AID*((-E2P*SINEI*(3.+2.*E2P2)+E2P3*AID3)*AID2+
12.*E2P3*AID4*(5.+(32.*THETA2)/FUN2+(80.*THETA4)/FUN22))
C3=1.-9.*THETA2-(24.*THETA4)/FUN2
AID5=CJ31P/CJ21P
C4=.25D0*AID5*(-E2P*AID3)+5./64.*AID*(-E2P*AID3*(4.+3.*E2P2)+
1E2P*SINEI*(26.+9.*E2P2))*C3-15./32.*AID*E2P*AID4*(4.+3.*E2P2)*
2(3.+(16.*THETA2)/FUN2+(40.*THETA4)/FUN22))
C5=E2P/(1.+ETA3)*(3.-E2P2*(3.-E2P2))
C6=(E2P*(-32.+81.*(E2P2*E2P2)))/((4.+3.*E2P2)+ETA*(4.+9.*E2P2))
C7=.25D0*AID5*SINEI*C5+5./64.*C3*AID*ETA2*SINEI*C6
C8=-.25D0*AID5*ETA3*SINEI-5./64.*AID*ETA3*SINEI*(4.+9.*E2P2)*C3
0510 T=DT
CL2P=CL12P*DT+CL22P*DT**2+CL02P + RND*DT*DT
CL2P=AMOD(CL2P,6.2831853071796D0)
IF(CL2P)520,530,530
520 CL2P=CL2P+6.2831853071796D0
530 G2P=G12P*DT+G02P
H2P=H12P*DT+H02P
SINEG=SIN(G2P)
COSING=COS(G2P)
D1E=SINEG*(SINEG*(E31P*SINEG+E21P)+E11P)+E01P
H1P=((H31P*SINEG+H21P)*SINEG+H11P)*COSING+H2P
GPLP=G2P+CL2P+.5D0*(CL21P+G21P)*SIN(2.*G2P)+(C1+C2)*COS(3.* G2P)
1+(C4+C7)*COSING
CL1P=CL2P
U=CL2P
100 DELTAU=(U-E2P*SIN(U)-CL2P)/(1.-E2P*COS(U))
U=U-DELTAU
IF(ABS(DELTAU)-1.E-10)200,100,100
200 U=U-(U-E2P*SIN(U)-CL2P)/(1.-E2P*COS(U))
E=U
SINE1P=SIN(E)
COSE1P=COS(E)
G1P=G2P
ADIVR=1./(1.-E2P*COSE1P)
SINF1P=ADIVR*ETA*SINE1P
COSF1P=ADIVR*(COSE1P-E2P)
F1P=ATAN2(SINF1P,COSF1P)
IF(ABS(F1P-CL2P)-3.1415926535898D0)220,210,210
210 STOP
220 FUN3=(1.+CN2*T)**.66666667D0
COSFG=COS(2.*(G1P+F1P))
SINFG=SIN(2.*(G1P+F1P))
ADIVR2=ADIVR**2
ADIVR3=ADIVR**3
CI=CI2P+CI0*D1E+CI1*SINF1P*SINFG+(2.*CI1*COSF1P+CI2)*COSFG
FUN8=F1P-CL1P+E2P*SINF1P
8018 H=H1P+(2.*H1*COSF1P+H2)*SINFG-H1*SINF1P*COSFG+H3*FUN8
KFUN=H/6.2831853071796D0
FUN9=KFUN
H=H-FUN9*6.2831853071796D0
IF(H)8022,8023,8023
8022 H=H+6.2831853071796D0
8023 A=A2P/FUN3+A0+(A1+A2*COSFG)*ADIVR + ADT*DT
AID6=ADIVR2*ETA2+ADIVR
AID7=SIN(2.*G2P+F1P)
AID8=SIN(2.*G2P+3.*F1P)
D1=.25D0*CJ21P*(6.*(5.*THETA2-1.)*FUN8+(3.-5.*THETA2)*(3.*SINFG+
13.*E2P*AID7 +E2P*AID8 ))
D2=.25D0*CJ21P*(2.*(3.*THETA2-1.)*(AID6+1.)*SINF1P+3.*(1.-THETA2)*

```

```

1  ((-AID6+1.)*AID7+(AID6+.33333333D0)*AID8))
  AID9=COS(2.*G2P+F1P)
  AID10=COS(2.*G2P+3.*F1P)
  D3=-ETA2*.5D0*CJ21P*(1.-THETA2)*(3.*AID9+AID10)
  ETA6I=1./(ETA3*ETA3)
  D4=ETA6I*(C5 +COSF1P*(3.+E2P*COSF1P*(3.+E2P*COSF1P)))
  D5=ETA6I*(E2P+COSF1P*(3.+E2P*COSF1P*(3.+E2P*COSF1P)))
  D6= ETA2*CJ2*.5D0*((3.*THETA2-1.)*D4+3.*(1.-THETA2)*D5*COSFG)+D3
  GAL=GPLP+D1+(E2P*ETA2)/(1.+ETA)*D2
  CE=(E2P-1.)*(1.+CN2*DT)**.666666666666667D0+1.+D1E+D6 + ESD*DT
  EDL=.5D0*E2P*CL21P*SIN (2.*G2P)+C8*COSING+E2P*CL1*COS (3.*G2P)-
1  ETA3*D2
  AID14=SIN(CL2P)
  AID15=COS(CL2P)
  ESL=CE *AID14+EDL*AID15
  ECL=CE *AID15-EDL*AID14
  CE=SQRT(ECL*ECL+ESL*ESL)
  CL=ATAN2(ESL,ECL)
  G=GAL-CL
  G=AMOD(G,6.2831853071796D0)
  IF(G)8024,8025,8025
8024 G = G + 6.2831853071796D0
8025 RETURN
END

```

```

*
*
*
*
*
*
*
*
*
*
*
*

```

```

*****
*****
**
**      SUBROUTINE POSVEL      **
**                                **
*****
*****

```

```

SUBROUTINE POSVEL (A,CE,CI,CL,G,H,B0,R1,R2,R3,V1,V2,V3,R,VEL)
CALL NWTRPH (CL,CE,E,SINEP,COSEP)
HSIN=SIN(H)
HCOS=COS(H)
GSIN=SIN(G)
GCOS=COS(G)
CISIN=SIN(CI)
CICOS=COS(CI)
A11=HCOS*GCOS-HSIN*CICOS*GSIN
A12=-HCOS*GSIN-HSIN*CICOS*GCOS
A21=HSIN*GCOS+HCOS*CICOS*GSIN
A22=HCOS*CICOS*GCOS-HSIN*GSIN
A31=CISIN*GSIN
A32=CISIN*GCOS
FUN=SQRT(1.-CE*CE)
R1=A*(A11*(COSEP-CE)+A12*(FUN*SINEP))
R2=A*(A21*(COSEP-CE)+A22*(FUN*SINEP))
R3=A*(A31*(COSEP-CE)+A32*(FUN*SINEP))
R=A*(1.-CE*COSEP)
FUN1=(SQRT(B0*A))/R
V1=FUN1*(A11*(-SINEP)+A12*FUN*COSEP)
V2=FUN1*(A21*(-SINEP)+A22*FUN*COSEP)
V3=FUN1*(A31*(-SINEP)+A32*FUN*COSEP)
VEL=FUN1*SQRT(1.-(CE*COSEP)**2)
RETURN
END

```

```

*
*
*
*
*
*
*
*
*
*
*
*

```

```

*****
*****
**
**      SUBROUTINE NWTRPH      **
**                                **
*****
*****

```



```

RETURN
END

```

```

*****
*****
**                                     **
**               FUNCTION XSPI       **
**                                     **
*****
*****

```

```

FUNCTION XSPI(XM)
DIMENSION XM(6)
REAL J(4)
DATA J,R/1.,0.00108276D0,-0.00000255D0,-0.00000156D0,6378.165D0/
F = XM(6)+(2.*XM(2)-XM(2)**3./4+5./96.*XM(2)**5.)*SIN(XM(6))
1+(1.25D0*XM(2)**2.-11./24.*XM(2)**4.+17./192.*XM(2)**6.)*SIN(2.*
2XM(
36))+(13./12.*XM(2)**2.-43./192.*XM(2)**5.)*SIN(3.*XM(6))
P = XM(1)*(1.-XM(2)**2.)
XSPI = 3./8.*J(2)*(R/P)**2.*SIN(2.*XM(3))*(XM(2)*COS(2.*XM(4)+F)
1 +COS(2.*(XM(4)+F))+XM(2)/3.*COS(2.*XM(4)+3.*F))
RETURN
END

```

```

*****
*****
**                                     **
**               FUNCTION XSPW       **
**                                     **
*****
*****

```

```

FUNCTION XSPW(XM)
DIMENSION XM(6)
REAL J(4)
DATA J,R/1.,0.00108276D0,-0.00000255D0,-0.00000156D0,6378.165D0/
F = XM(6)+(2.*XM(2)-XM(2)**3./4+5./96.*XM(2)**5.)*SIN(XM(6))
1+(1.25D0*XM(2)**2.-11./24.*XM(2)**4.+17./192.*XM(2)**6.)*SIN(2.*
2XM(
26))+(13./12.*XM(2)**2.-43./192.*XM(2)**5.)*SIN(3.*XM(6))
P = XM(1)*(1.-XM(2)**2.)
XSPW = 3./4.*J(2)*(R/P)**2.*(4.-5.*SIN(XM(3))*SIN(XM(3)))
1*(F-XM(6)+XM(2)*SIN(F))+1.5D0*J(2)*(R/P)**2.*(1.-1.5D0*SIN(XM(3))
2**2.)
3*((1.-XM(2)*XM(2)/4.)/XM(2)*SIN(F)+.5D0*SIN(2.*F)+XM(2)*SIN(3.*F)
4/12
5.))-1.5D0*J(2)*(R/P)**2.*((SIN(XM(3))*SIN(XM(3)))/4.+XM(2)**2./2.*(
61.-15./8.*SIN(XM(3))**2.)/XM(2)*SIN(2.*XM(4)+F)+XM(2)/16.*SIN
7(XM(3))**2.*SIN(2.*XM(4)-F)+.5D0*(1.-2.5D0*SIN(XM(3))**2.)*SIN(2.*
8(XM(4)+F))-(7./12.*SIN(XM(3))**2.-XM(2)*XM(2)/6.*(1.-19./8.*SIN
9(XM(3))**2.)/XM(2)*SIN(2.*XM(4)+3.*F)-3./8.*SIN(XM(3))**2.*SIN
11(2.*XM(4)+4.*F)-XM(2)/16.*SIN(XM(3))**2.*SIN(2.*XM(4)+5.*F))
12-9./16.*J(2)*(R/P)**2.*SIN(XM(3))**2.*SIN(2.*XM(4))
RETURN
END

```

```

*****
*****
**                                     **
**               FUNCTION XSPO       **
**                                     **
*****
*****

```







```
*
*
* *****
* *****
* **                                     **
* **          SUBROUTINE MEAN          **
* **                                     **
* *****
* *****
*
SUBROUTINE MEAN(XOSC,XM)
*...
*... COMPUTES THE MEAN ORBITAL ELEMENTS FROM THE OSCILATORY ELEMENTS
*... AND THE FIRST ORDER PERIODIC VARIATIONS BY THE RELATIONS,
*... XM = XOSC -XSP(XM).
*...
DIMENSION XOSC(6),XM(6),XMN(6),XSP(6),TOL(6),DELXM(6)
DATA TOL/.01D0,.00001D0,.00001D0,.00001D0,.00001D0,.00001D0/
KOUNT = 0
*... INITIAL GUESS FOR MEAN ELEMENTA.
DO 10 I=1,6
10 XM(I) = XOSC(I)
*... CALCULATE THE SHORT PERIODIC VARIATIONS.
20 XSP(1) = XSPA(XM)
   XSP(2) = XSPE(XM)
   XSP(3) = XSPI(XM)
   XSP(4) = XSPW(XM)
   XSP(5) = XSPQ(XM)
   XSP(6) = XSPM(XM)
   KOUNT = KOUNT+1
   DO 50 J=1,6
     XMN(J) = XOSC(J)-XSP(J)
     DELXM(J) = ABS(XMN(J)-XM(J))
     IF(DELXM(J).GT.TOL(J)) XM(J) = XMN(J)
50 CONTINUE
   DO 60 K=1,6
     IF(DELXM(K).GT.TOL(K).AND.KOUNT.LT.30) GO TO 20
60 CONTINUE
70 IF(KOUNT.GT.30) WRITE(6,100) DELXM
90 CONTINUE
100 FORMAT(/T5,'CONVERGENCE OF ONE OR MORE MEAN ELEMENTS WAS NOT MET.'
1/'THE ABSOLUTE DIFFERENCE IN THE ELEMENTS ARE SHOWN.'//7E12.5)
RETURN
END
*
*
* *****
* *****
* **                                     **
* **          SUBROUTINE GEOP          **
* **                                     **
* *****
* *****
*
SUBROUTINE GEOP (XM,DXT)
DIMENSION XM(6) , DXT(6)
REAL N,NCONS,NCONST,NCON
REAL J(4)
DATA J,R/1.,0.00108276D0,-0.00000255D0,-0.00000156D0,6378.165D0/
DATA U/398600./
N = SQRT(U/(XM(1)**3.))
P = XM(1)*(1.-XM(2)**2.)
DXT(1) = 0.
S3 = SIN(XM(3))*SIN(XM(3))
XS = 1.-XM(2)**2.
CS = COS(XM(3))
DED = (-3.)/32.*N**J(2)*J(2)*(R/P)**4.*S3*(14.-15.*S3)*XM(2)*
1XS*SIN(2.*XM(4))
```

```

DED0 = 3./8.*N*J(3)*(R/P)**3.*SIN(XM(3))*(4.-5.*S3)*XS*COS(XM(4))
DEDOT = 15./32.*N*J(4)*(R/P)**4.*S3*(6.-7.*S3)*(XM(2)*XS)
1XSIN(2.*XM(4))
DXDT(2) = DED-DED0-DEDOT
DID = 3./64.*N*J(2)*J(2)*(R/P)**4.*SIN(XM(3)*2.)*(14.-15.*S3)*
1XM(2)**2.*SIN(2.*XM(4))
DIDO = 3./8.*N*J(3)*(R/P)**3.*COS(XM(3))*(4.-5.*S3)*XM(2)*COS(XM(4)
1))
DIDOT = 15./64.*N*J(4)*(R/P)**4.*SIN(2.*XM(3))*(6.-7.*S3)*XM(2)*
1XM(2)*SIN(2.*XM(4))
DXDT(3) = DID+DIDO+DIDOT
DWD = .75D0*N*J(2)*(R/P)**2.*(4.-5.*S3)
DW = 2.*(14.-15.*S3)*S3-(23.-158.*S3+135.*S3**2.)*XM(2)**2.
DWD0 = 3./16.*N*J(2)**2.*(R/P)**4.*(48-103.*S3 + 215./4.*S3**2.+
1(7.-4.5D0*S3-45./8.*S3**2.)*XM(2)**2.+6.*(1.-1.5D0*S3)*(4.-5.*S3)*
2SQR(XS)-.25D0*DW*COS(2.*XM(4)))
*... PRINT *, XM(2), XM(3), XM(4), R, P, N, J(3), S3
DWDOT = 3./8.*N*J(3)*(R/P)**3*((4.-5.*S3)*(S3-XM(2)**2)*COS(XM(3)
1)**2)/(XM(2)*SIN(XM(3)))+2.*SIN(XM(3))*(13.-15.*S3)*XM(2))*SIN(XM
2(4))
DWN = S3*(6.-7.*S3)-(6.-35.*S3+31.5*S3**2.)*XM(2)**2.
DWDOTT=15./32.*N*J(4)*(R/P)**4.*(16.-62.*S3+49.*S3**2.+75D0*(24.-
184.*S3+63.*S3**2.)*XM(2)**2.+DWN*COS(2.*XM(4)))
DXDT(4) = DWD+DWD0+DWDGT-DWDOTT
DOD = (-1.5D0)*N*J(2)*(R/P)**2.*CS
DODO = 1.5D0*N*J(2)**2.*(R/P)**4.*CS*(2.25D0+1.5*SQR(XS)-S3
1*(2.5D0+2.25D0*SQR(XS))+XM(2)**2./4.*(1.+1.25D0*S3)-XM(2)**2.
2/8.*(7.-15.*S3)*COS(2.*XM(4)))
DODOT = 3./8.*N*J(3)*(R/P)**3.*(15.*S3-4)*XM(2)*CS/SIN(XM(3))*SIN(
1XM(4))
DODOTT=15./16.*N*J(4)*(R/P)**4.*CS*((4.-7.*S3)*(1.+1.5D0*XM(2)**2.
2)-(3.-7.*S3)*XM(2)**2.*COS(XM(4)*2.))
DXDT(5) = DOD-DODO-DODOT+DODOTT
NCON = 3./8.*N*J(2)**2.
NCONS = N*J(4)*(R/P)**4.
NCONST = 3./8.*N*J(3)*(R/P)**3.
DM = N*(1.+1.5D0*J(2)*(R/P)**2.*(1.-1.5D0*S3)*SQR(XS))
DMD=1.5D0*N*J(2)**2*(R/P)**4*((1.-1.5D0*S3)**2*XS+(1.25D0*(1.-
12.5D0*
1S3+13./8.*S3*S3)+5./8.*(1.-S3+5./8.*S3*S3)*XM(2)**2+S3/16.*(14.-
215.*S3)*(1.-2.5D0*XM(2)**2)*COS(2.*XM(4)))*SQR(XS))
DM1=(3.-7.5D0*S3+47./8.*S3*S3+(1.5D0-5.*S3+117./6.*S3*S3)*XM(2)**2
1-(1.+5.*S3-101./8.*S3*S3)/8.*XM(2)**4.)
DM2 = XM(2)**2./8.*S3*(70.-123.*S3+(56.-66.*S3)*XM(2)**2.)*COS(2.*
1XM(4))+27./128.*XM(2)**4.*S3*S3*COS(4.*XM(4))
DMD0 = NCON*(R/P)**4./(SQR(XS))*(3.*DM1+DM2)
DMDOT = NCONST*SIN(XM(3))*(4.-5.*S3)*(1.-4.*XM(2)**2.)/XM(2)*
1SQR(XS)*
1SIN(XM(4))-45./128.*NCONS*(8.-40.*S3+35.*S3*S3)*XM(2)**2.*SQR(XS)

DMDOTT=15./64.*NCONS*S3*(6.-7.*S3)*(2.-5.*XM(2)**2.)*SQR(XS)*COS(
12.*XM(4))
DXDT(6) = DM+DMD+DMD0-DMDOT+DMDOTT
RETURN
END

```

\*  
\*  
\*  
\*  
\*  
\*  
\*  
\*  
\*  
\*

```

*****
*****
**          SUBROUTINE SOLOC          **
**                                     **
*****
*****

```

```

SUBROUTINE SOLOC ( TVE , T , BLA , DS , AS , AB )
DATA EPS1/ 23.5D0 / , PI / 3.14159D0/ , TOL/ 0.0001D0 /
PI1 = 0.5D0*PI
PI2 = 2. * PI
PI3 = 1.5D0* PI

```

```

RPD = PI / 180.0D0
DELT = T - TVE
EPS = EPS1 * RPD
CLON = 0.985647D0 * RPD * DELT
IF (CLON.LT. 0.0 ) CLON = PI2 + CLON
IF (CLON.GT.PI2) CLON = AMOD(CLON,PI2)
SDS = SIN(EPS) * SIN ( CLON )
DS = ASIN ( SDS )
BLAR = BLA * RPD
DO 10 I = 1 , 5
J = I - 1
ARG = 0.5D0 * J * PI
TST = ARG - CLON
TST1 = ABS( TST )
IF ( TST1 . LE . TOL ) GO TO 20
10 CONTINUE
ETA1 = TAN(DS) / TAN(EPS)
ETA = ASIN(ETA1)
ETA = ABS(ETA)
IF (( CLON . LT . PI1 ) . AND . ( CLON . GT . 0.0)) AS = ETA
IF((CLON.LT.PI).AND.(CLON.GT.PI1)) AS = PI - ETA
IF ((CLON.LT.PI3).AND.(CLON.GT.PI)) AS = PI + ETA
IF ((CLON.LT.PI2).AND.(CLON.GT.PI3)) AS = PI2 - ETA
GO TO 21
20 AS = CLON
21 AS = AS + BLAR
RETURN
END

```

```

*
*
*
*
*
*
*
*
*
*

```

```

*****
*****
**
**      SUBROUTINE DATPRP      **
**                               **
*****
*****

```

```

SUBROUTINE DATPRP ( X,Y,XX,YY )
COMMON / PREP / ASUN, DSUN, RAS, DECS
X = ASUN
Y = DSUN
XX = RAS
YY = DECS
RETURN
END

```

```

*
*
*
*
*
*
*
*
*
*

```

```

*****
*****
**
**      SUBROUTINE PERIOD      **
**                               **
*****
*****

```

```

SUBROUTINE PERIOD ( A0, ES, XI, PA )
REAL J2
COMMON / XXXX / IET
DATA J2 / 0.00108276D0/, R/ 6378.165D0/, U/398600./,PI/3.14159D0/
PA = 2.*PI*(SQRT(A0*A0*(1.-ES*ES)*1.5D0))
1 IF ( IET . EQ. 0 ) RETURN
WRITE (6,100) PA
100 FORMAT(/10X,'INITIAL ANOMALISTIC PERIOD= ',F12.3,' SEC',/)
RETURN
END

```

```

*
*
*

```

```

*****

```

✕ ✕ ✕ ✕ ✕ ✕ ✕

✕ ✕ ✕ ✕ ✕ ✕ ✕ ✕ ✕ ✕ ✕

✕  
✕



```

      IF ( DECS . LT . 0.0 ) RAS = OMA + ALP
42  IF ( MTYPE . EQ . 1 ) RAS = RAS + PI
      RAS = AMOD ( RAS , PI2 )
      GO TO 10
50  IF ( CI . GE . PI02 ) GO TO 51
      RAS = OMA + PI - ALP
      IF ( DECS . LT . 0.0 ) RAS = OMA + PI + ALP
      GO TO 42
51  RAS = OMA + PI + ALP
      IF ( DECS . LT . 0.0 ) RAS = OMA + PI - ALP
      GO TO 42
10  ELNG = RAS - AG
      IF ( ELNG . LT . 0.0 ) ELNG = PI2 + ELNG
      ELNG = AMOD(ELNG,PI2)
      GMGLT = ASIN ( 0.9792D0*SIN(DECS)+0.2028D0*COS(DECS)*COS(ELNG -
1  (291.*PI/180.)) )
      RETURN
      END

```

```

*
*
*
*
*
*
*
*
*
*
*

```

```

*****
*****
**
**          SUBROUTINE DRAG          **
**
*****
*****

```

```

SUBROUTINE DRAG( XM, DEL, TT, DELMG )
REAL N,I0,I1,I2,I3,I4,I5,I6,I7
COMMON / SOLAR / F107,FBAR,AKP,TVE
COMMON / PREP / ASUN,DSUN,RAS,DECS
DIMENSION XM(6), SUN(4), SAT(2), GEO(3), BF(8)
DATA B0/398603.254D0/,BLA/30./,PI/3.14159D0/,EOE/.00335D0/
DATA IYR/1981D0/,TVD/1./,THR/17./,TM/14./,TS/56.243D0/
PI2 = 2. * PI
SUN(3) = 23.5D0*(PI/180.)
SUN(4) = 1.0
GEO(1) = F107
GEO(2) = FBAR
GEO(3) = AKP
N = SQRT(B0/(XM(1)**3))
TCOR = AMOD ( XM(6) , PI2 )
TCOR = TCOR / N
TTT = TT - ( TCOR / 86400. )
TTR = 1721044. + 367*IYR - (7*IYR/4) + TVD + (( THR*3600. + TM*60.
1  + TS ) / 86400. ) - 2400001.0D0
DELT = TTT - TTR
CALL SOLOC(TVE,TTT,BLA,DSUN,ASUN,ABLG)
MTYPE = 0
CALL SATLOC(MTYPE,XM,DELT,DSUN,ASUN,DECS,RAS,GMGLT,RM)
STR = XM(6)
XM(6) = 0.00
CALL SALT( DECS,XM,RM,HP,RE )
XM(6) = STR
*  CALL DATPRP( SUN(1),SUN(2),SAT(1),SAT(2) )
*  CALL ATMDEN(TTT,SUN,SAT,GMGLT,HP,GEO,RHO,DRDH,SH)
*  RHOP = RHO * ( 10. **9. )
*  SHP = SH * 0.001D0
CALL JAC60(DECS,DSUN,RAS,ASUN,BLA,HP,F107,RHOP,SHP)
MTYPE = 1
CALL SATLOC(MTYPE,XM,DELT,DSUN,ASUN,DECS,RAS,GMGLT,RM)
*  CALL DATPRP ( SUN(1),SUN(2),SAT(1),SAT(2) )
*  CALL ATMDEN(TTT,SUN,SAT,GMGLT,HP,GEO,RHO,DRDH,SH)
*  RHOMIN = RHO * ( 10.**9 )
*  SHMAX = SH * 0.001D0
CALL JAC60(DECS,DSUN,RAS,ASUN,BLA,HP,F107,RHOMIN,SHMAX)
MTYPE = 2
CALL SATLOC(MTYPE,XM,DELT,DSUN,ASUN,DECS,RAS,GMGLT,RM)
*  CALL DATPRP ( SUN(1), SUN(2), SAT(1), SAT(2) )
*  CALL ATMDEN(TTT,SUN,SAT,GMGLT,HP,GEO,RHO,DRDH,SH )

```



```

* RHOMAX=RHO * (10.**9 )
* SHMIN = SH*0.001D0
CALL JAC60(DECS,DSUN,RAS,ASUN,BLA,HP,F107,RHOMAX,SHMIN)
A = SIN(DSUN)*SIN(XM(3))*SIN(XM(4))+COS(DECS)*(COS(XM(5))-ABLG)*
1 COS(XM(4))-COS(XM(3))*SIN(XM(5))-ABLG)*SIN(XM(4))
B = SIN(DSUN)*SIN(XM(3))*COS(XM(4))-COS(DECS)*(COS(XM(5))-ABLG)*
1 SIN(XM(4))+COS(XM(3))*SIN(XM(5))-ABLG)*COS(XM(4))
F = (RHOMAX - RHOMIN) / (RHOMAX + RHOMIN )
RH00 = RHOP - 0.5D0*(RHOMAX + RHOMIN) * F * A
Z = XM(1) * XM(2) / SHP
Z1 = Z*(Z - 1.) - ( F*A / (1. + F * A ))
Z2 = ( 1. / ( 1. + F * A )) - Z * ( 1. - 0.5D0*Z) - 0.5D0
TM1 = -Z1*Z1 - 2. * Z*Z*Z2
CTHAVG = 0.0
IF ( TM1 .GT. 0.00 ) CTHAVG=(Z1+SQRT(TM1))/(Z*Z)
SHNM = ABS( SHMAX - SHMIN )
HAVG = 0.5D0*(SHMAX+SHMIN)+ ( SHNM / (SHMAX+SHMIN))*A*CTHAVG
BETA = 1.0 / HAVG
C = 0.5D0*BETA*EOE*SIN(XM(3))*SIN(XM(3))*(RE+HP)
CC = C * C
ZZ = BETA * XM(1) * XM(2)
ALP = 0.00
MO = 1
NN = 8
CALL MMBSIR(ZZ,ALP,NN,MO,BF,NZ)
I0 = BF(1)
I1 = BF(2)
I2 = BF(3)
I3 = BF(4)
I4 = BF(5)
I5 = BF(6)
I6 = BF(7)
I7 = BF(8)
FA = F*A
FB = F*B
E = XM(2)
C2W = COS(2.*XM(4))
S2W = SIN(2.*XM(4))
C4W = COS(4.*XM(4))
S4W = SIN(4.*XM(4))
DELMG=-DEL*(SQRT(B0*XM(1)))*RH00*EXP(-ZZ-C*C2W)*((1.+0.25D0*
1C*C)*
1(I0+E*I1)+FA*((1.+0.25D0*CC)*(I1+E*I2))+0.5D0*C*((2.*I2-E*(I1-3.*
2I3))+FA*(I1+I3+2.*E*I4))*C2W-0.5D0*C*FB*((I1-I3)+2.*E*(I2-I4))*
3 S2W +0.125D0*C*C*((2.*I4-E*(3.*I3-5.*I5))+FA*((I3+I5)+E*(3.*I6-I2
4 )))*C4W + 0.125D0*C*C*FB*((I5-I3)+E*(I2-4.*I4+3.*I6))*S4W)
XT1 = DEL*(SQRT(B0*XM(1)))*RH00
XT2 = DELMG / XT1
XT3 = EXP(-ZZ)*(I0 + E*I1)
XT4 = XT2 / XT3
DELMG = 1000. * DELMG / 9.8D0
*... PRINT *, ZZ, RH00, XT1, XT2, XT3, XT4, DELMG , DEL
RETURN
END

```

```

*
*
* *****
* *****
* **
* **      SUBROUTINE JAC60      **
* **
* *****
* *****

```

```

SUBROUTINE JAC60 (D,DS,A,AS,BLA,Z,F107,RHO,SH )
BL = BLA*3.14159D0 / 180.
XP = -16.021D0 - 0.001985D0*Z + 6.363D0*EXP( -0.0026D0*Z)
R0 = 10.**XP
CSPSI = SIN(D)*SIN(DS) + COS(D)*COS(DS)*COS(A-AS-BL)
F = (0.5D0*(1. + CSPSI))*3.
RHQ1 = 1. + 0.19D0*(EXP(0.0055D0*Z) - 1.9D0) *F

```

```

RHO = 0.01D0 * F107 * R0 * RH01 * (10.**12)
DRODZ = 2.3026D0*R0*(-.001985D0 - .016544D0*EXP(-.0026D0*Z))
DR1DZ = .001045D0*F*EXP(.0055D0*Z)
SH = -(R0*RH01)/(R0*DR1DZ+RH01*DRODZ)
RETURN
END

```

```

*
*
*
*
*
*
*
*
*
*

```

```

*****
*****
**          SUBROUTINE THRST          **
**                                     **
*****
*****

```

```

SUBROUTINE THRST( XM, DXM, IRC, K, PA, DWOA )
DIMENSION XM(6) , DXM(6), IRV(10), DA(10)
COMMON / OADJ / NOA, IRV, DA, SPI, WT, PSENS
DATA B0 / 398603.254D0/, PI/3.14159D0/
DO 10 I = 1,6
DXM(I) = 0.0
10 CONTINUE
DWOA = 0.0
IF ( IRC .EQ. 0) RETURN
THT = XM(6) + 2.*XM(2)*SIN(XM(6)) + (5./4.)*XM(2)*XM(2)*SIN(2.*XM
1 (6))
R = XM(1)*(1. - XM(2)*XM(2))/(1. + XM(2)*COS(THT))
V2 = B0 * ((2./R) - (1./XM(1)))
V = SQRT(V2)
DVI = DA(K)*B0/(2.*XM(1)*XM(1)*V)
DXM(1)= DA(K)
DXM(2) = 2.*((COS(THT)+XM(2))/V)*DVI
DXM(4) = 2.*SIN(THT)*DVI/(XM(2)*V)
DXM(6) = (2.*PI/PA)-(1./(XM(1)*(SQRT(1.-XM(2)*XM(2)))*V))*2.*
1 SIN(THT)*((XM(1)*(1.-XM(2)*XM(2))/XM(2)) + R*XM(2))*DVI
PA = 3.*PA*XM(1)*(V/B0)*DVI
DWOA = (WT/(SPI*9.8D0))*1000.*DVI
IF (PSENS .EQ. 0) THEN
PRINT *, THT,R,V,IRV(K),DA(K),DVI,DXM(2),DXM(4),DXM(6),PA,
1 DWOA
END IF
RETURN
END

```

# APPENDIX B

## SAMPLE INPUT AND OUTPUT

```

05000,001,0,1,0,025
2.2, .0000500, 1.0, 230.,100.,09100.
100., 100., 2.0 ,43222.7382
1 10947 U 90070 78 060 A 0 1.0 014791 1015 0 0 ++
2 10947 44619.98716775 150.0000 095.0000 200.0000 .0100000 095.0000 ++
3 10947 15.71356734 .000783912 1.00112 -3.81308 -0.23959E-00 0 ++
4 10947 000000000-0 0 0 0 0 ++
5 10947 01.06000000 -701.8652 E-00 ++
CCCC X.X XXXXXX.XXXXXXXXXX XXXXXX.XXXXXXXXXX
CD 1.0 000001.000000000 000003.500000000
A 0.0 000000.000010000 000000.001000000
D 0.0 000000.100000000 000010.000000000
SPI 0.0 000200.000000000 003000.000000000
W 0.0 000005.000000000 000200.000000000
WT 0.0 000100.000000000 100000.000000000
F107 0.0 000050.000000000 000300.000000000
FBAR 0.0 000050.000000000 000300.000000000
AKP 0.0 000000.000000000 000007.000000000
TVE 0.0 038422.000000000 039422.000000000
UJD 0.0 043223.000000000 044223.000000000
ETU 0.0 000000.000000000 000179.000000000
HO 0.0 000000.000000000 000360.000000000
GO 0.0 000000.000000000 000360.000000000
ES 0.0 000000.010000000 000000.100000000
XI 0.0 000022.500000000 000157.500000000
RND 0.0 000000.000010000 000000.000000000
ESD 0.0 000000.000000000 000000.000000000
AO 0.0 000001.025940000 000001.168470000
ADOT 0.0 000000.000000000 000000.000000000

```

```

1000, 0.1
2000, 0.3
3000, 0.5

```

```

*****
* ONLY THE ABOVE IS ACTUAL INPUT FILE DATA. AN INPUT ELEMENT *
* DESCRIPTION IS PRESENTED NEXT TO AID THE USER IN PLACING VALUES *
* *****

```

### INPUT FILE FOR PROPELLANT LONGEVITY MODEL (VARIABLE ORGANIZATION)

```

IETR1, IETR2, NOA, PSENS, IET, PSIZE
CD, A, D, SPI, W, WT,
F107, FBAR, AKP, TVE,
1 SKIP LINE ONE NAVSPASUR FIVE CARD DATA
2 8X, UJD, 1X, ETU, 1X, HO, 1X, GO, 1X, ES, 1X, XI
3 20X, RND, 19X, ESD
4 SKIP LINE FOUR NAVSPASUR FIVE CARD DATA
5 3X, AO, 1X, ADOT
IRV(1), DA(1)
IRV(2), DA(2)
IRV(3), DA(3)
.
.
IRV(K), DA(K)

```

NOTE: WARNING OMIT ALL ORBIT ADJUST DATA IF  
NO ORBIT ADJUSTS ARE SCHEDULED (NOA=0)

### SENSITIVITY ANALYSIS TABLE

CHAR	SNSAR	SNSMIN	SNSMAX
A4	F3.1	F16.8	F16.8

-----  
INITIAL INPUT CONDITIONS  
-----

ATMOSPHERIC INPUT PARAMETERS

D (RELATIVE ATMOSPHERIC ROTATION) = 1.0000  
F107 (DECIMETRIC SOLAR FLUX) = 100.00  
FBAR (90 DAY AVG. F107) = 100.00  
AKP (GEO MAGNETIC INDEX) = 2.000  
TVE (TIME OF VERNAL EQUINOX PASSAGE) = 43222.738200000 MODIFIED JULIAN DAYS

SATELLITE PHYSICAL PARAMETERS

CD (DRAG COEFFICIENT) = 2.20 UNITLESS  
A (CROSSECTIONAL AREA) = 0.000050000 SQUARE KILOMETERS  
SPI (MOTOR SPECIFIC IMPULSE) = 230.00 SECONDS  
W (INITIAL FUEL MASS) = 10.00 KILOGRAMS  
WT (INITIAL SATELLITE MASS) = 9100.00 KILOGRAMS

NAVSPASUR ORBITAL ELEMENTS

UJD (EPOCH) = 44619.98716775 MEAN JULIAN DAYS  
ETU (MEAN ANOMALY) = 150.0000 DEGREES  
H0 (MEAN RIGHT ASCENSION OF THE ASCENDING NODE) = 95.0000 DEGREES  
G0 (MEAN ARGUMENT OF PERIGEE) = 200.0000 DEGREES  
XI (MEAN INCLINATION) = 95.0000 DEGREES  
RND (RATE OF CHANGE OF MEAN MOTION) = 0.000783912 REVOLUTIONS PER DAY SQUARED  
ES (MEAN ECCENTRICITY) = 0.0100 UNITLESS  
ESD (ECCENTRICITY DECAY RATE) = -0.239590000 1/SECONDS  
A0 (KAULA SEMI-MAJOR AXIS) = 1.06000 MEAN EARTH RADII  
ADOT (SEMI-MAJOR AXIS DECAY RATE) = -701.865200000

CONTROL INPUT PARAMETERS

MAXIMUM REVOLUTIONS PER ITERATION 5000  
NUMBER OF SCHEDULED ORBIT ADJUSTS TO SEMI-MAJOR AXIS 0  
  
-----  
  
-----

SENSITIVITY ANALYSIS FOR  
LOW EARTH ORBIT SATELLITES  
PROPELLENT LONGEVITY

-----

TABLE OF INPUT PARAMETERS SCANNED FROM MINIMUM TO  
 MAXIMUM WITH THE INDICATED INCREMENT PER RUN.  
 THE GRANULARITY IS 1/ 25.  
 ALL OTHER INPUT PARAMETERS ARE RETURNED TO THEIR  
 INITIAL VALUES AT EACH INCREMENT.

INPUT PARAMETER	MINIMUM	MAXIMUM	INCREMENT
CD	1.000000000	3.500000000	0.100000000

-----

SENSITIVITY SCAN RESULTS FOR ABOVE SPECIFICS

REV NUMBER	TIME(DAYS)	FRACTION OF SCAN
495	31.58	1.000000000
448	28.57	1.100000000
409	26.08	1.200000000
376	23.97	1.300000000
348	22.18	1.400000000
324	20.65	1.500000000
303	19.30	1.600000000
285	18.15	1.700000000
268	17.07	1.800000000
254	16.17	1.900000000
241	15.34	2.000000000
229	14.57	2.100000000
218	13.87	2.200000000
208	13.23	2.300000000
200	12.72	2.400000000
191	12.14	2.500000000
184	11.70	2.600000000
177	11.25	2.700000000
170	10.80	2.800000000
164	10.42	2.900000000
159	10.10	3.000000000
154	9.78	3.100000000
149	9.46	3.200000000
144	9.14	3.300000000
140	8.88	3.400000000
136	8.63	3.500000000



```

05000,001,0,1,0,025
2.2, .0000500, 1.0, 230.,901.,09100.
100., 100., 2.0 ,43222.7382
1 10947 U 90070 78 060 A 0 1.0 014791 1015 0 0 ++ |
2 10947 44619.98716775 150.0000 095.0000 200.0000 .0100000 095.0000 ++ |
3 10947 15.71356734 .000783912 1.00112 -3.81308 -0.23959E-00 0 ++ |
4 10947 0000000000-0 0 0 0 0 ++ |
5 10947 01.06000000 -701.8652 E-00 ++ |
CCCC X.X XXXXXX.XXXXXXXXXX XXXXXX.XXXXXXXXXX
CD 0.0 000001.000000000 000003.500000000
A 0.0 000000.000010000 000000.001000000
D 0.0 000000.100000000 000010.000000000
SPI 0.0 000200.000000000 003000.000000000
W 0.0 000005.000000000 000200.000000000
WT 0.0 000100.000000000 100000.000000000
F107 0.0 000050.000000000 000300.000000000
FBAR 0.0 000050.000000000 000300.000000000
AKP 0.0 000000.000000000 000007.000000000
TVE 0.0 038422.000000000 039422.000000000
UJD 0.0 043223.000000000 044223.000000000
ETU 0.0 000000.000000000 000179.000000000
HO 0.0 000000.000000000 000360.000000000
GO 0.0 000000.000000000 000360.000000000
ES 0.0 000000.010000000 000000.100000000
XI 0.0 000022.500000000 000157.500000000
RND 0.0 000000.000010000 000000.000000000
ESD 0.0 000000.000000000 000000.000000000
AO 1.0 000001.025940000 000001.168470000
ADOT 0.0 000000.000000000 000000.000000000

1000, 0.1
2000, 0.3
3000, 0.5

```

```

*****
* ONLY THE ABOVE IS ACTUAL INPUT FILE DATA. AN INPUT ELEMENT *
* DESCRIPTION IS PRESENTED NEXT TO AID THE USER IN PLACING VALUES *
* *****

```

# INPUT FILE FOR PROPELLANT LONGEVITY MODEL (VARIABLE ORGANIZATION)

```

IETR1, IETR2, NOA, PSENS, IET, PSIZE
CD, A, D, SPI, W, WT,
F107, FBAR, AKP, TVE,
1 SKIP LINE ONE NAVSPASUR FIVE CARD DATA
2 8X, UJD, 1X, ETU, 1X, HO, 1X, GO, 1X, ES, 1X, XI
3 20X, RND, 19X, ESD
4 SKIP LINE FOUR NAVSPASUR FIVE CARD DATA
5 8X, AO, 1X, ADOT
IRV(1), DA(1)
IRV(2), DA(2)
IRV(3), DA(3)
.
.
IRV(K), DA(K)

```

NOTE: WARNING OMIT ALL ORBIT ADJUST DATA IF  
NO ORBIT ADJUSTS ARE SCHEDULED (NOA=0)

## SENSITIVITY ANALYSIS TABLE

CHAR	SNSAR	SNSMIN	SNSMAX
A4	F3.1	F16.8	F16.8

```

*****

```

-----

INITIAL INPUT CONDITIONS

-----

ATMOSPHERIC INPUT PARAMETERS

D (RELATIVE ATMOSPHERIC ROTATION) = 1.0000  
F107 (DECIMETRIC SOLAR FLUX) = 100.00  
F2AR (90 DAY AVG. F107) = 100.00  
AKP (GEOMAGNETIC INDEX) = 2.000  
TVE (TIME OF VERNAL EQUINOX PASSAGE) = 43222.738200000 MODIFIED JULIAN DAYS

SATELLITE PHYSICAL PARAMETERS

CD (DRAG COEFFICIENT) = 2.20 UNITLESS  
A (CROSSSECTIONAL AREA) = 0.000050000 SQUARE KILOMETERS  
SPI (MOTOR SPECIFIC IMPULSE) = 230.00 SECONDS  
W (INITIAL FUEL MASS) = 1.00 KILOGRAMS  
WT (INITIAL SATELLITE MASS) = 9100.00 KILOGRAMS

NAVSPASUR ORBITAL ELEMENTS

UJD (EPOCH) = 44619.98716775 MEAN JULIAN DAYS  
ETU (MEAN ANOMALY) = 150.0000 DEGREES  
HO (MEAN RIGHT ASCENSION OF THE ASCENDING NODE) = 95.0000 DEGREES  
GO (MEAN ARGUMENT OF PERIGEE) = 200.0000 DEGREES  
XI (MEAN INCLINATION) = 95.0000 DEGREES  
RND (RATE OF CHANGE OF MEAN MOTION) = 0.000783912 REVOLUTIONS PER DAY SQUARED  
ES (MEAN ECCENTRICITY) = 0.0100 UNITLESS  
ESD (ECCENTRICITY DECAY RATE) = -0.239590000 1/SECONDS  
AO (KAULA SEMI-MAJOR AXIS) = 1.06000 MEAN EARTH RADII  
ADOT (SEMI-MAJOR AXIS DECAY RATE) = -701.865200000

CONTROL INPUT PARAMETERS

MAXIMUM REVOLUTIONS PER ITERATION 5000  
NUMBER OF SCHEDULED ORBIT ADJUSTS TO SEMI-MAJOR AXIS 0

-----

-----

SENSITIVITY ANALYSIS FOR  
LOW EARTH ORBIT SATELLITES  
PROPELLENT LONGEVITY

-----

TABLE OF INPUT PARAMETERS SCANNED FROM MINIMUM TO  
 MAXIMUM WITH THE INDICATED INCREMENT PER RUN.  
 THE GRANULARITY IS 1/ 25.  
 ALL OTHER INPUT PARAMETERS ARE RETURNED TO THEIR  
 INITIAL VALUES AT EACH INCREMENT.

INPUT PARAMETER	MINIMUM	MAXIMUM	INCREMENT
AO	1.025940000	1.168470000	0.005701200

-----

SENSITIVITY SCAN RESULTS FOR ABOVE SPECIFICS

REV NUMBER	TIME(DAYS)	FRACTION OF SCAN
1	0.00	1.025940000
1	0.00	1.031641200
1	0.00	1.037342400
3	0.12	1.043043600
6	0.31	1.048744800
12	0.70	1.054446000
22	1.34	1.060147200
40	2.51	1.065848400
69	4.42	1.071549600
115	7.47	1.077250800
186	12.21	1.082952000
298	19.76	1.088653200
473	31.65	1.094354400
747	50.42	1.100055600
1149	78.19	1.105756800
1652	113.33	1.111458000
2033	140.55	1.117159200
2270	158.15	1.122860400
2514	176.50	1.128561600
2942	208.13	1.134262800
3349	238.73	1.139964000
3648	262.00	1.145665200
4026	291.32	1.151366400
4373	318.80	1.157067600
4555	334.53	1.162768800
4712	348.62	1.168470000

```

05000,001,0,1,0,025
2.2, .0000500, 1.0, 230.,100.,09100.
100., 100., 2.0 ,43222.7382
1 10947 U 90070 78 060 A 0 1.0 014791 1015 0 0 ++ |
2 10947 44619.98716775 150.0000 095.0000 200.0000 .0100000 095.0000 ++ |
3 10947 15.71356734 .000783912 1.00112 -3.81308 -0.23959E-00 0 ++ |
4 10947 000000000-0 0 0 0 0 ++ |
5 10947 01.06000000 -701.8652 E-00 ++ |
CCCC X.X XXXXXX.XXXXXXXXXX XXXXXX.XXXXXXXXXX
CD 0.0 000001.000000000 000003.500000000
A 0.0 000000.000010000 000000.001000000
D 0.0 000000.100000000 000010.000000000
SPI 0.0 000200.000000000 003000.000000000
W 0.0 000005.000000000 000200.000000000
WT 0.0 000100.000000000 100000.000000000
F107 1.0 000050.000000000 000300.000000000
FBAR 0.0 000050.000000000 000300.000000000
AKP 0.0 000050.000000000 000007.000000000
TVE 0.0 038422.000000000 038422.000000000
UJD 0.0 043223.000000000 044223.000000000
ETU 0.0 000000.000000000 000179.000000000
HO 0.0 000000.000000000 000360.000000000
GO 0.0 000000.000000000 000360.000000000
ES 0.0 000000.010000000 000000.100000000
XI 0.0 000022.500000000 000157.500000000
RND 0.0 000000.000010000 000000.000000000
ESD 0.0 000000.000000000 000000.000000000
AO 0.0 000001.025940000 000001.168470000
ADOT 0.0 000000.000000000 000000.000000000

1000, 0.1
2000, 0.3
3000, 0.5

```

```

*****
*
* ONLY THE ABOVE IS ACTUAL INPUT FILE DATA. AN INPUT ELEMENT
* DESCRIPTION IS PRESENTED NEXT TO AID THE USER IN PLACING VALUES
*
*****

```

# INPUT FILE FOR PROPELLANT LONGEVITY MODEL (VARIABLE ORGANIZATION)

```

IETR1, IETR2, NOA, PSENS, IET, PSIZE
CD, A, D, SPI, W, WT,
F107, FBAR, AKP, TVE,
1 SKIP LINE ONE NAVSPASUR FIVE CARD DATA
2 8X, UJD, 1X, ETU, 1X, HO, 1X, GO, 1X, ES, 1X, XI
3 20X, RND, 19X, ESD
4 SKIP LINE FOUR NAVSPASUR FIVE CARD DATA
5 8X, AO, 1X, ADOT
IRV(1), DA(1)
IRV(2), DA(2)
IRV(3), DA(3)
.
.
.
IRV(K), DA(K)

```

NOTE: WARNING OMIT ALL ORBIT ADJUST DATA IF  
NO ORBIT ADJUSTS ARE SCHEDULED (NOA=0)

## SENSITIVITY ANALYSIS TABLE

CHAR	SNSAR	SNSMIN	SNSMAX
A4	F3.1	F16.8	F16.8

```

*****

```

-----

INITIAL INPUT CONDITIONS

-----

ATMOSPHERIC INPUT PARAMETERS

D (RELATIVE ATMOSPHERIC ROTATION) = 1.0000  
F107 (DECIMETRIC SOLAR FLUX) = 100.00  
FBAR (90 DAY AVG. F107) = 100.00  
AKP (GEOMAGNETIC INDEX) = 2.000  
TVE (TIME OF VERNAL EQUINOX PASSAGE) = 43222.738200000 MODIFIED JULIAN DAYS

SATELLITE PHYSICAL PARAMETERS

CD (DRAG COEFFICIENT) = 2.50 UNITLESS  
A (CROSSECTIONAL AREA) = 0.000050000 SQUARE KILOMETERS  
SPI (MOTOR SPECIFIC IMPULSE) = 230.00 SECONDS  
W (INITIAL FUEL MASS) = 10.00 KILOGRAMS  
WT (INITIAL SATELLITE MASS) = 9100.00 KILOGRAMS

NAVSPASUR ORBITAL ELEMENTS

UJD (EPOCH) = 44619.98716775 MEAN JULIAN DAYS  
ETU (MEAN ANOMALY) = 150.0000 DEGREES  
H0 (MEAN RIGHT ASCENSION OF THE ASCENDING NODE) = 95.0000 DEGREES  
G0 (MEAN ARGUMENT OF PERIGEE) = 200.0000 DEGREES  
XI (MEAN INCLINATION) = 95.0000 DEGREES  
RND (RATE OF CHANGE OF MEAN MOTION) = 0.000783912 REVOLUTIONS PER DAY SQUARED  
ES (MEAN ECCENTRICITY) = 0.0100 UNITLESS  
ESD (ECCENTRICITY DECAY RATE) = -0.239590000 1/SECONDS  
A0 (KAULA SEMI-MAJOR AXIS) = 1.06000 MEAN EARTH RADII  
ADOT (SEMI-MAJOR AXIS DECAY RATE) = -701.865200000

CONTROL INPUT PARAMETERS

MAXIMUM REVOLUTIONS PER ITERATION 5000  
NUMBER OF SCHEDULED ORBIT ADJUSTS TO SEMI-MAJOR AXIS 0

-----

-----

SENSITIVITY ANALYSIS FOR  
LOW EARTH ORBIT SATELLITES  
PROPELLENT LONGEVITY



-----

TABLE OF INPUT PARAMETERS SCANNED FROM MINIMUM TO  
 MAXIMUM WITH THE INDICATED INCREMENT PER RUN.  
 THE GRANULARITY IS 1/ 25.  
 ALL OTHER INPUT PARAMETERS ARE RETURNED TO THEIR  
 INITIAL VALUES AT EACH INCREMENT.

INPUT PARAMETER	MINIMUM	MAXIMUM	INCREMENT
F107	50.000000000	300.000000000	10.000000000

-----

SENSITIVITY SCAN RESULTS FOR ABOVE SPECIFICS

REV NUMBER	TIME(DAYS)	FRACTION OF SCAN
392	24.99	50.000000000
324	20.65	60.000000000
276	17.58	70.000000000
241	15.34	80.000000000
213	13.55	90.000000000
191	12.14	100.000000000
174	11.06	110.000000000
159	10.10	120.000000000
146	9.27	130.000000000
136	8.63	140.000000000
127	8.05	150.000000000
119	7.54	160.000000000
112	7.10	170.000000000
105	6.65	180.000000000
100	6.33	190.000000000
95	6.01	200.000000000
90	5.69	210.000000000
86	5.43	220.000000000
82	5.18	230.000000000
79	4.99	240.000000000
76	4.79	250.000000000
73	4.60	260.000000000
70	4.41	270.000000000
67	4.22	280.000000000
65	4.09	290.000000000
63	3.96	300.000000000

-----  
INITIAL INPUT CONDITIONS  
-----

ATMOSPHERIC INPUT PARAMETERS

D (RELATIVE ATMOSPHERIC ROTATION) = 1.0000  
F107 (DECIMETRIC SOLAR FLUX) = 100.00  
FBAR (90 DAY AVG. F107) = 100.00  
AKP (GEOMAGNETIC INDEX) = 2.000  
TVE (TIME OF VERNAL EQUINOX PASSAGE) = 43222.738200000 MODIFIED JULIAN DAYS

SATELLITE PHYSICAL PARAMETERS

CD (DRAG COEFFICIENT) = 2.20 UNITLESS  
A (CROSSSECTIONAL AREA) = 0.000050000 SQUARE KILOMETERS  
SPI (MOTOR SPECIFIC IMPULSE) = 230.00 SECONDS  
W (INITIAL FUEL MASS) = 150.00 KILOGRAMS  
WT (INITIAL SATELLITE MASS) = 9100.00 KILOGRAMS

NAVSPASUR ORBITAL ELEMENTS

UJD (EPOCH) = 44619.98716775 MEAN JULIAN DAYS  
ETU (MEAN ANOMALY) = 150.0000 DEGREES  
HO (MEAN RIGHT ASCENSION OF THE ASCENDING NODE) = 95.0000 DEGREES  
GO (MEAN ARGUMENT OF PERIGEE) = 200.0000 DEGREES  
XI (MEAN INCLINATION) = 95.0000 DEGREES  
RND (RATE OF CHANGE OF MEAN MOTION) = 0.000783912 REVOLUTIONS PER DAY SQUARED  
ES (MEAN ECCENTRICITY) = 0.0100 UNITLESS  
ESD (ECCENTRICITY DECAY RATE) = -0.239590000 1/SECONDS  
AO (KAULA SEMI-MAJOR AXIS) = 1.06000 MEAN EARTH RADII  
ADOT (SEMI-MAJOR AXIS DECAY RATE) = -701.865200000

CONTROL INPUT PARAMETERS

MAXIMUM REVOLUTIONS PER ITERATION 5000  
NUMBER OF SCHEDULED ORBIT ADJUSTS TO SEMI-MAJOR AXIS 0

-----

L

-----

PROPELLANT LIFE ESTIMATOR

-----

CDA= 0.11000E-03 SQ KM  
 SPECIFIC IMPULSE= 230.00 SEC  
 INITIAL WEIGHT OF PROPELLANT= 150.00 KG

F107= 100.00  
 FBAR= 100.00  
 TIME OF VERNAL EQUINOX= 0.43222738200000E+05

MAXIMUM NUMBER OF ORBITAL REVOLUTIONS= 5000

DATA PRINTED EVERY 100 ORBITAL REVOLUTIONS

KOZAI MEAN ELEMENT SET

SEMIMAJOR AXIS= 0.67562054107790E+04 KM  
 ECCENTRICITY= 0.96561132904615E-02  
 INCLINATION= 0.94999964849617E+02 DEG  
 ARGUMENT OF PERIGEE= 0.19333742463643E+03 DEG  
 ASCENDING NODE= 0.95000149668470E+02 DEG  
 MEAN ANOMALY= 0.15661152641309E+03 DEG

REV NUMBER	TIME(MJD)	TIME(DAYS)	PROPELLANT REMAINING(KG)
100	44626.32	6.33	145.28
200	44632.71	12.72	140.69
300	44639.10	19.11	136.21
400	44645.49	25.50	131.83
500	44651.88	31.90	127.54
600	44658.27	38.29	123.37
700	44664.67	44.68	119.33
800	44671.06	51.07	115.45
900	44677.45	57.46	111.72
1000	44683.84	63.86	108.07
1100	44690.23	70.25	104.42
1200	44696.63	76.64	100.72
1300	44703.02	83.03	96.94
1400	44709.41	89.42	93.05
1500	44715.80	95.82	88.96
1600	44722.19	102.21	84.60
1700	44728.59	108.60	79.92
1800	44734.93	114.99	74.98
1900	44741.37	121.33	69.93
2000	44747.76	127.77	64.97
2100	44754.15	134.17	60.27
2200	44760.55	140.56	55.92
2300	44766.94	146.95	51.91
2400	44773.33	153.34	48.18
2500	44779.72	159.73	44.59
2600	44786.11	166.13	41.07
2700	44792.51	172.52	37.58
2800	44798.90	178.91	34.10
2900	44805.29	185.30	30.53
3000	44811.68	191.69	26.78
3100	44818.07	198.09	22.74
3200	44824.47	204.48	18.37
3300	44830.86	210.87	13.66
3400	44837.25	217.26	8.68
3500	44843.64	223.65	3.58
3600	44850.03	230.05	-1.49
3600	230.05		0.000000000

## LIST OF REFERENCES

1. Naval Surface Weapons Center Report 83-243, Low-Altitude Earth Satellite Propellant Longevity Prediction with Application Flight Profile Trade-off Analysis, by A.D. Parks, September 1983.
2. Taff, L.G., Celestial Mechanics: a Computational Guide for the Practitioner, John Wiley & Sons, Inc., 1985.
3. Bate, R.B., Mueller, D.D., and White, J.E., Fundamentals of Astrodynamics, Dover Publications, Inc., 1971.
4. Fleagle, R.G., An Introduction to Atmospheric Physics, Academic Press, 1980.
5. Air Force Geophysics Laboratory Report 81-0195, Empirical Models for the Thermosphere and Requirements for Improvements, by L.G. Jacchia, June 1981.
6. Air Force Geophysics Laboratory Report 81-230, Analysis of Data for Development of Density and Composition Models of the Upper Atmosphere, by L.G. Jacchia, and J. W. Slowey, July 1981.
7. Smithsonian Astrophysical Observatory Special Report 375, Thermospheric Temperature, Density, and Composition: New Models, by L.G. Jacchia, 15 March 1977.
8. National Aerodynamics and Space Administration Technical Memorandum 87587, User's Guide for Langely Research Center Orbital Lifetime Program, by L.H. Orr, September 1985.

# INITIAL DISTRIBUTION LIST

	No. Copies
1. Defense Technical Information Center Cameron Station Alexandria, Virginia 22304-6145	2
2. Library, Code 0142 Naval Postgraduate School Monterey, California 93943-5002	2
3. Naval Surface Weapons Center ATTN: Dr. A. D. Parks (Code K13) Dahlgren, Virginia 22448	2
4. Dr. R.D. Wood, Code 67Wr Department of Aeronautics Naval Postgraduate School Monterey, California 93943-5000	2
5. Dr. M.D. Weir, Code 53Wc Department of Mathematics Naval Postgraduate School Monterey, California 93943-5000	2
6. Lt. C.D. Noble Department Head School Class 100 Surface Warfare Officers School Command Newport, Rhode Island 02841-5012	2









Thesis

N63 Noble

c.1 Verification of a micro-  
thrusting model to main-  
tain satellites in low  
orbit.

Thesis

N63 Noble

c.1 Verification of a micro-  
thrusting model to main-  
tain satellites in low  
orbit.

thesN63

Verification of a micro-thrusting model



3 2768 000 75459 2

DUDLEY KNOX LIBRARY